



LUND UNIVERSITY

Experimental Studies on the Regulation of Glomerular Filtration Barrier Permeability In Vivo. Intra- and intercellular signaling mechanisms.

Dolinina, Julia

2020

Document Version:

Publisher's PDF, also known as Version of record

[Link to publication](#)

Citation for published version (APA):

Dolinina, J. (2020). *Experimental Studies on the Regulation of Glomerular Filtration Barrier Permeability In Vivo. Intra- and intercellular signaling mechanisms*. [Doctoral Thesis (compilation), Department of Clinical Sciences, Lund]. Lund University, Faculty of Medicine.

Total number of authors:

1

General rights

Unless other specific re-use rights are stated the following general rights apply:

Copyright and moral rights for the publications made accessible in the public portal are retained by the authors and/or other copyright owners and it is a condition of accessing publications that users recognise and abide by the legal requirements associated with these rights.

- Users may download and print one copy of any publication from the public portal for the purpose of private study or research.
- You may not further distribute the material or use it for any profit-making activity or commercial gain
- You may freely distribute the URL identifying the publication in the public portal

Read more about Creative commons licenses: <https://creativecommons.org/licenses/>

Take down policy

If you believe that this document breaches copyright please contact us providing details, and we will remove access to the work immediately and investigate your claim.

LUND UNIVERSITY

PO Box 117
221 00 Lund
+46 46-222 00 00

Experimental Studies on the Regulation of Glomerular Filtration Barrier Permeability *In Vivo*

Intra- and intercellular signaling mechanisms

JULIA DOLININA

DEPARTMENT OF CLINICAL SCIENCES, LUND | LUND UNIVERSITY



Experimental Studies on the Regulation of Glomerular
Filtration Barrier Permeability *In Vivo*

Experimental Studies on the Regulation of Glomerular Filtration Barrier Permeability *In Vivo*

Intra- and intercellular signaling mechanisms

by Julia Dolinina



LUND
UNIVERSITY

Thesis for the degree of Doctor of Philosophy

Thesis advisors: assoc. prof. Carl M. Öberg, assoc. prof. Peter Bentzer
Faculty opponent: assoc. prof. Robert Frithiof, Uppsala University, Sweden

To be presented, by due permission of the Faculty of Medicine at Lund University, for
public criticism at the Department of Clinical Sciences, Lund on Thursday the 10th of
December 2020 at 10 am.

Organization LUND UNIVERSITY		Document name Doctoral dissertation	
		Date of issue DECEMBER 10, 2020	
Author(s) JULIA DOLININA		Sponsoring organization	
Title and subtitle Experimental studies on the regulation of glomerular filtration barrier permeability in vivo: Intra- and intercellular signaling mechanisms			
Abstract Increased permeability of large molecules in the glomerular filtration barrier (GFB) leading to proteinuria is a hallmark of glomerular disease, and a well-known contributing factor to the progression of chronic kidney disease. The balance between oxidative stress (ROS) and NO signaling as well as intracellular Ca ⁺⁺ signaling seems to play an important role in permeability changes in the GFB. This thesis presents studies on the effects of nitric oxide, endothelin-1, angiotensin II, and unilateral ureteral obstruction on glomerular microvascular permeability <i>in vivo</i> in a well-established rat model. We studied the fractional clearance of a polydisperse, protein-like probe molecule (a 1:24 mixture of Ficoll 70 kDa and Ficoll 400 kDa). The molecule was infused intravenously and the urine was collected. Presence of the probe molecule in the urine was detected by high-performance size exclusion chromatography (HPSEC). Since Ficoll is not affected by tubular mechanisms, its fractional clearance can be used as a good estimate of the glomerular sieving coefficient and thus the permeability across the kidney filter. After a control period, one or more pharmacological stimuli were given to study the effects on glomerular permeability: Study 1: Bioavailability of endogenous NO was reduced with an infusion of an endothelial NO synthase (L-NAME) blocker, which led to increased permeability. This was counteracted by treatment with a ROS scavenger (Tempol) and cyclic GMP (an intracellular signaling molecule downstream of the NO receptor). Study 2: In acute unilateral ureteral obstruction, an increase in permeability was observed which was mitigated by Tempol. Study 3: Administration of endothelin-1 (ET-1) resulted in increased permeability in GFB which was attenuated after use of ET-1 receptor A blockers but not by an ET-1 receptor B blocker. Study 4: Blockers of TRPC5/6 channels counteracted increased permeability after intravenous administration of angiotensin II. Blockers of TRPC6 appear to have an effect on both proteinuria and blood pressure, whereas blockade of TRPC5 only reduces proteinuria. In this thesis, it was shown that several different intracellular signaling pathways are involved in permeability changes in the glomerular filter. Better understanding of the underlying mechanisms that lead to proteinuria may provide opportunities to develop new drugs with anti-proteinuric effect.			
Key words Glomerular filtration barrier, Nitric oxide, Endothelin-1, Angiotensin II, TRPC5, TRPC6			
Classification system and/or index terms (if any)			
Supplementary bibliographical information		Language English	
ISSN and key title ISSN 1652-8220 Lund University, <i>Faculty of Medicine Doctoral Dissertation Series</i> 2020:134		ISBN 978-91-8021-001-0	
Recipient's notes	Number of pages 54		Price
	Security classification		

I, the undersigned, being the copyright owner of the abstract of the above-mentioned dissertation, hereby grant to all reference sources permission to publish and disseminate the abstract of the above-mentioned dissertation.

Signature



Date 2020-11-04

Experimental Studies on the Regulation of Glomerular Filtration Barrier Permeability *In Vivo*

Intra- and intercellular signaling mechanisms

by Julia Dolinina



LUND
UNIVERSITY

In Sweden, a doctoral thesis takes either the form of a single cohesive research study (monograph) or a summary of research papers (compilation thesis) written by the doctoral student alone or together with one or several co-author(s).

A compilation thesis consists of two parts. First, an introductory text (“kappa”) puts the research into context and summarizes the key points of the papers. Second, the research papers are reproduced, which may already have been published or are manuscripts at various stages (in press, submitted or in draft)

Copyright pp 1-54 Julia Dolinina

Paper 1 © the American Physiological Society 2016

Paper 2 © the American Physiological Society 2018

Paper 3 © the American Physiological Society 2019

Paper 4 © by the Authors (Manuscript unpublished)

Faculty of Medicine
Department of Clinical Sciences Lund


ISBN 978-91-8021-001-0

ISSN 1652-8220

Printed in Sweden by Media-Tryck, Lund University
Lund 2020



Media-Tryck is a Nordic Swan Ecolabel certified provider of printed material. Read more about our environmental work at www.mediatryck.lu.se

MADE IN SWEDEN 

To my daughter Polina

Table of Contents

List of publications	10
Abbreviations	11
Swedish summary (Populärvetenskaplig sammanfattning)	12
Introduction	15
Proteinuria is a hallmark of kidney disease.....	15
The kidney.....	16
The glomerular filtration barrier	17
Protein transport across the glomerular filtration barrier: theory and current knowledge	18
Aims of the thesis	23
Methods	25
Laboratory animals and experimental protocols	25
Animals	25
Surgery	25
Experimental protocols.....	25
Molecular probe and determination of proteinuria.....	28
Two-pore analysis and transport physiology.....	29
Statistical analysis	32
Results.....	35
Study I	35
Study II.....	36
Study III	39
Study IV	40

Discussion	41
Glomerular permeability and hemodynamic aspects.....	47
Study II – some considerations.....	48
Conclusions	48
Further perspectives	48
Acknowledgements	49
References	51

List of publications

This thesis is based on the following publications

- I. Dolinina, J., Sverrisson, K., Rippe, A., Öberg, C. M., & Rippe, B. (2016). Nitric oxide synthase inhibition causes acute increases in glomerular permeability in vivo, dependent upon reactive oxygen species. *American Journal of Physiology - Renal Physiology*, 311(5), F984-F990.
- II. Dolinina, J., Rippe, A., Bentzer, P., & Öberg, C. M. (2018). Glomerular hyperpermeability after acute unilateral ureteral obstruction: effects of Tempol, NOS, RhoA, and Rac-1 inhibition. *American Journal of Physiology - Renal Physiology*, 315(3), F445-F453.
- III. Dolinina, J., Rippe, A., & Öberg, C. M. (2019). Sustained, delayed and small increments in glomerular permeability to macromolecules during systemic endothelin-1 infusion mediated via the ETA receptor. *American Journal of Physiology-Renal Physiology* 316(6), F1173-F1179.
- IV. Dolinina, J., Rippe, A., Bentzer, P., & Öberg, C. M. Inhibition of TRPC5 ameliorates angiotensin II induced glomerular hyperpermeability in vivo without hemodynamic effects. Manuscript.

Abbreviations

AG	Angiotensin
CL	Clearance
Da	Dalton
FITC	Fluorescein isothiocyanate
GBM	Glomerular basement membrane
GFB	Glomerular filtration barrier
GFR	Glomerular filtration rate
PKC	Protein kinase C
PSD	Podocyte slit diafragn
PTR	Proximal tubular re-absorption
Å	Ångström (0.1 nm)
VEC	Visceral epithelial cell, podocyte
IPK	Isolated perfused kidney

Swedish summary (Populärvetenskaplig sammanfattning)

Njurarna är parade, bönformade organ som ligger vid sidan om ryggraden. En frisk njure är cirka 11-12 cm lång och väger ungefär 150-160 g. Njurarna utför flera viktiga funktioner i kroppen, inklusive filtrering och utsöndring av metabola avfallsprodukter, reglering av salter, vätska och syrlighets grad i kroppen; samt stimulering av produktion av röda blodkroppar. De deltar i reglering av blodtrycket och skelettets metabolism genom aktivering av D-vitamin.

Den funktionella enheten i njuren är nefronet. Nefron saknar reparationsförmåga, man föds med cirka 1 million nefron per njure. Människan bildar således inga nya nefron under sin livstid och förlust av nefron leder till utveckling av kronisk njursvikt. Blodet filteras i nefronet över den glomerulära kapillärväggen vars lager utgör den så kallade glomerulära filtrationsbarriären (GFB) som är genomsläpplig för vatten och salter, men har mycket låg genomsläpplighet för stora plasmaproteiner, framförallt för albumin och andra proteinmolekyler som är större än albumin. Cirka 180L vätska filtreras via njurarna dagligen och bildar så kallad primär urin som bearbetas och finjusteras via ett välutvecklat system av tubuli till 1,5L sekundär urin per dygn hos friska individer.

Albumin är ett protein som har en svagt negativ laddning (-22) vid fysiologiska förhållanden. Albuminmolekylen är hård, har en radie på 35,5 Å och väger 66 kDa. Hos människor ligger plasma-albumin nivån på 40 g/l. Vid fysiologiska förhållanden är genomsläppligheten för medelstora molekyler så som albumin låg i glomerulära filtret och enbart 1 på 10000 albumin molekyler passerar till primär urinen. 99% av allt filtrerat albumin återupptas i proximala tubuli så det återstår endast en liten mängd 10-30 mg albumin i sekundärurinen. När dessa system inte fungerar som de ska och släpper igenom högre halter av albumin och andra proteiner över GFB leder det till så-kallad proteinuri.

Proteinuri är en välkänd bidragande riskfaktor till njurfunktionens nedsättning och på sikt leder det till organskada med utveckling av terminal uremi och tillkomst av dialysbehov. Mortaliteten hos dialysbehandlade patienter ligger på cirka 19% vilket är avsevärt högre än i den genomsnittliga populationen. Behandling av terminal njursjukdom innebär en betydande samhällskostnad, till exempel ligger behandlingskostnaden för hemodialysbehandling på 800.000 kr/patient/år. Genom att skapa en bättre förståelse av mekanismer för proteinuri kan man utveckla nya antiproteinuriska läkemedel och därigenom förbättra behandling av proteinuriska njursjukdomar.

Mitt forskningssyfte är att studera permeabilitets-mekanismer av GFB för albumin och andra stora molekyler. Mitt forskningsprojekt är djurexperimentellt (råtta). Djur

experiment ger möjlighet att studera permeabilitet i GFB i fysiologiska förhållandet där alla cellstrukturerna i GFB befinner sig i sin fysiologiska miljö.

Permeabiliteten för ämnen i GFB uttrycks som en silkoeficient (sieving coefficient Θ) dvs. kvoten mellan koncentrationen av ämnet i primär urin och plasma. Med hjälp av en surrogatmolekyl Ficoll_{70A}, (märkt med fluorescerande markör) studerar vi fraktionellt clearance av molekylen till urin, vilket är det samma som den över GFB (den s.k. sievingkoefficienten). En välutvecklad mätningsmetod med HPLC-teknik ger oss möjlighet att detektera små mängder av surrogatmolekylen i urin. Kompletterande matematisk analys med uträkning av porfördelningen över GFB ger möjlighet att klarlägga komplexiteten i glomerulär filtrets reaktion. Experiment utförs på sövd Sprague-Dawley råttor där först en tillgång till råttans blodkärl anbringas för blodprovstagning samt tillförsel av testmedel. I råttans vänster urinledare (uretären) sattes en kateter för urinsamling. Efter 20 minuters viloperiod tas blod och urin prover för uträkning av basal sievingkoefficient och GFR. Därefter ges ett testmedel i råttans blodkärl som infusion eller så görs en avstängning av råttans vänstra urinledare. Blod och urin prover för uträkning av silkoefiient för surrogatmolekyl (FITC Ficoll_{70A}) tas 5, 15 och 30 min efter testmedlets infusionsstart eller efter att uretärobstruktion frisläppts.

I den första studien (Study I) undersöktes om oxidativ stress kan påverka njurfiltrets genomsläpplighet. Vi sänkte biotillgänglighet av NO genom blockering av dess produktion via NO-syntas. I samband med sänkt biotillgänglighet av NO såg vi en övergående ökning av permeabilitet i GFB inom loppet av 30 minuter. Permeabilitet av njurfilter var helt återställd vid samtidigt behandling med Tempol, en borttagbare av skadliga oxidativa ämnen eller vid tillförsel av cyklisk GMP, en intracellulär förmedlare av NO-effekter. Vår data talar för att NO-systemet är involverat i regleringen av genomsläpplighet i glomerulär filtret.

I den andra studien (Study II) undersöktes om akuta permeabilitets förändringar i GFB föreligger vid uretär obstruktion, och i ett separat uppsättnings försök, huruvida oxidativ stress orsakar dessa permeabilitetsförändringar. Vi såg en tydlig permeabilites ökning i GFB efter 120 min av uretär obstruktion som var orsakad av oxidativ stress. Däremot sågs tecken på strukturell skada av njurens filter efter 180 min av uretär obstruktion.

I den tredje studien (Study III) undersöktes om Endothelin-1, ett potent kärlsammandragande ämne, är involverat i regleringen av GFB genomsläpplighet *in vivo* och via vilka receptorer dessa förändringar sker. Studien visade att Endotelin ökar övergående permeabilitet av GFB och effekten förmedlas via ET_A receptorer.

I studie nummer fyra (Study IV) studerar vi om Angiotensin II-utlöst hyperpermeabilitet över GFB förmedlas via TRPC5/TRPC6 jon kanaler *in vivo*. Vår data visar att effekten förmedlas via bägge receptorerna, dock fanns det ingen påverkan på systemiskt blodtryck vid blockering av TRPC5 receptorer.

Vår samlade data i Studie I, III-IV talar för att det föreligger en övergående, dynamisk permeabilitets ökning över GFB vid Angiotensin II, Endotelin samt oxidativ påverkan. Effekten förmedlas via olika intracellulära signalvägar som dock verkar ha ett gemensamt mål med påverkan på reorganisation av cytoskelettet i glomerulära celler. Således, förutom podocyter och endotelceller skulle mesangialceller kunna delta i GFB permeabilitets reglering. Rollen av TRPC5 kanaler i permeabilitetsregleringen av GFB bör kartläggas vidare med både experimentella och kliniska studier

Introduction

Proteinuria is a hallmark of kidney disease

Proteinuria is a well-known contributory cause of renal failure and the development of kidney injury that requires treatment (Gansevoort et al., 2011; Iseki et al., 2003). According to the Swedish Renal Registry, at the start of 2018, there were 9,918 renal patients (a prevalence of 980 per million population) who underwent some form of active treatment for uraemia such as dialysis or a kidney transplant. Mortality in this group of patients is higher than in the general population and is 2.9% among kidney transplant patients and 18.8% among those on dialysis.

The rate of progression of the impairment of kidney function is determined by the degree of tubulointerstitial injury in the renal tissue. Proteinuria induces a large number of cellular and chemotoxic reactions in the interstitium, which lead to inflammation, with the development of accompanying fibrosis and atrophy of the renal tubuli (Abbate et al., 2006; Eddy, 2004). In modern clinical practice, the majority of proteinuric renal diseases are treated using causal therapy such as immunosuppressive therapy in, for example, systemic vasculitis, membranoproliferative glomerulonephritis or proteinuric states secondary to diabetes, cardiovascular disease or myeloma. Angiotensin converting enzyme inhibitors (ACE inhibitors) and/or angiotensin receptor blockers (ARBs) are often involved in the treatment of proteinuric renal diseases, which have well-known anti-proteinuric and antihypertensive effects. ACE inhibitors and ARBs dilate the efferent arteriole in glomeruli to a greater extent than the afferent and thereby have an impact on intrarenal hemodynamics and impair the kidney's autoregulation, i.e. its ability to maintain a constant GFR despite variations in systemic blood pressure. Consequently, in conditions where there is a simultaneous presence of low blood volume as a result of, for example, sepsis, vomiting, haemorrhage or diarrhoea, simultaneous treatment with ACE inhibitors/ARBs can lead to the development of acute kidney injury (AKI), especially among patients with underlying chronic kidney injury where the ability to autoregulate is commonly impaired. The presence of AKI among intensive care unit patients increases their mortality by 30% (McCarthy, 1996). Mortality is also higher than average among generally ill hospitalised patients with newly developed AKI. In addition, treatment with ACE inhibitors/ARBs may be contraindicated in patients with normal or low blood pressure among whom symptomatic hypotension may occur.

Accordingly, there is a clear need to develop new medications with an antiproteinuric effect that do not have an impact on intrarenal hemodynamics or systemic blood pressure. Gaining a better understanding of the physiological mechanisms that give rise to proteinuria creates the potential to develop new antiproteinuric drugs.

The kidney

The kidneys are paired, bean-shaped retroperitoneal organs that lie alongside the spine at the level of the T12–L3 vertebrae, with the left kidney normally being slightly higher than the right. A healthy kidney is approximately 11–12 cm long and weighs around 150–160 g.

The kidneys perform several important functions in the body, including filtration and excretion of metabolic waste products (urea and ammonium), regulation of the electrolyte balance, fluid balance and acid-base balance, and stimulation of erythrocyte production. They participate in the regulation of blood pressure via the renin-angiotensin-aldosterone system, control reabsorption of water and maintain intravascular volume and blood pressure. They regulate skeletal metabolism through the activation of vitamin D.

The functional unit of the kidney is the nephron. Humans are born with approximately one million nephrons per kidney that do not have the ability to be repaired. Consequently, humans do not create any new nephrons during their lifetime and the loss of nephrons thus leads in the long term to a permanent reduction in GFR and the development of chronic kidney injury. Plasma is filtered in the nephron across the glomerular capillary wall, the layers of which constitute what is known as the glomerular filtration barrier (GFB), which is permeable to water and salts, but has a very low permeability to large plasma proteins, especially for albumin and other protein molecules that are larger than albumin, for example immunoglobulins. Approximately 180 litres of plasma is filtered through the kidneys each day and forms what is known as primary urine that is processed and fine-tuned via a well-developed system of tubuli into circa 1.5 litres of secondary urine per 24 hours in healthy individuals. The kidney's filtration and reabsorption processes require adequate blood flow, which is reflected in the complexity of the kidneys' vascular anatomy. The blood supply to the kidneys comprises 20 % of cardiac output at rest, the majority of the oxygen content of which remains unused, and the arteriovenous oxygen difference (difference in partial pressure of oxygen pO_2 between venous and arterial blood) is lower than in any other organ in the body.

The glomerular filtration barrier

The endothelial layer consists of unique flat fenestrated endothelial cells that are approximately 60–80 nm in size and can constitute 30–50% of the capillary lumen (Rostgaard & Qvortrup, 1997). Endothelial cells on the interior of the capillary lumen are covered with glycocalyx and glycoproteins (Hjalmarsson et al., 2004) (Figure 1). Glycocalyx is made up of glycosaminoglycan and proteoglycans and has a weak negative charge (Weinbaum et al., 2007). The thickness of the glycocalyx layer varies between different capillary beds.

The glomerular basal membrane (GBM) consists of collagen type IV, heparan sulphate, proteoglycan and glycoproteins such as laminin, nidogen/entactin, agrin and perlecan (Miner, 1999).

The visceral layer of Bowman's capsule consists of specialised visceral epithelial cells – podocytes (VEC). Podocytes are in contact with one another via well-developed foot-like appendages called pedicels that hold onto one another with the aid of a slit diaphragm. The Bowman's space side of the body of the podocytes, pedicels and slit diaphragm are covered with a weakly negatively charged glycocalyx.

A fourth actor, the mesangial cells with surrounding extracellular matrix (the mesangium), has been studied in recent years. The mesangium is not directly included in the structure of the GFB but may have an impact on its permeability characteristics as regards both water in the plasma and substances dissolved in blood plasma. The glomerulus is suspended from the mesangium, a little bit like scaffolding, and this provides the glomerular capillary bundles with robust support for withstanding the high capillary pressure (about 50 mmHg) in the glomerular circulation. The mesangium consists of a matrix that contains type IV collagen and associated proteins such as proteoglycan and two types of cells: stellate cells phagocytic cells. Stellate cells have a cytoskeleton, respond to hormonal stimuli such as angiotensin II and also produce the mesangial matrix. Phagocytic cells participate in the local immune response. Microfibrils run through the mesangial matrix. Microfibrils connect the mesangial cells to the lamina densa in the GBM. In mesangial cells, the microfibrils are connected with F-actin (Mundel et al., 1988).

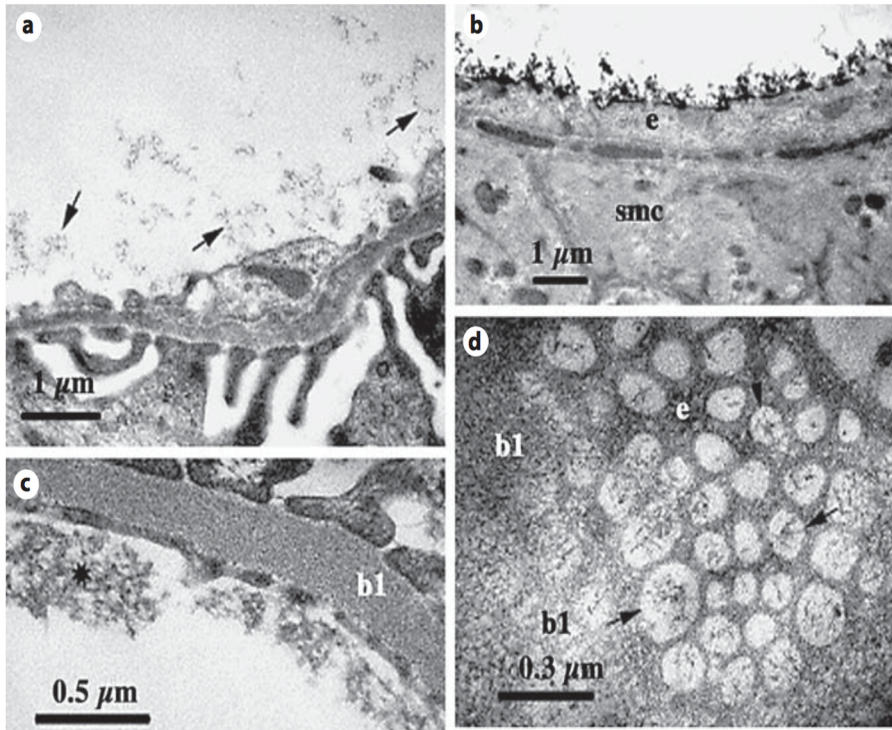


Figure 1. Electron micrographs of the glomerular capillary wall. From Hjalmarsson C, Johansson BR, Haraldsson B: Electron microscopic evaluation of the endothelial surface layer of glomerular capillaries. *Microvascular Research* 2004;67:9–17 (with permission).

Protein transport across the glomerular filtration barrier: theory and current knowledge

Albumin is a monomeric protein that has a negative charge (-22) at physiological pH (pH 7.4). The albumin molecule has a dense structure, having a radius of 35.5 \AA (3.55 nm) and a molecular weight of 66 kDa (Ohlson et al., 2001). In humans, albumin is the most abundant protein in blood plasma, and occurs at a concentration of 40 g/l , whereas only a very small amount, a maximum of 30 mg/24 hours , is present in final urine. Under physiological conditions, the permeability of the glomerular filter to large molecules such as albumin is very low. In the normal state, only about 1 in 10,000 albumin molecules pass across the renal filter into primary urine. With a plasma albumin concentration of 40 g/l , this means that the concentration in Bowman's capsule is only about 4 mg/l . Thus, if 180 liters of primary urine is created per 24 hours, this means that circa $180 \times 4 \text{ mg} = 720 \text{ mg}$ of albumin is filtered. Given that 99% of all filtered albumin is reabsorbed in the

proximal tubuli, only a small amount of albumin (10–30 mg) remains in the secondary urine. For example, in patients with Dent-1 disease (*CLCN5* mutation), having a near complete abolishment (~90%) of proximal tubular reuptake of albumin (but intact glomerular permeability), lose about 560 mg/24h of albumin, corresponding to a urinary albumin-creatinine index of 38 mg/mmol (Edwards et al., 2020).

The permeability of the GFB to substances is commonly expressed as a sieving coefficient (Θ), i.e. the ratio of the concentration of the substances in the Bowman's capsule to that in the plasma. Direct measurements of albumin in Bowman's capsule using micropuncture investigations on rats found a sieving coefficient at the level of 10^{-5} ($\Theta = 0.000080$) (Tojo & Endou, 1992).

The sieving coefficient of molecules of various sizes in the glomerular filter has been subject to very intensive study in recent years (Figure 2). The sieving coefficient values measured differed depending on which model and measurement method was used in the investigation. For example, measurements from animal experiments on rats using the tissue uptake technique show an albumin sieving coefficient of $\Theta = 0.00066$ (Lund et al., 2003), while in cooled isolated perfused kidney (IPK) the albumin sieving coefficient has been measured at $\Theta = 0.0015$ (Ohlson et al., 2000), and in fixed kidney at $\Theta = 0.0087$ (Ciarimboli et al., 1999). In studies using IPK with impaired tubular reabsorption, an albumin sieving coefficient of $\Theta = 0.0080$ has been measured that has risen to $\Theta = 0.080$ during the experimental period (Ciarimboli et al., 1999). The 'albumin retrieval' hypothesis is partly based on these rather high sieving coefficients. This theory proposes that there are two ways of dealing with albumin in the proximal tubuli. One is a well-known mechanism in which proteins are taken up via the megalin/cubilin system (Christensen & Birn, 2001) and degraded to amino acids, which are returned to the circulation. The other mechanism is transcytosis of intact albumin via the proximal tubuli (Comper et al., 2016), which in this hypothesis is presumed to play a major role. Support for a high albumin sieving coefficient was found in studies of healthy individuals who demonstrated high GFB permeability to Ficoll 36 Å, a surrogate polysaccharide probe having the size of albumin (Blouch et al., 1997). However, papers from our laboratory have shown that molecular density and structure, in addition to molecular size, may have significance for permeability characteristics when the molecule approaches a radius of 36 Å (i.e. close to the size of the transport-limiting structures in the renal filter – 'the small pores'). The Ficoll molecule is thus 'softer' than albumin, which may explain its high permeability characteristics at the 36 Å-size compared with the albumin molecule (Asgeirsson et al., 2007). Rising sieving coefficient values for albumin in the IPK model may be explained by the emergence of kidney injury over time, which has an impact on the structural characteristics of the renal filter (Haraldsson et al., 2008).

Accordingly, there is a predominant perception that the sieving coefficient for albumin in the GFB is very low under normal physiological conditions. This is further supported by a measured sieving coefficient for albumin at the level of 10^{-5} in individuals with congenitally impaired tubular reabsorption of proteins (Dent's disease with preserved GFR) (Norden et al., 2001).

The GFB has a strict size-limiting permselectivity with progressively limited permeability for molecules up to the size of albumin (36 Å). Low molecular weight (LMW) molecules, such as α_1 -microglobulin and myeloma light chains, with molecular weights < 30 kDa and molecular radii < 25 Å pass pretty much freely through the GFB and are thus transported primarily by convection (Lund et al., 2003).

The GFB is a barrier to the passage of molecules depending on size (Figure 2), and several theories have been developed in order to describe the transport characteristics of the GFB. The 'fiber matrix theory'. The GFB is represented by fibers with a distinct radius that form a fiber matrix of a certain density (which is described using the parameter $\phi = 1 - \text{void volume}$). The denser the arrangement of fibers (higher ϕ) in the membrane, the more difficult it is for molecules to pass through it (Curry & Michel, 1980). The two-pore theory is based on the assumption that transport across the GFB can be described as that which takes place across an 'equivalent' membrane with two different types of pore (known as pore populations). First, a large population of small pores that, to an increasing extent, impede passage of molecules of sizes greater than 25 Å. In addition, a population of large pores that are rare and through which large molecules such as albumin are lost into primary urine. The size of small pores has been calculated at approximately 35–50 Å and the size of large pores at 80–100 Å (Ohlson et al., 2000). Histologically, there is no corresponding structure in the glomerular filter that would form either the small or the large pores, instead it is endothelial fenestrae and/or slit diaphragm of podocytes or their interaction with each other that may constitute potential structures.

Aside from the significance of molecular size to glomerular permselectivity, discussion has been taking place since 1970 of molecular charge as being a strong contributory factor in the low permselectivity of the GFB to (anionic) plasma proteins. This phenomenon was studied in a seminal paper by Brenner and colleagues (Bohrer et al., 1978). Their study investigated permeability of the glomerular filter to dextran molecules with different charges: negative, neutral and positive charges. Low GFB permeability was demonstrated for a negatively charged dextran molecule (dextran sulphate) (Bohrer et al., 1978). Subsequently, there have been attempts to reproduce Brenner's experiment and these found the same low permselectivity for a similar anionic dextran molecule (Schaeffer Jr et al., 2002). This phenomenon was explained through negatively charged dextran sulphate having the ability to bind to plasma proteins and, to a certain extent, to also be

reabsorbed and degraded in the renal tubuli, which in turn reduced the apparent permeability of the GFB.

The negative anionic charge of the GFB is linked to the heparin sulphate chain, which is included in proteoglycan. Heparan sulphate is found in glycocalyx, which coats the surface of both endothelial cells and podocytes and is also included in agrin and perlecan in the GBM.

Mutated mice that do not have the heparan sulphate chain in perlecan showed no morpho-histological differences in their GBM and did not have proteinuria under physiological conditions (Morita et al., 2005). In the fiber matrix model, some difference has been seen in the permeability of the GFB to anionic and neutral molecules when their size is around 30–40 Å (Haraldsson et al., 2008). In our laboratory, it has also been demonstrated that molecular density and shape may have significance for the permeability of the GFB when approaching a molecular size of 36 Å.

Accordingly, molecular size, structure and charge interact to affect the permeability of the GFB to the molecule when molecular size approaches 30–40 Å. Otherwise, molecular size appears to be the decisive factor influencing the permeability of the GFB to the molecule.

Despite the high permselectivity of the GFB, small quantities of albumin are detected in primary urine. This finding may be explained in part by applying the theoretical two-pore model where large molecules are able, to some extent, to pass through large pores by convective flow (Rippe & Haraldsson, 1987). Convective transport is influenced by the hydrostatic pressure gradient across the membrane. For example, in glomeruli, the efferent arteriole contracts under the influence of angiotensin, which may lead to increased hydrostatic pressure across the GFB. In clinical practice, proteinuria is seen in hypertension. The leaking of protein decreases once treatment with ARBs is started.

In our laboratory, it has been demonstrated that a transient increase in the permeability of the GFB to large molecules (Ficoll 70 Å) takes place under the influence of angiotensin II. However, this effect appears to be independent of the pressure in the glomeruli (Axelsson et al., 2012).

These findings may instead be explained by changes in the permeability of the GFB to large molecules, which may have a cellular component in which cells that have a contractile cytoskeleton appear to be involved.

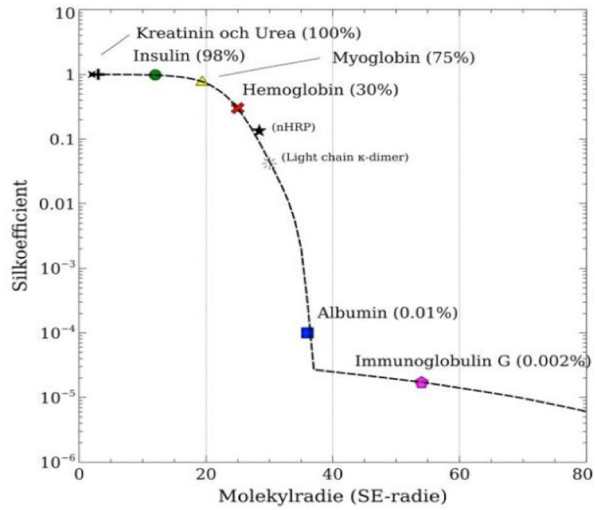


Figure 2. The renal filter restricts molecules based on their molecular size.

The larger the molecule, the lower its glomerular permeability and sieving coefficient (*Swedish* 'Silkoefficient'). Adapted from (Öberg & Rippe, 2014).

Aims of the thesis

Paper I

The purpose of Paper I is to investigate if intercellular NO-signaling is involved in the regulation of GFB permeability *in vivo*, Is the permeability over the GFB affected by lowered bioavailability for NO?

Paper II

It is well established that ureteral obstruction evokes tubular proteinuria. The purpose of Paper II is to investigate whether there is also changes in glomerular permeability following ureteral obstruction and, in a separate set of trials, if the ROS system is involved in such changes.

Paper III

Angiotensin II increases the permeability over GFB. Here, I investigated if endothelin-1, another potent vasoconstrictor, is involved in the regulation of GFB permeability *in vivo*. By application of selective blockers of ET-1 receptor A and B, it is also possible to elucidate through which receptor such changes may occur.

Paper IV

The purpose of study IV is to elucidate whether the effects of angiotensin II on glomerular permeability are dependent on signaling via TRPC5/TRPC6 ion channels *in vivo*.

Methods

Laboratory animals and experimental protocols

Animals

The experimental studies in this thesis were performed in either male Wistar rats or male Sprague-Dawley rats. The rats had free access to water and standard chow until the day of the experiment. The Malmö/Lund Committee for Animal Experiment Ethics approved of the experiments.

Surgery

Induction of anaesthesia was accomplished by an intraperitoneal injection of pentobarbital sodium (90mg/kg) and maintained during the experimental period by repeated (i.a.) injections of the same drug via the tail artery. Body temperature was kept at 37°C using a thermostatically controlled heating pad. To facilitate breathing a tracheotomy was performed. The tail artery was cannulated (PE-50 cannula) for continuous monitoring of mean arterial blood pressure (MAP) and registration of heart rate (HR) (MP 150 system, with AcqKnowledge from MAC, Biopac System), and for maintenance of anaesthesia. The left carotid artery was cannulated for blood sampling and the left jugular vein for infusion purposes (PE-50 cannulas). The left ureter was firstly exposed by a small incision in the abdominal wall and then cannulated (PE-10 cannula) for urine sampling. Furosemide (Furosemide, Recip, 0.375 mg/kg body weight) was administered in the tail artery to temporarily increase urine flow in order to facilitate the cannulation of the ureter. Animals had a resting period (20min) after surgery. After the experimental period, animals were euthanized with an over-dose of KCl intravenously under deep anaesthesia.

Experimental protocols

We did not utilize SHAM-animals. Instead, each animal was their own control in which longitudinal samples after interventions were compared to baseline samples. Baseline samples of blood and urine were taken at the end of the resting period (at time 0) to determine the baseline sieving coefficients (θ) to Ficoll.

Paper I

A competitive eNOS inhibitor N-nitro-L-arginine methyl ester hydrochloride (L-NAME) was administered to the animals as an initial bolus ($470 \mu\text{g kg}^{-1}$) followed by a continuous intravenous infusion ($93 \mu\text{g kg}^{-1} \text{min}^{-1}$). Urine and blood samples for the determination of glomerular sieving coefficients (θ) of Ficoll were obtained at 5, 15, 30 min, and in L-NAME arm also at 60 and 120 min. To elucidate the underlying mechanisms of the L-NAME effect on glomerular permeability, we tested various substances such as Tempol (a ROS scavenger), L-arginine (substrate for NOS), DEA-NONOate (a potent NO-donor) and 8-bromo-cGMP (a cyclic GMP analogue):

1. In the Tempol–L-NAME group the SOD mimetic compound 4-hydroxy-tempo (Tempol) was started 5 min before the start of L-NAME infusion, the Tempol-infusion continuing throughout the experiment at $1 \text{ mg kg}^{-1} \text{min}^{-1}$ together with L-NAME.
2. In the L-Arginine–L-Name group, L-2-Amino-5-guanidino-n-valerianic acid (L-arginine) was given in a bolus dose (1.56 mg kg^{-1}) followed by a continuous infusion of $470 \mu\text{g kg}^{-1} \text{min}^{-1}$. Animals were pre-treated with L-arginine during 30 min before the start of the L-NAME infusion and thus received L-arginine throughout the experiment.
3. In the DEA-NONOate–L-NAME group, Diethylamine-NONOate (DEA-NONOate). was infused together with L-NAME at a rate on $0.65 \mu\text{g kg}^{-1} \text{min}^{-1}$.
4. Lastly, in the 8-Bromo-cGMP–L-Name group, 8-Bromoguanosine 3',5'-cyclic monophosphate was tested in two doses. This two groups of animals received 8-bromo-cGMP firstly as a bolus ($38.91 \mu\text{g kg}^{-1}$ and $77.82 \mu\text{g kg}^{-1}$ respectively) which was followed by continuous infusion ($38.91 \mu\text{g kg}^{-1} \text{min}^{-1}$ and $77.82 \mu\text{g kg}^{-1} \text{min}^{-1}$ respectively) 5 minutes before the start of the L-NAME infusion.

Paper II

A left ureter obstruction was established using a thin rubber band. After either 120- or 180-min, the obstruction was carefully released and measurements of GFR, sieving coefficients to Ficoll, mean arterial pressure (MAP), and heart rate (HR) were obtained at 5, 15 and 30 min.

In the 120-min UUO arm, the rats were divided into two groups: UUO only and UUO-Tempol group. In the UUO-Tempol group, the superoxide $\text{O}_2\cdot$ scavenger Tempol (Sigma-Aldrich, St. Louis, MO) was given as a continuous infusion ($1.0 \text{ mg kg}^{-1} \text{min}^{-1}$ iv) starting directly after ureteral obstruction.

In the 180-min UUO group, animals were divided into four groups:

- UUO only group
- UUO–Tempol group, the SOD mimetic compound, 4-hydroxy-tempo was started directly after ureteral obstruction at $1.0 \text{ mg kg}^{-1} \text{ min}^{-1}$ continuously.
- UUO–RAC1i group and UUO–RHOi groups: Inhibitors of small GTPases, RHOi (Y-27632; Mitsubishi Pharma, Osaka, Japan) and RAC1i (NSC-23766, Calbiochem, San Diego, CA), were given as an intravenous bolus (RHOi bolus of $15 \mu\text{g}$; and RAC1i bolus of $12.5 \mu\text{g}$) followed by continuous infusion (RHOi: $8.9 \mu\text{g kg}^{-1} \text{ min}^{-1}$ iv and RAC1i: $9.3 \mu\text{g kg}^{-1} \text{ min}^{-1}$ iv).

Paper III

A non-pressor dose of ET-1 (Sigma-Aldrich, St. Louis, MO) was administered as a bolus ($0.41 \mu\text{g} \cdot \text{kg}^{-1}$, $166 \text{ pmol} \cdot \text{kg}^{-1}$) followed by a continuous infusion ($0.14 \mu\text{g kg}^{-1} \text{ min}^{-1}$, $55 \text{ pmol} \cdot \text{kg}^{-1} \cdot \text{min}^{-1}$). In two experimental groups, equimolar doses (200 nmol/kg) of the ET_A receptor antagonist JKC-301 (Sigma-Aldrich) or the ET_B receptor antagonist BQ-788 (Sigma-Aldrich) were given before the administration of the non-pressor dose of ET-1.

Paper IV

Glomerular hyperpermeability was induced by a bolus dose ($160 \text{ ng} \cdot \text{kg}^{-1}$) of angiotensin II followed by an iv infusion ($80 \text{ ng} \cdot \text{kg}^{-1} \cdot \text{min}^{-1}$). The animals were divided into 5 different experimental groups: Ang II only, Ang II+Hi La₃⁺, Ang II + Lo La₃⁺, AngII+clemizole and Ang II + Low La₃⁺ + clemizole. In the AngII+La₃⁺ groups, lanthanum(III)chloride heptahydrate (Sigma-Aldrich, St. Louis, MO) was given as an iv bolus dose (18 mg kg^{-1} for Hi; 3 mg kg^{-1} for Lo) followed by a continuous infusion ($220 \text{ mg kg}^{-1} \text{ min}^{-1}$ iv for Hi; $60 \text{ mg kg}^{-1} \text{ min}^{-1}$ for Lo).

For the AngII+TRPC5i group, we used clemizole, a potent TRPC5 inhibitor Clemizole (Sigma-Aldrich, St. Louis, MO), was administered a bolus dose (0.4 mg kg^{-1} iv) and a continuous infusion ($24 \mu\text{g kg}^{-1} \text{ min}^{-1}$).

Urine and blood samples for determination of sieving coefficients (θ) to Ficoll and GFR and measurements for HR, MAP were obtained at 5, 15, 30 min. Serum concentrations of La₃⁺ were assessed by means of inductively coupled mass spectrometry (ICP-MS) on a Perkin Elmer Optima 8300 (Perkin Elmer Instruments, Shelton, CT).

Molecular probe and determination of proteinuria

In order to study the permeability of the GFB, we have used a polydisperse probe molecule that provides a wide range of molecular sizes whose different permeabilities characterize the permselectivity of the glomerular filter. Ficoll is a cross-linked polysaccharide that has a spherical shape and a radius of approximately 15–100 Å. In spite of its cross links, which make the molecule more rigid than dextran, for example, the molecule is somewhat flexible and able to change structure slightly, and has a neutral charge at neutral pH. Ficoll passes through the GFB but is not affected by tubuli. Consequently, it is possible to assume that the fractional clearance of Ficoll from the plasma to secondary urine is identical to its fractional clearance from plasma to primary urine (i.e. the glomerular sieving coefficient).

Two different molecular weights have been used in the experiments, 70 kDa and 400 kDa, and they were labelled with a small fluorescent molecule (fluorescein isothiocyanate, FITC). Prior to any interventions, FITC-Ficoll_{70Å} (10 mg/ml) and FITC-Ficoll_{400Å} (10 mg/ml) were administered to the animal as an i.v. bolus (40 µg and 960 µg) at the beginning of the resting period. This was followed by a continuous i.v. infusion of the mixture of FITC-Ficoll_{70Å}/Ficoll_{400Å} at a ratio of 1:24 and an infusion rate of 10 ml/kg⁻¹/h⁻¹ during the resting period and throughout the rest of the experiments. The concentration of FITC-Ficoll in plasma and urine samples was assessed using high-pressure size exclusion chromatography (HPSEC) followed by fluorescence detection (Waters).

Determination of the glomerular sieving coefficient

The sieving coefficients for Ficolls were calculated as their fractional clearances:

$$\theta = \frac{C_u F C_p \text{In}}{C_p F C_u \text{In}}$$

Thus, the glomerular sieving coefficient values for Ficoll are calculated by dividing the concentration of Ficoll in primary urine ($C_u F$) by the average concentration of Ficoll in plasma ($C_p F$). The concentration of Ficoll in primary urine is obtained by dividing the (final) concentration of Ficoll in urine ($C_u F$) by the final ratio between the concentration of inulin in the urine and the plasma ($C_u \text{In} / C_p \text{In}$). The sieving coefficient for Ficoll_{70Å} is a measure of increased protein loss via large pores according to the theoretical two-pore model of glomerular transport.

Glomerular filtration rate estimation

To determine the GFR we used both radiolabelled chromium-EDTA (51Cr-EDTA 0.3 MBq/ml) and fluorescein-labelled inulin (FITC-inulin 10 mg/ml). Both probes were administered as a bolus at a dose of 0.3 MBq and 500 µg at the beginning of the resting period and continued to be administered at an infusion rate of 10 ml/kg-

1/h-1 during the resting period and throughout the rest of the experiments. The concentration of FITC-inulin in plasma and urine samples was measured by fluorescence detection. The radioactivity (51Cr-EDTA) of blood and urine samples was detected using a gamma counter. When determining the fluorescence of the FITC-inulin, the measurement error is close to 10%, which is why GFR was mainly determined using the radiolabelled chromium-EDTA. Clearance of inulin and 51Cr-EDTA from plasma to urine is used in order to assess the GFR and is calculated from

$$\text{GFR} = \frac{C_u V_u}{C_p}$$

where C_u represents the concentration of 51Cr-EDTA or inulin in the urine, V_u represents the flow of urine (ml/min) and C_p is the plasma concentration of 51Cr-EDTA or inulin.

Two-pore analysis and transport physiology

The transport of water and solute matter across a semipermeable membrane does not generally occur at the same rate. Two types of hindered solute transport across a semipermeable membrane have been described: restricted diffusion (i.e. dependent on the concentration gradient) (A/A_0) and restricted convection ($1-\sigma$) (Renkin, 1954). Mason et al. (Mason et al., 1980) developed a pore model based on a permeability hindrance factor λ , which is calculated as the ratio between molecular size in SE (a_e) and pore size (r_p)

$$\lambda = \frac{A_e}{R_p}$$

λ the value can thus be between 1 and 0, i.e. $\lambda = 1$ indicates a total barrier to the passage of molecules. The hindrance factor for diffusive transport (between 0 and 1) is

$$\frac{A}{A_0} = \frac{(1-\lambda)^{9/2}}{1-0,3956\lambda+1,0616\lambda^2}$$

The corresponding hindrance factor for convective transport (between 0 and 1) is

$$(1-\sigma) = \frac{(1-\lambda)^2 [2-(1-\lambda)^2] (1-\frac{\lambda}{3})}{1-\frac{\lambda}{3} + \frac{2}{3\lambda^2}}$$

On the basis of irreversible thermodynamics, equations have been derived for the transport of water (J_v) and molecules (solutes) (J_s) across a semipermeable membrane (Kedem & Katchalsky, 1958; Kedem & Katchalsky, 1961). For water transport:

$$J_v = L_p S (\Delta P - \sigma \Delta \pi)$$

Here, $L_p S$ is the hydraulic conductance, which reflects how easily water passes through the membrane; ΔP is the transmembrane hydrostatic pressure gradient; σ is the membrane's osmotic reflection coefficient with respect to the osmotically active substance; and $\Delta \pi$ is the transvascular osmotic pressure gradient. Similarly, for solute transport:

$$J_s = J_v (1 - \sigma) \bar{C} + PS \Delta C$$

Here J_v is the flow of water across the membrane; $(1 - \sigma)$ is the hindrance factor for convective solute transport; \bar{C} is the transmembrane solute concentration gradient; ΔC is the transmembrane solute gradient, i.e. the gradient between the concentration of solutes in the plasma and in Bowman's capsule ($C_p - C_{bk}$).

Lastly, PS is the permeability surface area product, which determines the capacity for diffusion and is a measure of hindrance to diffusive transport. PS is calculated using the following formula

$$PS = \frac{A}{A_0} D \frac{A_0}{\Delta x}$$

where D is the diffusion coefficient, $\frac{A_0}{\Delta x}$ is the ratio between the area of the diffusion surface (A_0) and the thickness of the membrane (Δx).

In summary, it is possible to describe transport across the membrane as follows:

- Water transport is the sum of two flows: the flow due to the hydrostatic pressure gradient, with L_p as the coefficient, and the flow due to osmotic pressure, with $L_p S \times \sigma$ as the coefficient. The product $L_p S \times \sigma$ is also called osmotic conductance (Martus et al., 2020).
- Solute transport is in turn the sum of the flow due to convection, with $(1 - \sigma)$ as the hindrance factor, and flow due to diffusion, with the coefficient PS (where A/A_0 is included as the hindrance factor).

Glomerular clearance

To calculate the clearance of a certain substance (CL) across the renal filter, solute transport (J_s) has to be divided by the concentration of this substance in plasma.

$$CL = \frac{\text{solute transport (mmol/min)}}{\text{plasma concentration (mmol/ml)}}$$

To calculate the sieving coefficient (Θ) for a certain substance, the clearance is divided by the GFR.

$$\Theta = \frac{CL}{GFR}$$

and thus, if the glomerular clearance is identical to GFR, the sieving coefficient equals unity. The hindrance factor for the sieving coefficient (Θ) is therefore dependent exclusively on $\lambda = \frac{Ae}{Rp}$. Because the solute flow across the renal filter can be calculated as the concentration in Bowman's capsule multiplied by the GFR, we can re-arrange the above equation to

$$\Theta = \frac{\text{Bowman's capsule concentration}}{\text{plasma concentration}}$$

In studies of the sieving coefficient of the GFB for molecules of various sizes, a steep part (cut-off) is seen in the curve, which corresponds to molecular sizes of 36–40 Å (Lund et al., 2003). Molecules with a small molecular size (< 20 Å) pass freely across the GFB and it is thus not possible for a concentration gradient to develop across the GFB for LMW molecules, with these molecules instead being transported primarily by convective transport. When the molecules become larger, the formation of a concentration gradient occur as the membrane presents more hindrance to solute transport and diffusive transport thus becomes increasingly important. At the same time, large molecules have a worse ability to be transported by diffusion because they are 'heavy'; in other words, the diffusion coefficient, D , in Fick's law

Diffusive flow = $D \times$ concentration gradient

becomes lower. Molecular transport through small pores appears to have ceased when molecular size has approached 36-37 Å and $\lambda = 1$, i.e. when molecular size approaches the pore radius. However, it is known that small quantities of albumin are present in urine. This phenomenon can be explained by the fact that the renal filter also contains large pores, according to the theoretical two-pore model produced by Rippe et al. (Rippe & Haraldsson, 1987). According to the two-pore model, there are two populations of pores; small pores with a radius of 37.5 Å and rare large pores with a radius of approximately 110 Å. Solute transport via small pores takes place about 40% by diffusion and, when the filtration rate is rising, occurs mostly by convection. Solute transport via large pores takes place mostly via convection. There are however very few large pores, which is why there is only a small quantity of albumin in primary urine.

In terms of the distributed two-pore model (Öberg & Rippe, 2014), calculations for the following have been produced in our work:

r_s – the radius of small pores

s_s – the spread of the small pore size distribution

r_L – the radius of large pores

s_L – the spread of the small pore size distribution

α_L – fractional hydraulic conductance via large pores. Reflects the number of large pores.

α_L is calculated with the aid of fractional GFR via large pores (J_{vL}/GFR) according to the following formula:

$$\alpha_L = \frac{J_{vL}/GFR}{\frac{\Delta\pi}{P_{UF}}(1-\sigma_L)+1}$$

Accordingly, the fractional hydraulic conductance through large pores (α_L) is always lower than the fractional GFR through large pores. If the membrane consisted of only one pore size, r_L , the following would instead have applied $\alpha_L = J_{vL}/GFR$.

Statistical analysis

The choice of non-parametric methods in the present articles is due to a low number of observations and hence an increased risk for a lack of normal distribution in the data. Also, in unfortunate cases single points of extreme (but valid) data can confer a false significance between groups (type I error). Thus, non-parametric tests are more robust in scenarios with small groups. Measurements were performed repeatedly in the same animals, therefore statistical tests for paired measurements were used. The collected data is longitudinal, i.e. reflects the effect change over time. We also have various treatments in our studies, and are in Study II-IV using non-parametric multiple analysis of variance for several groups. This statistical method gives the possibility to test the effects of time and treatment separately, and for potential interaction (time \times treatment) between the groups. The main rationale is to assess whether or not an observed effect is due to the treatment. If there is an effect from the treatment we expect it to express itself as an interaction, since all animals (including treated animals) should have the same baseline (time 0). Statistical calculations in Study II-IV were performed using R 3.5.1 for macOS (The R Foundation for Statistical Computing). Statistical calculations in Study I were made using IBM SPSS Statistics 20.0 for Windows (SPSS, Chicago, IL). Values are presented as means \pm SE. Significance levels were set at * $P < 0.05$, ** $P < 0.01$, *** $P < 0.001$.

Paper I

Differences among experimental groups were tested using nonparametric analysis of variance with the Kruskal-Wallis test. Post-hoc tests were performed using Mann-Whitney U-tests.

Paper II

Main and interaction effects (time \times treatment) were assessed using a nonparametric factorial omnibus test as provided in the nparLD package (version 2.1) for R (version 3.4.0, The R Foundation for Statistical Computing) giving a nonparametric ANOVA-like test. In the presence of significant main effects without interactions, *post hoc* testing was performed using either a Friedman test (for time main effects) or a Kruskal-Wallis test (for treatment main effects) followed by pairwise comparisons using either a Wilcoxon-Nemenyi-McDonald-Thompson test (for Friedman) or Wilcoxon tests (for Kruskal-Wallis) when appropriate. Significant interactions were tested using a 2×2 -factorial design (using the nparLD package). Holm-Bonferroni corrections for multiple comparisons were made when applicable.

Paper III

Friedman tests were assessed to determine differences between samples taken at the different time points. In the case of significant omnibus test, *post hoc* testing was performed using a Wilcoxon-Nemenyi-McDonald-Thompson test. *Post hoc* nonparametric 2x2 ANOVA was performed using the nparLD package for R.

Paper IV

Differences were assessed using an ANOVA on aligned rank transformed data (using ARTool version 0.10.5). Bonferroni corrections for multiple comparisons were made.

Results

Study I

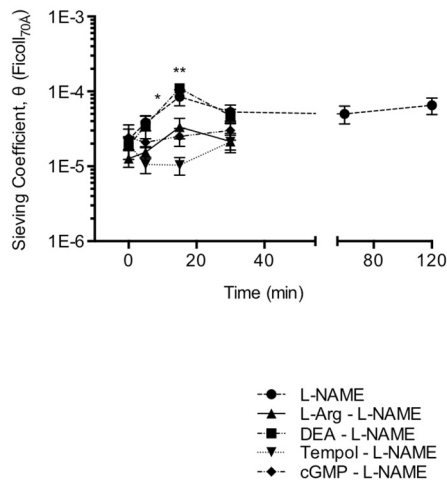


Figure 3 Ficoll 70 Å sieving coefficients as a function of time during eNOS inhibition (L-NAME)

The bioavailability of endogenous NO was reduced by L-NAME, an eNOS-blocker which induced marked glomerular hyperpermeability, which was ameliorated by ROS-scavenger Tempol, a cyclic GMP analogue (cGMP) and L-arginine (substrate for NO production by eNOS).

An increased permeability of GFB to FITC-Ficoll 70Å was observed with decreased bioavailability of NO (Figure 3). The barrier was restored during treatment with ROS scavenger Tempol, and in part also by co-administration of L-arginine and secondary intracellular messenger cyclic GMP (analogue).

Study II

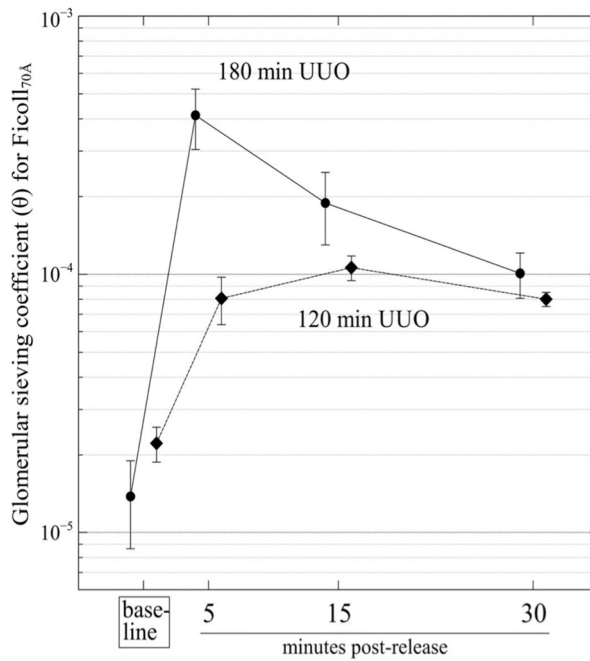


Figure 4 Sieving coefficients for Ficoll 70 A at baseline, 5, 15 and 30 min post-release of UUO
Unilateral ureteral obstruction (UUO) evoked marked glomerular hyperpermeability, both after 120 and 180 minutes.

A unilateral ureteral obstruction (UUO) was applied. First, marked permeability changes in GFB were observed after 120 min of obstruction which became more pronounced after 180 min of obstruction.

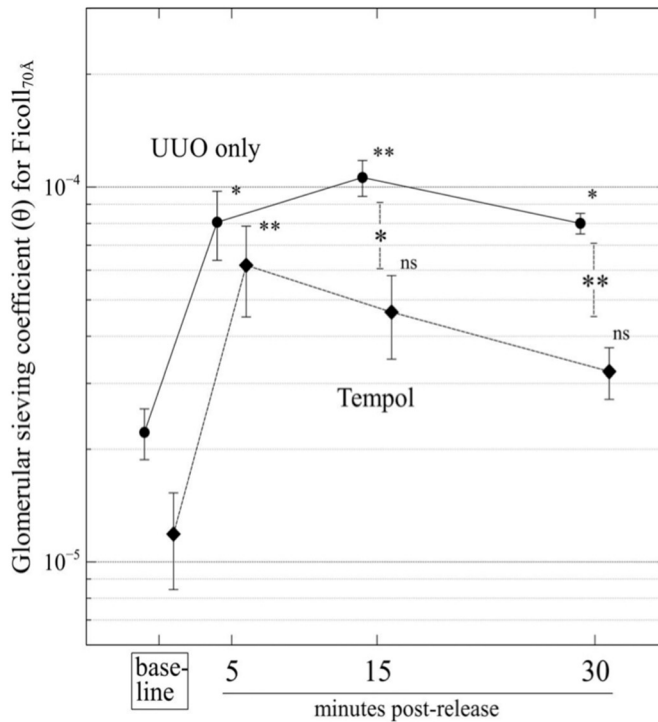


Figure 5. Sieving coefficients for Ficoll 70 Å at baseline, 5, 15 and 30 min post-release of 120 min UUU. 120 min unilateral ureteral obstruction was partly ameliorated by ROS scavenger Tempol.

The increase in permeability of the GFB after 120 min urinary obstruction was ameliorated by administration of ROS scavenger Tempol. By contrast, treatment with ROS scavenger Tempol, e-NOS inhibition (L-NAME) or intervention on RaC-1 / RoA systems could not counteract the permeability increase in GFB for FITC-Ficoll70Å after 180 min ureteral obstruction. Complementary pore analysis modelling also showed signs of structural filter damage with impact on small pore size as well as its distribution.

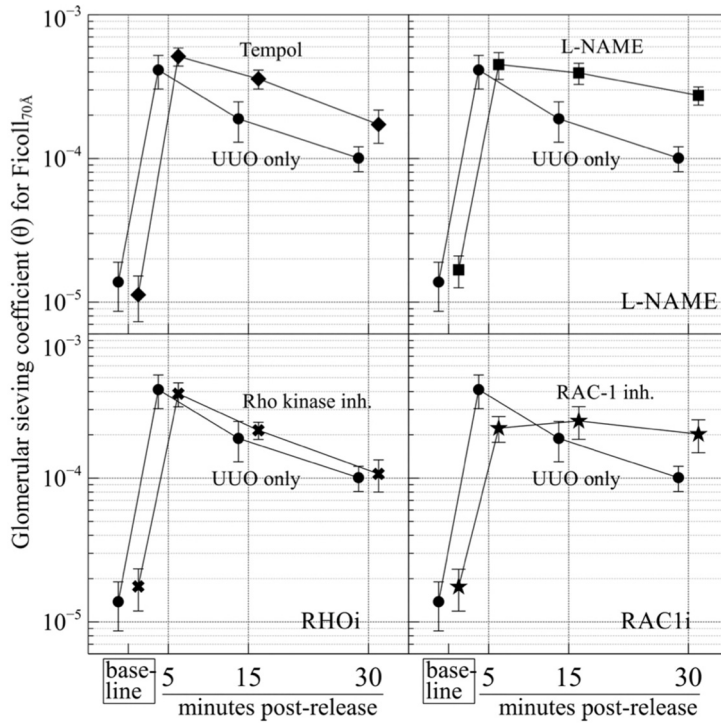


Figure 6. Glomerular sieving coefficients for 70 Å Ficoll as a function of time (baseline and 5, 15, and 30 min after release of ureteral obstruction).

180-min UUO alone (filled circle), 180-min UUO with treatment using either Tempol (rhombus), Rac-1 inhibition (RAC1i), Rho kinase inhibition (RHOi), or endothelial NOS inhibition (eNOSi).

Study III

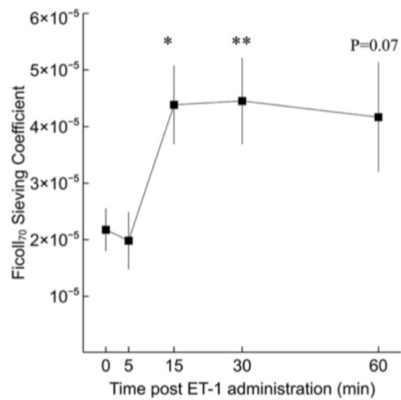


Figure 7. Glomerular sieving coefficients for 70 Å Ficoll as a function of time (baseline and 5, 15, 30 and 60 min start of ET-1 administration).

Systemic endothelin-1 evoked sustained, delayed but small increments in glomerular permeability to 70 Å Ficoll (Figure 7). The observed increments in glomerular permeability were mitigated after use of Endothelin receptor A blockers but not Endothelin B receptor blockers (Figure 8).

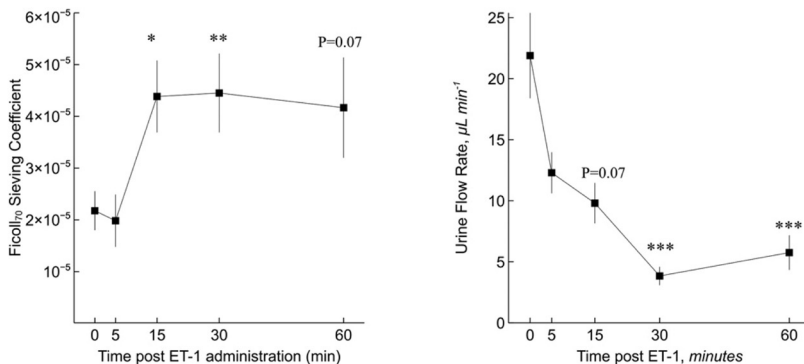


Figure 8. Glomerular sieving coefficients for 70 Å Ficoll as a function of time (baseline and 5, 15, 30 and 60 min start of ET-1 administration).

Study IV

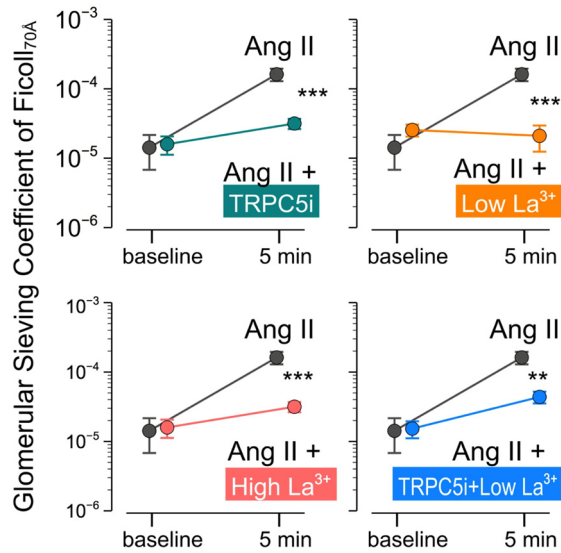


Figure 9. Glomerular sieving coefficients of Ficoll 70 Å after administration of angiotensin II and inhibitors of TRPC5/6.

It is well established that angiotensin II leads to glomerular hyperpermeability. Here we used TRPC5 channel blocker (Clemizole), low concentration of Lantan salt (activates TRPC5 / blocks TRPC6) and high concentration Lantan salt infusion (dual TRPC6 / TRPC5 blockade), and combined treatment with low concentration La³⁺ and clemizole. Whereas all of these interventions appeared to ameliorate angiotensin-induced permeability increase in GFB. TRPC6 channel blockers appear to have both an effect on proteinuria and blood pressure (see Paper IV).

Discussion

ROS (reactive oxygen species) have attracted attention in the past 20 years and are presumed to play a central role as both intercellular and intracellular signalling molecules. It has also been established that nitric oxide (NO) plays an important role in the management of oxidative stress, influences vascular permeability, counteracts thrombocyte/leukocyte aggregation and their adherence to the vascular wall, counteracts cell proliferation, mediates vasodilation and relaxation of smooth muscle cells. In recent years, evidence has been obtained that excess NO may favour the production of ROS through the formation of peroxynitrite radicals (ONOO⁻) (Bendall et al., 2005) and has a negative impact on several biochemical processes through nitrosation of proteins and lipids (Sánchez et al., 2013). Peroxynitrite radicals (ONOO⁻) may also have an impact on DNA. Consequently, the collected data suggest there is a duality to the physiological effects of NO where the quantity of NO and also its origin is able to tip the scales in the opposite direction. In light of this, we would like to study the role of NO in the regulation of GFB permeability *in vivo*.

NO is produced by intracellular NO synthase (NOS). There are three types of NOS:

Type 1 Neurogenic NOS (n-NOS/b-NOS), is found in the central nervous system, cardiomyocytes, the placenta, tubular epithelial cells and, according to some sources, also in the mesangium. May be activated via the Ca-calmodulin complex.

Type 2 inducible NOS (i-NOS), can be induced in many tissues, macrophages, cytokines, liposaccharides may induce i-NOS up-regulation. Inducible NOS is not inhibited by increased NO production.

Type 3 Endothelial NOS (e-NOS), is found primarily in endothelial cells, and in the kidney, e-NOS is seen in both the cortex and the medulla but also has some prevalence in the renal medulla. E-NOS is up-regulated in conjunction with shear stress, under the influence of Ca-calmodulin, but is inhibited by caveolin. E-NOS is also able to transition to a decoupled conformation that is able to produce ROS (ONOO⁻) (Alderton et al., 2001).

In Study I, the bioavailability of endogenous NO was reduced using an infusion of e-NOS inhibitor (L-NAME). A clear increase in the permeability of GFB to FITC-Ficoll 70 Å was observed when the bioavailability of NO was reduced. The barrier was reinstated when treated with the ROS scavenger Tempol and cyclic GMP.

Consequently, reduced bioavailability of NO affects the permeability of the GFB. This effect is mediated through the activation of the sGC-cGMP signalling pathway. Our data show that the balance between ROS and NO contributes to the permeability characteristics of the glomerular filter in vivo. The intracellular effects of atrial natriuretic peptide (ANP) and carbon monoxide (CO) are also mediated through the GC-cGMP signalling pathway.

In earlier work by Axelsson (Axelsson et al., 2011), a transient increase in the permeability of the GFB was seen under the influence of ANP. This effect was observed as early as five minutes after the start of the ANP infusion and the permeability of the GFB was spontaneously reset within 30 minutes. This finding diverges from our results where the NO system, which uses the same intracellular signalling pathway, has the opposite effect on the permeability of the GFB. The shorter activation time for the ANP effect may be explained by the fact that ANP binds directly to the membrane-bound GC-A, which in turn generates secondary messenger cGMP (Lucas et al., 2000). The difference in effect between these two studies may be due to the fact that they involve two different cells that are responding to stimuli via the same intracellular signalling pathway (Pavenstadt et al., 2003). For example, in studies by Chevalier et al. (Chevalier et al., 1992), the cGMP level was measured in tissue from the kidney of an adult rat following the addition of nitroprusside (a powerful NO donor) or ANP. When the NO donor was used, a high cGMP level was seen in the mesangium and when ANP was used, this was seen in podocytes. Accordingly, cGMP appears to have different effects in different tissues. For example, in cardiomyocytes, cGMP blocks hydrolysis of cAMP by blocking phosphodiesterase 3 (PDE3) and thereby increases the influx of calcium into cells via L-type calcium channels (Maurice, 2005).

Calcium influx into cells plays a major role in remodulation of the cytoskeleton. Changes in the intracellular calcium level activate secondary intracellular mediators for the arrangement of the cytoskeleton that are known as small GTPases (RhoA, Rac1, Cdc42) (Figure 10). In cultured podocytes (Greka & Mundel, 2011), the remodelling of actin with stress fibres has been demonstrated upon activation of RhoA, and activation of Rac1 induces the formation of lamellipodia, which gives a cell phenotype that has a migratory tendency.

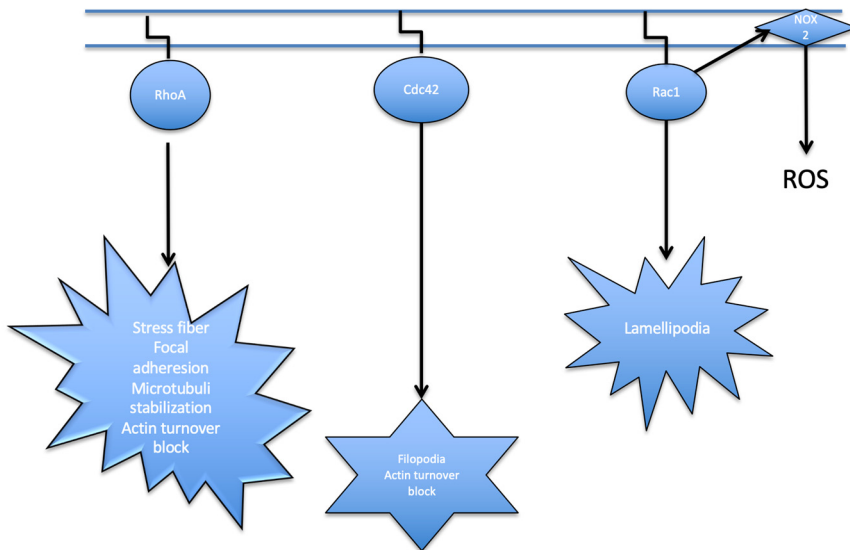


Figure 10. Downstream signaling of Rho-GTPases.

Angiotensin II induces a transitory increase in the permeability of the GFB. This effect is mediated by the influx of calcium into the cell. In our laboratory, it has been demonstrated that blocking both small GTPases (RhoA/ Rac1) counteracts angiotensin-induced increases in the permeability of the GFB (Axelsson et al., 2013).

Extracellular influx of calcium takes place through mechanisms including membrane-bound calcium channels that belong to the TRP (transient receptor potential) family. According to studies of cultured podocytes, TRPC5 channels appear to be linked to Rac1-Cdc42 activation, while TRPC6 activates RhoA (Greka & Mundel, 2011). TRPC5/TRPC6 are represented on the cell surface on podocytes but not on fenestrated endothelial cells. Activation of TRPC5/TRPC6 receptors takes place during angiotensin receptor activation.

In Study IV, we studied whether blocking TRPC5/TRPC6 receptors *in vivo* affects the angiotensin-induced increases in GFB permeability. We are using a TRPC5 channel blocker (clemizole) and lanthanum salt at two different concentrations. Low-concentration lanthanum salt activates TRPC5 and blocks TRPC6. High-concentration lanthanum salt blocks both TRPC5 and TRPC6 channels.

Angiotensin-induced increases in GFB permeability were completely blocked by TRPC5 channel blockers. TRPC6 channel blockers appeared to have an effect on both proteinuria and blood pressure. TRPC6 channels regulate vascular tone, which

may explain the dose-dependent reduction in blood pressure during TRPC6 blockade.

One weakness of Study IV is that the TRPC5 blocker used (clemizole) may have other effects that are not due to its blockade of the TRPC5 channel. Clemizole is also a first-generation antihistamine that was previously also registered as a medicinal product in Sweden (Allercur). A further development is to try the same experiments, but with a more selective blocker (e.g. AC1903).

Attention has been drawn in recent years to the role played by endothelin in the development of various diseases of the kidney such as hypertensive nephropathy and diabetic nephropathy. It was noted that non-selective blocking of endothelin receptors may reduce inflammation and the development of fibrosis in the kidneys and may alleviate proteinuria. Endothelin is a potent vasoconstrictor that is manufactured in an inactive form (Big-ET-1) and, as with angiotensin, needs to be activated by cleaving into its active form (ET-1). Endothelin signalling involves both paracrine and autocrine signalling. High concentrations of endothelin have been observed locally in tissues without a high concentration of endothelin having been seen systemically. Endothelin occurs in the body in three isoforms: ET-1, ET-2 and ET-3. The ET-1 isoform is predominant in the kidneys.

There are two types of endothelin receptor. ET_A and ET_B . While all isoforms of endothelin have the same affinity for the ET_B receptor, the ET-3 isoform has an affinity for the ET_A receptor that is 100 times lower than that of the ET-1 and ET-2 isoforms. The distribution of ET receptors in the body varies. In the kidneys, ET_A receptors are present in mesangial cells; fenestrated endothelial cells have ET_B receptors, podocytes predominantly express ET_B and to a lesser extent ET_A .

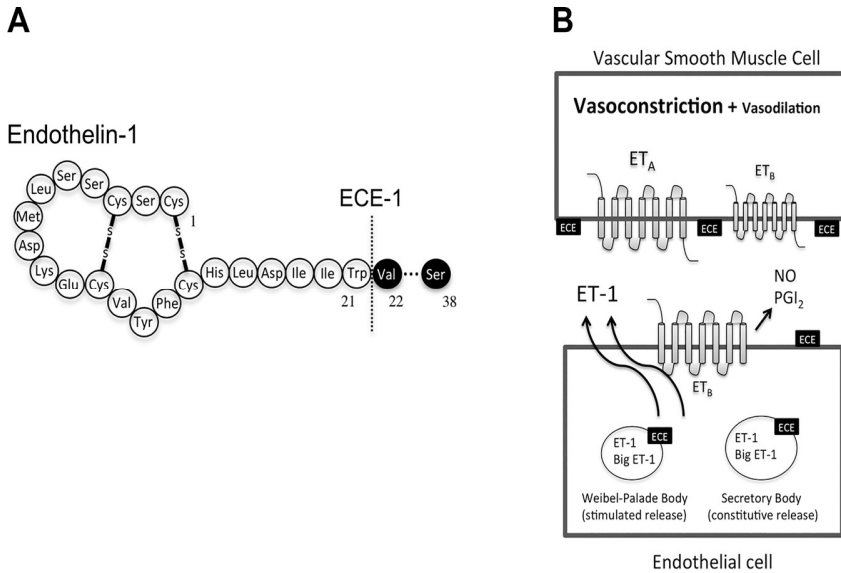


Figure 11. Schematic illustration of Endothelin-1 synthesis and signaling.

Endothelin (ET)-1 is a potent vasoconstrictor peptide hormone synthesized by endothelial cells. It binds to ET type A (ET_A) and type B (ET_B) receptors on vascular smooth muscle cells, mediating vasoconstriction and vasodilation, respectively. Synthesis of ET-1 is accomplished by enzymatic cleavage of a precursor (big ET) by an endothelin-converting enzyme (ECE) (similar to angiotensin converting enzyme). PGI₂, prostaglandin I₂; NO, nitric oxide;

In Study III we have demonstrated that ET-1 is involved in regulating the permeability of the GFB *in vivo*. The effect of ET-1 is mediated primarily via ET_A receptors.

AG-1 and ET_A receptors belong to the G protein-coupled family (GPCR) (Horinouchi et al., 2009).

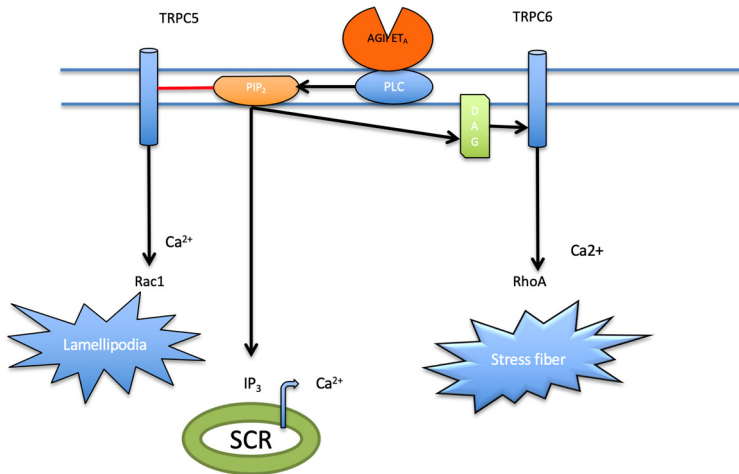


Figure 12. Illustration of a G-protein coupled receptor.

AGI-angiotensin II, ET_A – Endothelin A, TRPC 5/6- transient receptor potential channels, PLC-phospholipase C, PIP₂-phosphatidylinositol(4,5)bisphosphate, DAG- diacylglycerol, IP₃ - inositol-1,4,5-trisphosphate, SCR- sarcoplasmic reticulum, RhoA/Rac1- small GTP-ases

When these receptors are activated, membrane-bound phospholipase C (PLC) is activated. PLC mediates its intracellular effects via the breakdown of membrane-bound phosphatidylinositol 4,5-bisphosphate (PIP₂). PIP₂ is a regulatory factor that is homogeneously distributed in eukaryotic cell membranes and mediates a large number of different effects, including having a braking effect on membrane-bound TRPC5 channels (Czech, 2000; van Rheenen et al., 2005). When PLC is activated, degradation of PIP₂ to two intracellular transmitters begins: diacylglycerol (DAG) (Wang, 2006) and inositol 1,4,5-trisphosphate (IP₃). DAG is membrane bound and is able to activate TRPC6 channels (Clapham, 2003), protein kinase C and protein kinase D (Wang, 2006). IP₃ moves freely in the cytosol and activates receptors on the surface of the sarcoplasmic reticulum and by doing so promotes calcium flux from the extracellular space to the cytosol.

In studies of cultured podocytes, a skew distribution was seen of TRPC receptor expression on the cell surface where there was an increased expression of TRPC6 channels under physiological conditions. When angiotensin is supplied continuously, recruitment of TRPC5 channels from the cytosol of podocytes to the cell surface takes place. Studies of ET_A receptors on HEK cells showed that ET_A receptors have a connection to TRPC 6,3,5,7 receptors, however, it was not possible to prove there is activity via TRPC5 channels in conjunction with ET_A receptor activation (Horinouchi et al., 2011). At the same time, it was demonstrated in diabetes studies that during inflammation, podocytes produce ET-1, which diffuses

locally to the mesangium and activates ET_A receptors in the mesangial cells (Giehl et al., 2008; Peng et al., 2008; Sasser et al., 2007). The mesangial cell is a smooth muscle cell that has a cytoskeleton and, in addition to ET_A , also expresses AG-1 receptors on its cell surface. In diabetes studies, histological reorganisation of the cytoskeleton is seen in mesangial cells with the formation of lamellipodia, i.e. signs of an active Rac-1 signalling pathway in the cell.

Accordingly, it could be the case that mesangial cells, in addition to podocytes and endothelial cells, also participate in the regulation of GFB permeability. The role of TRPC5 channels in regulation of GFB permeability should be examined further in both experimental and clinical studies. In this context, it is interesting that empirical treatment of proteinuric IgA nephropathy with fish oil has been used in clinical practice. Interestingly, fish oil contains ω -3 fatty acid, which is also a TRPC5 blocker (Sukumar et al., 2012).

Glomerular permeability and hemodynamic aspects

Angiotensin II and endothelin 1 are potent vasoconstrictors. When capillary pressure rises, GFR increases and the flow over large pores rises as a result (J_{vL}). In conjunction with increased J_{vL} clearance of albumin rises but fractional clearance (and thus the sieving coefficient) remains the same (J_{vL}/GFR). Consequently, the observation that the sieving coefficient rises for large molecules cannot be explained by increased capillary pressure. Instead this is due to structural changes to the filter that also take place. Accordingly, it has been demonstrated in the work by C Rippe et al. (Rippe et al., 2006) that when GFR is increasing, the fractional clearance of FITC-Ficoll 55 Å (equivalent to 36 Å albumin molecule) is in principal unchanged.

In the endothelin-1 study, a transitory increase is seen in the sieving coefficient for FITC-Ficoll 70 Å without a simultaneous change in GFR or evident increase in blood pressure. There are no signs of structural filter injury with unchanged small pore size, however there is a clear increase in the flow over large pores within a widespread increase in their radius. Thus, our data suggest a cellular component to the regulation of GFR permeability.

Study II – some considerations

Harmful effects of ureteral obstruction are normally linked to inflammatory processes that are started in the renal interstitium in conjunction with increased pressure in the tubuli system. Mobilization of ROS and activation of cytokines lies behind inflammation in ureteral obstruction. In our study, we find a glomerular component to the change in permeability of the GFB as early as after 120 minutes of ureteral obstruction. This effect appears to be, at least in part, mediated by ROS. After 180 minutes of ureteral obstruction, pronounced damage occurs to the structure of the renal filter, with an effect on both the size of small pores and their distribution. In this situation, the dynamic permeability increments caused by ROS may be made permanent and non-responsive towards ROS scavenger tempol.

Conclusions

- Nitric oxide signaling appears to be playing an important part in the maintenance and regulation of glomerular permeability, and its physiological effects seem to involve a balance with ROS.
- During ureteral obstruction there are permeability changes in the glomerular filter, that to some extent seem to be brought about by oxidative stress.
- Endothelin receptor A seems to be involved in the permeability changes of the GFB.
- Intracellular Ca^{2+} signaling via TRPC5 and TRPC6 channels the effects of AGII on the glomerular filter.

Further perspectives

An ultimate goal would be the development of drugs that counteract glomerular proteinuria without additive effect on the hemodynamics of the kidney, or effects on systemic blood pressure. We found evidence to suggest that TRCP5 channel blocking lacks hemodynamic effect, both in glomerular and peripheral capillaries. Thus, TRCP5 channel blockers may have potential to become new anti-proteuric drugs.

Acknowledgements

I would like to thank everyone who has contributed to my dissertation. And especially I would like to express my greatest appreciation to the following people:

Bengt Rippe - I remember him as a dedicated and engaged supervisor. He had profound knowledge of renal physiology and was interested in related areas of science such as molecular cell biology. It was important for Bengt that I could get to know the research work from scratch. He would always welcome a discussion and appreciate my opinion. I feel privileged and grateful that I got to know Professor Bengt Rippe and could work under his supervision.

I would like to thank Carl M Öberg for taking over the supervision. Under Carl Öberg's guidance, we were able to execute Professor Bengt Rippe's ideas and plans during the latter part of the dissertation. Carl Öberg has excellent pedagogical skills. I really appreciate his ability to explain incredibly complicated concepts in a structured and logical way.

Peter Bentzer, my co-supervisor, I am grateful for all the advice regarding the research education and a lot of practical help to get it.

Anna Rippe, laboratory assistant and an amazingly experienced colleague. I would like to thank Anna for sharing her knowledge and skills with me, and for being so patient and supportive. Without her great input, my dissertation would not have been as structured as it is now.

Big thanks to Helen Axelberg and Per-Olof Grände for scientific discussions and philosophical conversations about life in general during lunch and coffee breaks.

My mentor and colleague, Sophie Ohlsson, for great advice and insights on how to get a better balance between the research work and my daily routine at the clinic.

Naomi Clyne, my senior mentor, for all the support and recommendations regarding the research world and my daily work.

To all colleagues at the Kidney Clinic in Lund, I would like to express my gratitude for all the support and help in taking care of my patients while I researched and wrote the dissertation.

My friends: Inese Dubnika Hauksson, Maria Lundgren, Yana Strekalovskaia, Pyotr Platonov, Natalia Martynova, Marina Popova and Sergey Peredkov - thank you for

being there for me, as solid as rocks that I can lean on. I always get advice, support, and warmth from you.

My dear family - daughter Polina, my parents Tatiana and Nikolay and my sister Alexandra, I want to thank you for all the love you give me.

References

- Abbate, M., Zoja, C., & Remuzzi, G. (2006). How Does Proteinuria Cause Progressive Renal Damage? *Journal of the American Society of Nephrology*, 17(11), 2974-2984. <https://doi.org/10.1681/asn.2006040377>
- Alderton, W. K., Cooper, C. E., & Knowles, R. G. (2001). Nitric oxide synthases: structure, function and inhibition. *Biochemical journal*, 357(3), 593-615.
- Asgeirsson, D., Venturoli, D., Fries, E., Rippe, B., & Rippe, C. (2007). Glomerular sieving of three neutral polysaccharides, polyethylene oxide and bikunin in rat. Effects of molecular size and conformation. *Acta Physiologica*, 191(3), 237-246.
- Axelsson, J., Rippe, A., & Rippe, B. (2011). Transient and sustained increases in glomerular permeability following ANP infusion in rats. *American Journal of Physiology-Renal Physiology*, 300(1), F24-F30.
- Axelsson, J., Rippe, A., Sverrisson, K., & Rippe, B. (2013). Scavengers of reactive oxygen species, paracalcitol, RhoA, and Rac-1 inhibitors and tacrolimus inhibit angiotensin II-induced actions on glomerular permeability. *Am J Physiol Renal Physiol*, 305(3), F237-243. <https://doi.org/10.1152/ajprenal.00154.2013>
- Axelsson, J., Rippe, A., Öberg, C. M., & Rippe, B. (2012). Rapid, dynamic changes in glomerular permeability to macromolecules during systemic angiotensin II (ANG II) infusion in rats. *American Journal of Physiology-Renal Physiology*, 303(6), F790-F799.
- Bendall, J. K., Alp, N. J., Warrick, N., Cai, S., Adlam, D., Rockett, K., Yokoyama, M., Kawashima, S., & Channon, K. M. (2005). Stoichiometric relationships between endothelial tetrahydrobiopterin, endothelial NO synthase (eNOS) activity, and eNOS coupling in vivo: insights from transgenic mice with endothelial-targeted GTP cyclohydrolase 1 and eNOS overexpression. *Circulation research*, 97(9), 864-871.
- Blouch, K., Deen, W. M., Fauvel, J. P., Bialek, J., Derby, G., & Myers, B. D. (1997). Molecular configuration and glomerular size selectivity in healthy and nephrotic humans [Article]. *American Journal of Physiology - Renal Physiology*, 273(3 42-3), F430-F437. <https://doi.org/10.1152/ajprenal.1997.273.3.f430>
- Bohrer, M. P., Baylis, C., Humes, H. D., Glasscock, R. J., Robertson, C. R., & Brenner, B. M. (1978). Permselectivity of the glomerular capillary wall: Facilitated filtration of circulating polycations. *The Journal of clinical investigation*, 61(1), 72-78.
- Chevalier, R. L., Fern, R. J., Garmey, M., el-Dahr, S. S., Gomez, R. A., & De Vente, J. (1992). Localization of cGMP after infusion of ANP or nitroprusside in the maturing rat. *American Journal of Physiology-Renal Physiology*, 262(3), F417-F424.

- Christensen, E. I., & Birn, H. (2001). Megalin and cubilin: synergistic endocytic receptors in renal proximal tubule. *American Journal of Physiology-Renal Physiology*, 280(4), F562-F573.
- Ciarimboli, G., Schurek, H.-J., Zeh, M., Flohr, H., Bökenkamp, A., Fels, L. M., Kilian, I., & Stolte, H. (1999). Role of albumin and glomerular capillary wall charge distribution on glomerular permselectivity: studies on the perfused-fixed rat kidney model. *Pflügers Archiv*, 438(6), 883-891.
- Clapham, D. E. (2003). TRP channels as cellular sensors. *Nature*, 426(6966), 517-524.
- Comper, W., Russo, L., & Vuchkova, J. (2016). Are filtered plasma proteins processed in the same way by the kidney? *Journal of Theoretical Biology*, 410, 18-24.
- Curry, F., & Michel, C. (1980). A fiber matrix model of capillary permeability. *Microvascular research*, 20(1), 96-99.
- Czech, M. P. (2000). PIP2 and PIP3: complex roles at the cell surface. *Cell*, 100(6), 603-606.
- Eddy, A. A. (2004). Proteinuria and interstitial injury. *Nephrology Dialysis Transplantation*, 19(2), 277-281.
- Edwards, A., Christensen E. I., Unwin, R. J., Norden, A.G.W. (2020). Predicting the protein composition of human urine in normal and pathological states: quantitative description based on dent1 disease (*CLCN5* mutation). *Journal of Physiology*, In press.
- Gansevoort, R. T., Matsushita, K., van der Velde, M., Astor, B. C., Woodward, M., Levey, A. S., de Jong, P. E., & Coresh, J. (2011). Lower estimated GFR and higher albuminuria are associated with adverse kidney outcomes. A collaborative meta-analysis of general and high-risk population cohorts. *Kidney international*, 80(1), 93-104. <https://doi.org/https://doi.org/10.1038/ki.2010.531>
- Giehl, K., Graness, A., & Goppelt-Strube, M. (2008). The small GTPase Rac-1 is a regulator of mesangial cell morphology and thrombospondin-1 expression. *American Journal of Physiology-Renal Physiology*.
- Greka, A., & Mundel, P. (2011). Balancing calcium signals through TRPC5 and TRPC6 in podocytes. *Journal of the American Society of Nephrology*, 22(11), 1969-1980.
- Haraldsson, B., Nyström, J., & Deen, W. M. (2008). Properties of the glomerular barrier and mechanisms of proteinuria. *Physiological reviews*, 88(2), 451-487.
- Hjalmarsson, C., Johansson, B. R., & Haraldsson, B. (2004). Electron microscopic evaluation of the endothelial surface layer of glomerular capillaries. *Microvascular research*, 67(1), 9-17.
- Horinouchi, T., Asano, H., Higa, T., Nishimoto, A., Nishiya, T., Muramatsu, I., & Miwa, S. (2009). Differential coupling of human endothelin type A receptor to Gq/11 and G12 proteins: the functional significance of receptor expression level in generating multiple receptor signaling. *Journal of pharmacological sciences*, 111(4), 338-351.
- Horinouchi, T., Terada, K., Higa, T., Aoyagi, H., Nishiya, T., Suzuki, H., & Miwa, S. (2011). Function and regulation of endothelin type A receptor-operated transient receptor potential canonical channels. *Journal of pharmacological sciences*, 117(4), 295-306.

- Iseki, K., Ikemiya, Y., Iseki, C., & Takishita, S. (2003). Proteinuria and the risk of developing end-stage renal disease. *Kidney international*, 63(4), 1468-1474.
- Kedem, O., & Katchalsky, A. (1958). Thermodynamic analysis of the permeability of biological membranes to non-electrolytes. *Biochimica et biophysica Acta*, 27, 229-246.
- Kedem, O., & Katchalsky, A. (1961). A physical interpretation of the phenomenological coefficients of membrane permeability. *The Journal of general physiology*, 45(1), 143-179.
- Lucas, K. A., Pitari, G. M., Kazerounian, S., Ruiz-Stewart, I., Park, J., Schulz, S., Chepenik, K. P., & Waldman, S. A. (2000). Guanylyl cyclases and signaling by cyclic GMP. *Pharmacological reviews*, 52(3), 375-414.
- Lund, U., Rippe, A., Venturoli, D., Tenstad, O., Grubb, A., & Rippe, B. (2003). Glomerular filtration rate dependence of sieving of albumin and some neutral proteins in rat kidneys. *American Journal of Physiology-Renal Physiology*, 284(6), F1226-F1234.
- Mason, E., Wendt, R., & Bresler, E. (1980). Similarity relations (dimensional analysis) for membrane transport. *Journal of Membrane science*, 6, 283-298.
- Maurice, D. H. (2005). Cyclic nucleotide phosphodiesterase-mediated integration of cGMP and cAMP signaling in cells of the cardiovascular system. *Front Biosci*, 10, 1221-1228.
- McCarthy, J. T. (1996). Prognosis of patients with acute renal failure in the intensive-care unit: a tale of two eras. *Mayo Clinic Proceedings*,
- Miner, J. H. (1999). Renal basement membrane components. *Kidney international*, 56(6), 2016-2024.
- Morita, H., Yoshimura, A., Inui, K., Ideura, T., Watanabe, H., Wang, L., Soininen, R., & Tryggvason, K. (2005). Heparan sulfate of perlecan is involved in glomerular filtration. *Journal of the American Society of Nephrology*, 16(6), 1703-1710.
- Mundel, P., Elger, M., Sakai, T., & Kriz, W. (1988). Microfibrils are a major component of the mesangial matrix in the glomerulus of the rat kidney. *Cell and Tissue Research*, 254(1), 183-187. <https://doi.org/10.1007/BF00220032>
- Norden, A. G., Lapsley, M., Lee, P. J., Pusey, C. D., Scheinman, S. J., Tam, F. W., Thakker, R. V., Unwin, R. J., & Wrong, O. (2001). Glomerular protein sieving and implications for renal failure in Fanconi syndrome. *Kidney international*, 60(5), 1885-1892.
- Ohlson, M., Sörensson, J., & Haraldsson, B. r. (2000). Glomerular size and charge selectivity in the rat as revealed by FITC-Ficoll and albumin. *American Journal of Physiology-Renal Physiology*, 279(1), F84-F91.
- Ohlson, M., Sörensson, J., Lindström, K., Blom, A. M., Fries, E., & Haraldsson, B. r. (2001). Effects of filtration rate on the glomerular barrier and clearance of four differently shaped molecules. *American Journal of Physiology-Renal Physiology*, 281(1), F103-F113.
- Pavenstadt, H., Kriz, W., & Kretzler, M. (2003). Cell biology of the glomerular podocyte. *Physiological reviews*, 83(1), 253-307.

- Peng, F., Zhang, B., Wu, D., Ingram, A. J., Gao, B., & Krepinsky, J. C. (2008). TGF β -induced RhoA activation and fibronectin production in mesangial cells require caveolae. *American Journal of Physiology-Renal Physiology*, 295(1), F153-F164.
- Renkin, E. M. (1954). Filtration, diffusion, and molecular sieving through porous cellulose membranes. *The Journal of general physiology*, 38(2), 225.
- Rippe, B., & Haraldsson, B. (1987). Fluid and protein fluxes across small and large pores in the microvasculature. Application of two-pore equations. *Acta physiologica scandinavica*, 131(3), 411-428.
- Rippe, C., Asgeirsson, D., Venturoli, D., Rippe, A., & Rippe, B. (2006). Effects of glomerular filtration rate on Ficoll sieving coefficients (θ) in rats. *Kidney international*, 69(8), 1326-1332.
- Rostgaard, J., & Qvortrup, K. (1997). Electron microscopic demonstrations of filamentous molecular sieve plugs in capillary fenestrae. *Microvascular research*, 53(1), 1-13.
- Sánchez, F. A., Ehrenfeld, I. P., & Durán, W. N. (2013). S-nitrosation of proteins: An emergent regulatory mechanism in microvascular permeability and vascular function. *Tissue Barriers*, 1(1), 553-563.
- Sasser, J. M., Sullivan, J. C., Hobbs, J. L., Yamamoto, T., Pollock, D. M., Carmines, P. K., & Pollock, J. S. (2007). Endothelin A receptor blockade reduces diabetic renal injury via an anti-inflammatory mechanism. *Journal of the American Society of Nephrology*, 18(1), 143-154.
- Schaeffer Jr, R. C., Gratrix, M. L., Mucha, D. R., & Carbajal, J. M. (2002). The rat glomerular filtration barrier does not show negative charge selectivity. *Microcirculation*, 9(5), 329-342.
- Sukumar, P., Sedo, A., Li, J., Wilson, L. A., O'Regan, D., Lippiat, J. D., Porter, K. E., Kearney, M. T., Ainscough, J. F., & Beech, D. J. (2012). Constitutively active TRPC channels of adipocytes confer a mechanism for sensing dietary fatty acids and regulating adiponectin. *Circulation research*, 111(2), 191-200.
- Tojo, A., & Endou, H. (1992). Intrarenal handling of proteins in rats using fractional micropuncture technique. *American Journal of Physiology-Renal Physiology*, 263(4), F601-F606.
- van Rheenen, J., Mulugeta Achame, E., Janssen, H., Calafat, J., & Jalink, K. (2005). PIP2 signaling in lipid domains: a critical re-evaluation. *The EMBO journal*, 24(9), 1664-1673.
- Wang, Q. J. (2006). PKD at the crossroads of DAG and PKC signaling. *Trends in pharmacological sciences*, 27(6), 317-323.
- Weinbaum, S., Tarbell, J. M., & Damiano, E. R. (2007). The structure and function of the endothelial glycocalyx layer. *Annu. Rev. Biomed. Eng.*, 9, 121-167.
- Öberg, C., Rippe, B. (2014). A distributed two-pore model: theoretical implications and practical application to the glomerular sieving of Ficoll. *American Journal of Physiology Renal Physiology*, 306(8), 844-854.

Paper I



Nitric oxide synthase inhibition causes acute increases in glomerular permeability in vivo, dependent upon reactive oxygen species

Julia Dolinina, Kristinn Sverrisson, Anna Rippe,  Carl M. Öberg, and Bengt Rippe

Department of Nephrology, Lund University, Lund, Sweden

Submitted 11 March 2016; accepted in final form 21 September 2016

Dolinina J, Sverrisson K, Rippe A, Öberg CM, Rippe B. Nitric oxide synthase inhibition causes acute increases in glomerular permeability in vivo, dependent upon reactive oxygen species. *Am J Physiol Renal Physiol* 311: F984–F990, 2016. First published September 28, 2016; doi:10.1152/ajprenal.00152.2016.—There is increasing evidence that the permeability of the glomerular filtration barrier (GFB) is partly regulated by a balance between the bioavailability of nitric oxide (NO) and that of reactive oxygen species (ROS). It has been postulated that normal or moderately elevated NO levels protect the GFB from permeability increases, whereas ROS, through reducing the bioavailability of NO, have the opposite effect. We tested the tentative antagonism between NO and ROS on glomerular permeability in anaesthetized Wistar rats, in which the left ureter was cannulated for urine collection while simultaneously blood access was achieved. Rats were systemically infused with either L-NAME or L-NAME together with the superoxide scavenger Tempol, or together with L-arginine or the NO-donor DEA-NONOate, or the cGMP agonist 8-bromo-cGMP. To measure glomerular sieving coefficients (θ , θ) to Ficoll, rats were infused with FITC-Ficoll 70/400 (mol/radius 10–80 Å). Plasma and urine samples were analyzed by high-performance size-exclusion chromatography (HPSEC) for determination of θ for Ficoll repeatedly during up to 2 h. L-NAME increased θ for Ficoll_{70Å} from $2.27 \pm 1.30 \times 10^{-5}$ to $8.46 \pm 2.06 \times 10^{-5}$ ($n = 6$, $P < 0.001$) in 15 min. Tempol abrogated these increases in glomerular permeability and an inhibition was also observed with L-arginine and with 8-bromo-cGMP. In conclusion, acute NO synthase inhibition in vivo by L-NAME caused rapid increases in glomerular permeability, which could be reversed by either an ROS antagonist or by activating the guanylyl cyclase-cGMP pathway. The data strongly suggest a protective effect of NO in maintaining normal glomerular permeability in vivo.

glomerular filtration; glomerular sieving coefficient; Ficoll; soluble guanylyl cyclase; cGMP; capillary permeability

PERMEABILITY OF THE MICROVASCULATURE IS tightly regulated and there is evidence that the continuous release of nitric oxide (NO) from the endothelium plays a central role in the maintenance of normal barrier permeability, partly by antagonizing the detrimental effects of reactive oxygen species (ROS) (13, 14). Early studies of vascular barrier function following inhibition of NO synthase (NOS) in vivo using N^G -nitro-L-arginine methyl ester hydrochloride (L-NAME) thus demonstrated marked increases in vascular permeability and in leukocyte adhesion in feline mesenteric microvessels after NOS inhibition (24, 25). These actions were reversed by potent NO donors such as nitroprusside, or by agonists of cGMP (24), as corroborated by later studies (22, 34, 35, 46). By contrast, NO has also been identified as a key signaling molecule in eliciting hyperpermeability following various permeability stimuli,

mostly in microvessels perfused with cell-free media or in cell cultures (28, 40, 41, 52, 53) via enhancement of the activity of endothelial NOS (eNOS). eNOS is regulated by a number of processes and factors, most notably by caveolin-1, causing tonic eNOS inhibition. Furthermore, if eNOS is markedly upregulated, but not its cofactor tetrahydrobiopterin (BH₄) (e.g., by oxidation), eNOS will produce ROS such as superoxide (O_2^-) and peroxynitrite ($ONOO^-$) instead of NO, denoting eNOS uncoupling (13). Furthermore, $ONOO^-$ will further uncouple eNOS in a feed-forward fashion, which may lead to endothelial dysfunction and increases in vascular permeability (14, 23).

In vitro, the permeability of the glomerular filtration barrier (GFB) has been shown to be quite sensitive to enhanced levels of ROS, particularly O_2^- (44, 45). In vivo, we recently demonstrated that systemically administered Ang II; the cytokines IL-1 β , TNF- α , and IL-6; fetal hemoglobin (HbF); and puromycin aminonucleoside (PAN) have the ability to produce acute increases in glomerular permeability, which can be inhibited by the superoxide dismutase (SOD) mimetic (O_2^- scavenger) Tempol (3, 5, 47, 48). Furthermore, there is good evidence that increases in ROS generation and oxidative stress play a role in the processes leading to chronic renal disease, and that antioxidative mechanisms are generally impaired in a variety of chronic kidney disorders (10, 15, 17, 18, 31). Furthermore, NO depletion has been shown to aggravate proteinuria and renal histological derangement in renal disease (7, 15, 43).

NO modulates a great number of cellular processes mediated by either cGMP-dependent or cGMP-independent processes (13, 14). One major action of NO is to induce the activation of soluble guanylyl cyclase (sGC), synthesizing cGMP, and acting as a second messenger for a number of cellular events such as activation of protein kinase G (PKG). NO can also cause a number of cGMP-independent actions such as nitration of proteins, activation of ion channels, and interaction with ROS and their metabolites, whereby NO acts as a (direct) ROS scavenger. Indeed, in acute experiments in isolated glomeruli in vitro, the direct ROS antagonizing effect of NO has been amply demonstrated (44, 45).

In the present study we attempted to assess the acute effects of systemic NOS inhibition on glomerular permeability in rats in vivo and to investigate the extent to which those effects can be reversed by the superoxide radical scavenger, Tempol. As mentioned above, an antagonism between NO and ROS has been shown to occur in vitro in isolated glomeruli; the latter, however, being likely to be subject to an increased baseline barrier permeability. Furthermore, in vitro, capillaries are not exposed to normal shear stress, a major stimulus for endogenous NO production (51). In addition, glomerular tufts in vitro may be subjected to slight (inflammatory) activation due to the

Address for reprint requests and other correspondence: B. Rippe, Clinical Sciences, Lund, Dept. of Nephrology, Lund Univ., Skåne Univ. Hospital, S-211 85 Lund, Sweden (e-mail: Bengt.Rippe@med.lu.se).

isolation procedure, the processing (sieving procedure), and the artificial environment. A parallel might be drawn to cultured endothelium *in vitro* compared with endothelium *in vivo*. Endothelial monolayers *in vitro* usually show a higher permeability and might be in an activated stage compared with endothelium in intact microvessels *in vivo* (9).

To assess glomerular permeability in intact rats *in vivo* we monitored the glomerular sieving coefficients (theta, θ ; i.e., the primary urine-to-plasma concentration ratios) of FITC-Ficoll 70/400 (70,000 and 400,000 M_n , respectively) of Stokes-Einstein radius (a_s) ranging from 10 to 80 Å after systemic infusion of L-NAME alone, or together with Tempol, L-arginine, a cGMP analog, and the NO-donor DEA-NONOate. Ficoll is a copolymer of sucrose and epichlorohydrin, which is not significantly reabsorbed in the proximal tubules. High-molecular-weight (HMW) Ficoll can thus be used as a direct probe of glomerular permeability in real time using highly sensitive urine detection of the test probes by a fine-tuned, high-performance, size-exclusion chromatograph (HPSEC). We found that NOS inhibition increased baseline glomerular permeability *in vivo*, which could be completely reversed by Tempol or by systemic infusion of L-arginine or by direct stimulation of cGMP, the major downhill effector of NO.

MATERIALS AND METHODS

Experiments were performed using male Wistar rats (Møllegaard, Lille Stensved, Denmark) with a mean body wt of 257 ± 2.69 g. The rats had free access to water and standard chow until the day of the experiment. The Malmö/Lund Committee for Animal Experiment Ethics approved the experiments. Anesthesia was initiated by an intraperitoneal injection of pentobarbital sodium (90 mg/kg; Pentobarbitalnatrium vet; Kungens Kurva, Sweden) and maintained by repeated intra-arterial injections of the same drug via the tail artery. Body temperature was kept at 37°C using a thermostatically controlled heating pad. To facilitate breathing a tracheotomy was performed. The tail artery was cannulated (PE-50 cannula) for continuous monitoring of mean arterial blood pressure (MAP) and registration of heart rate (HR) (MP 150 system, with AcqKnowledge from MAC; Biopac System) and for maintenance of anesthesia. The left carotid artery was cannulated for blood sampling, and the left jugular vein for infusion purposes (PE-50 cannulas). The left ureter was exposed by a small incision in the abdominal wall and cannulated (PE-10 cannula) for urine sampling, followed by closure of the incision by a small suture. Furosemide (0.375 mg/kg body wt) was administered in the tail artery to temporarily increase urine flow to facilitate the cannulation of the ureter.

Experimental procedures. All experiments started with an initial resting period of at least 20 min duration following cannulation of the left ureter. During the resting period and throughout the rest of the experiments, the animals were given a continuous intravenous (iv) infusion of a mixture of FITC-Ficoll_{70A} (10 mg/ml) and FITC-Ficoll_{400A} (10 mg/ml; TdB Consultancy, Uppsala, Sweden) in the relationship 1:24, together with FITC-inulin (10 mg/ml, TdB Consultancy) and ⁵¹Cr-EDTA (0.3 MBq/ml, Amersham Biosciences, Buckinghamshire, UK), following an initial iv bolus dose. This initial bolus dose contained 40 µg, 960 µg, 500 µg, and 0.3 MBq of FITC-Ficoll_{70A}, FITC-Ficoll_{400A}, FITC-inulin, and ⁵¹Cr-EDTA, respectively. The infusion rate was 10 ml·kg⁻¹·h⁻¹. Infusion concentrations were thus 20 µg/ml of FITC-Ficoll_{70A}, 0.48 mg/ml of FITC-Ficoll_{400A}, 0.5 mg/ml of FITC-inulin, and 0.3 MBq/ml of ⁵¹Cr-EDTA. Baseline samples of blood and urine were taken at the end of the resting period (at *time 0*) to determine the baseline sieving coefficients (θ) to Ficoll.

Five groups of rats exposed to L-NAME were investigated, and in all groups blood and urine samples were collected at 0, 5, 15, and 30 min, and for L-NAME alone, also at 60 and 120 min after the start of the (L-NAME) infusion. A maximal alteration in MAP of ± 15 mmHg was allowed during the experiments.

In the *L-NAME group* ($n = 7$), the competitive NOS inhibitor N^G-nitro-L-arginine methyl ester hydrochloride (L-NAME; Sigma-Aldrich, St. Louis, MO) was administered to the animals as an initial bolus (470 µg/kg iv) followed by a continuous infusion (93 µg·kg⁻¹·min⁻¹ iv). Because the maximal L-NAME effect on glomerular permeability occurred at 15 min (see below), all subsequent experiments in which we attempted to interact with the L-NAME effects on glomerular permeability were performed on a short time scale (up to 30 min).

In the *Tempol-L-NAME group* ($n = 12$), a continuous iv infusion of the SOD mimetic compound (and scavenging O₂⁻) 4-hydroxytempo (1 mg·kg⁻¹·min⁻¹, Tempol; Sigma-Aldrich) was started 5 min before the start of the L-NAME infusion (+bolus), the coinfusion together with L-NAME (93 µg·kg⁻¹·min⁻¹) continuing throughout the experiment (30 min).

In the *L-arginine-L-NAME group* ($n = 5$) the NO donor L-2-amino-5-guanidino-n-valerianic acid (L-arginine; AppliChem, Darmstadt, Germany), the substrate for NO synthesis by NOS, was given in an attempt to competitively inhibit the L-NAME effects. L-arginine was given in an iv bolus dose, 1.33 mg/kg, followed by a continuous infusion of 400 µg·kg⁻¹·min⁻¹. Animals were pretreated with L-arginine during 30 min before the start of the L-NAME infusion (+bolus) and received L-arginine throughout the experiment.

The *DEA-NONOate-L-NAME group* ($n = 6$) obtained the NO-donor, diethylamine-NONOate (DEA-NONOate; Sigma-Aldrich). DEA-NONOate was coinfused with L-NAME at a rate of 0.65 µg·kg⁻¹·min⁻¹, or at lower rates, depending on the concomitant reductions in MAP (max -15 mmHg).

In the *8-bromo-cGMP-L-NAME group* ($n = 7+7$), the cGMP analog 8-bromoguanosine 3',5'-cyclic monophosphate (8-bromo-cGMP; Sigma-Aldrich) was given together with L-NAME. cGMP is a target for NO via activation by sGC at the cellular level. Rats received 8-bromo-cGMP as an iv bolus 5 min before the start of the L-NAME infusion (78 µg/kg), followed by a continuous iv infusion of either 4 ($n = 7$) or 8 ($n = 7$) µg·kg⁻¹·min⁻¹ during the L-NAME administration.

Control experiments. Effect of Tempol, L-arginine, DEA-NONOate, and FeTPPS on basal glomerular permeability. Tempol ($n = 7$), L-arginine ($n = 6$), and DEA-NONOate ($n = 6$) were delivered in exactly the same doses (bolus + infusion) alone to animals in a control group without being coinfused with L-NAME. In five rats we delivered 10 mg/kg iv of the peroxynitrite scavenger 5,10,15,20-tetrakis(4-sulfonatophenyl)porphyrinato iron (III) chloride (FeTPPS, 341492; Merck, Darmstadt, Germany) 5 min before the start of measurements of sieving coefficients, θ for Ficoll, was measured at 5, 15, and 30 min.

Glomerular sieving of FITC-Ficoll. To assess glomerular sieving coefficients (θ) to Ficoll, urine was sampled for 5 min, and a blood sample (2 × 60 µl) was taken in the middle of each urine-collection period. A HPSEC (Waters, Milford, MA) was used for assessing the concentrations of FITC-Ficoll and FITC-inulin in urine and plasma samples. An autosampler (Waters 717 plus) was used for loading the samples on to the system. The mobile phase was driven by a pump (Waters 1525). Fluorescence was detected with a fluorescence detector (Waters 2475) at an excitation wavelength of 492 nm and an emission wavelength of 518 nm. The system was controlled by Breeze Software 3.3 (Waters). For size separation an Ultrahydrogel 500 column (Waters) was used and calibrated with Ficoll and protein standards as described at some length previously (1).

The sieving coefficients of FITC-Ficoll_{70A/400A} were determined as the fractional clearance (θ) from $\theta = (C_{FU} \times C_{IP}) / (C_{FP} \times C_{IU})$, where C_{FP} represents the concentration of Ficoll in the plasma and C_{FU}

represents the Ficoll concentration in the urine, C_{1P} represents the inulin concentration in the plasma, and C_{1U} the inulin concentration in the urine. The glomerular sieving coefficient to Ficoll 70Å (Ficoll_{70Å}) is, according to the so-called two-pore model (2–4, 6, 36, 47, 48), a representative marker of glomerular permeability due to alterations in the large pore number, and hence, Ficoll_{70Å} is presented as the main outcome variable throughout the study (Fig. 1).

In between Ficoll-sieving measurements, glomerular filtration rate (GFR) was measured (in the left kidney) throughout the experiments using ⁵¹Cr-EDTA. The urinary excretion of ⁵¹Cr-EDTA and/or FITC-inulin per minute ($U_i \times V_u$) divided by the concentration of tracer in plasma (P_i) was used to calculate GFR, where U_i represents the tracer concentration in the urine, and V_u represents the urine flow per minute. Blood (25 µl) was sampled for assessing the tracer concentration in the midpoint of the each urine-collecting period. Hematocrit was assessed throughout the experiments to convert blood radioactivity (⁵¹Cr-EDTA) to plasma radioactivity. The radioactivities in urine and blood were measured using a gamma counter (Wizard 1480; LKP, Wallak, Turku, Finland). Because the variability (coefficient of variance) of FITC-inulin-assessed GFR was slightly higher than that of ⁵¹Cr-EDTA-assessed GFR, we present the latter consistently throughout the study.

Statistical analysis. Values are presented as means ± SE. Statistical evaluation was performed in two steps. First, differences among groups were tested using a nonparametric ANOVA with the Kruskal-Wallis test and the Mann-Whitney *U*-test for post hoc testing, together with Bonferroni corrections. This analysis showed significant increases in θ for Ficoll_{70Å} after L-NAME alone and in the L-NAME-DEA-NONOate group at 15 min. In the second step we used a (parametric) mixed model ANOVA (type III SS) focusing on “phase” (baseline vs. 15 min) to analyze the difference in sieving coefficients between baseline and 15 min. Statistical calculations were performed with R software (version 3.3.0 for Windows) using the “afex” package. Post hoc contrasts were performed with the “lsmeans” package. The family-wise error rate was adjusted using the Holm-Bonferroni method. Significance levels were set at $P < 0.05$ (*), $P < 0.01$ (**), and $P < 0.001$ (***)

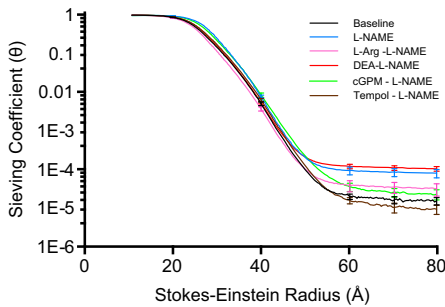


Fig. 1. Glomerular sieving coefficients (theta, θ) for Ficoll as a function of Stokes-Einstein radius (a_e) for baseline conditions in all groups (black line) and for the various interventions assessed at 15 min. During the permeability challenges there were no changes in θ for Ficoll_{10–49Å} in any of the experimental groups, indicating that there were no changes, according to the two-pore model, in the “small-pore radius”. Hence, all changes in θ occurred for high-molecular-weight Ficoll (Ficoll_{50–80Å}), reflecting an increase in large pore number during the permeability changes. (For levels of statistical significance, see Fig. 3.) Black line, baseline conditions ($t = 0$) for all experiments; blue line, L-NAME group; pink line, L-arginine-L-NAME group; red line, DEA-NONOate-L-NAME group; green line, 8-bromo-cGMP-L-NAME group; and brown line, Tempol-L-NAME group.

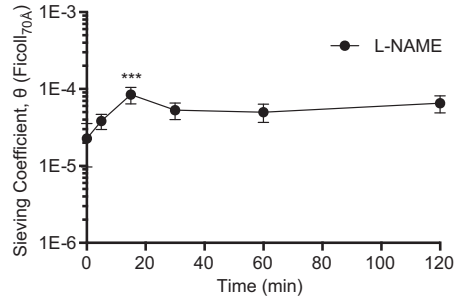


Fig. 2. Effects of L-NAME on θ for Ficoll_{70Å} as a function of infusion time. There was a significant increase in θ for Ficoll_{70Å} at 15 min, after which the permeability of the glomerular filtration barrier (GFB) tended to spontaneously reverse to baseline. Solid line, L-NAME group (***) $P < 0.001$ vs. baseline).

RESULTS

θ for Ficoll as a function of Stokes-Einstein radius (a_e). In Fig. 1 the glomerular sieving pattern for Ficoll_{10–80Å} is shown for baseline conditions (average baseline curve) and at 15 min for all experimental groups, illustrating that only the θ values for Ficoll_{50–80Å}, but not those for Ficoll_{10–49Å}, responded during the experimental interventions. According to the two-pore model of glomerular permeability (36), this implies that the so-called “small-pore pathway” (radius, approximately 45–47 Å) remained unaffected, whereas the “large-pore pathway” (radius, approximately 110–120 Å), permeable to HMW Ficoll and to albumin and larger proteins, was recruited to a variable extent during induced changes in glomerular permeability.

Effects of L-NAME on glomerular permeability. L-NAME increased the glomerular sieving coefficients (θ) to HMW Ficoll (Ficoll_{70Å}) at 15 min after the start of the L-NAME infusion, after which the permeability of the filtration barrier tended to spontaneously reverse to baseline at 30, 60, and 120 min (Fig. 2). For Ficoll_{70Å}, θ thus increased from $2.27 \times 10^{-5} \pm 1.31 \times 10^{-5}$ at baseline to $8.46 \times 10^{-5} \pm 2.07 \times 10^{-5}$ ($P < 0.001$) 15 min after the start of the L-NAME infusion, whereas θ values for Ficoll_{70Å} at 30 and 60 min were not found to be significantly elevated compared with baseline. Thus, θ for Ficoll_{70Å} was $5.29 \times 10^{-5} \pm 1.30 \times 10^{-5}$ ($P = 0.42$), $5.02 \times 10^{-5} \pm 1.33 \times 10^{-5}$ ($P = 0.30$), and $6.53 \times 10^{-5} \pm 1.61 \times 10^{-5}$ ($P = 0.14$) at 30, 60, and 120 min, respectively.

Effects of Tempol on L-NAME-induced increases in glomerular permeability. Tempol effectively counteracted the effects of L-NAME on glomerular permeability at 15 min. Thus, θ for Ficoll_{70Å} in the Tempol-L-NAME group was significantly lower ($1.04 \times 10^{-5} \pm 0.27 \times 10^{-5}$) than in the L-NAME group ($P < 0.001$) (Fig. 3).

Effects of L-arginine on L-NAME-induced increases in glomerular permeability. Systemic administration of L-arginine reduced the L-NAME-induced increase in glomerular permeability to Ficoll_{70Å} at 15 min after start of the L-NAME infusion (Fig. 3). Thus, θ values for Ficoll_{70Å} did not increase significantly at 15 min ($3.33 \times 10^{-5} \pm 1.02 \times 10^{-5}$) compared with baseline ($1.26 \times 10^{-5} \pm 0.10 \times 10^{-5}$, $P = 1.00$) (Fig. 3). The L-arginine-L-NAME group differed significantly ($P < 0.001$) from the L-NAME group at 15 min.

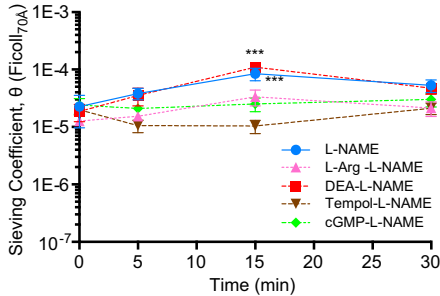


Fig. 3. Changes in θ for Ficoll_{70A} as a function of time for all the interventions made. Compared with L-NAME alone, Tempol, L-arginine, and 8-bromo-cGMP, when coinused with L-NAME, all prevented significant alterations in glomerular permeability at 15 min vs. baseline. However, there were no inhibitory effects of the NO-donor DEA-NONOate on the L-NAME induced increases in glomerular permeability at 15 min. Blue circles and solid blue line, L-NAME group; pink triangles and dotted pink line, L-arginine-L-NAME group; brown inverted triangles and brown dashed line, Tempol-L-NAME group; red squares and red dashed-dotted line, DEA-NONOate-L-NAME group; green diamonds and green dashed-double dotted line, 8-bromo-cGMP-L-NAME group. *** $P < 0.001$ vs. baseline.

Effects of DEA-NONOate on L-NAME-induced increases in glomerular permeability. DEA-NONOate given in a dose that did not allow more than a 15 mmHg reduction in MAP did not reverse the increased glomerular permeability at 15 min induced by L-NAME (Fig. 3). During the DEA-NONOate-L-NAME infusion, θ values for Ficoll_{70A} increased from $1.86 \times 10^{-5} \pm 0.62 \times 10^{-5}$ at baseline to $1.97 \times 10^{-5} \pm 1.49 \times 10^{-5}$ ($P < 0.001$) at 15 min (Fig. 3).

Effects of 8-bromo-cGMP on L-NAME-induced increases in glomerular permeability. 8-Bromo-cGMP in a dose-dependent manner inhibited the increases in glomerular permeability induced by L-NAME (Fig. 3). Thus, for an 8-bromo-cGMP dose of $8 \mu\text{g}\cdot\text{kg}^{-1}\cdot\text{min}^{-1}$, θ for Ficoll_{70A} remained largely unchanged at 15 min from baseline ($2.52 \times 10^{-5} \pm 0.67 \times 10^{-5}$ vs. $2.40 \times 10^{-5} \pm 0.73 \times 10^{-5}$, $P = 1.00$), whereas 50% of this dose of 8-bromo-cGMP was with borderline effect (data not shown).

Hemodynamics and GFR. Infusion rates were adjusted so as to maintain MAP within ± 15 mmHg from baseline. Hence, there were only small but significant ($P < 0.001$) increases in MAP for L-NAME alone, L-arginine-L-NAME, and Tempol-L-NAME during the course of the infusions except for DEA-NONOate (+L-NAME), which caused no significant changes in MAP at 15 min (Fig. 4). Not shown in the figure are the MAP values for L-NAME at 60 and 120 min, being 124.6 ± 4.7 and 126.3 ± 3.6 at 30 and 60 min, respectively. In the 8-bromo-cGMP-L-NAME group, the increase in MAP (at 15 min) was just borderline ($P = 0.048$). Although GFR remained largely unchanged over time in the L-NAME group, the L-arginine-L-NAME group, and the Tempol-L-NAME group, there were significant reductions in GFR, with a dip at 15 min (and 30 min) for the DEA-NONOate-L-NAME group ($P < 0.001$) and the 8-bromo-cGMP-L-NAME group ($P < 0.05$) (Fig. 5).

Control experiments. Effect of Tempol, L-arginine, DEA-NONOate, and FeTPPS on baseline glomerular permeability. In separate experiments, Tempol ($n = 7$), DEA-NONOate ($n =$

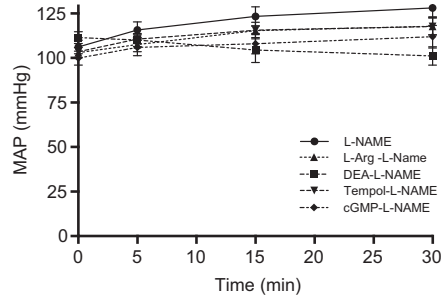


Fig. 4. Mean arterial pressure (MAP) as a function of time for the experimental groups. There were small but significant ($P < 0.001$) increases in blood pressure in the L-NAME group, the Tempol-L-NAME group, and the L-arginine-L-NAME group, whereas the MAP increase in the 8-bromo-cGMP-L-NAME group was barely significant ($P = 0.048$). The MAP changes in the DEA-NONOate-L-NAME group at 15 min vs. baseline were not statistically significant. Symbols are explained in Fig. 3, and used here without color coding.

6), and L-arginine ($n = 6$) were administered in exactly the same way as when they were coinused with L-NAME. To test whether peroxynitrite, the major reaction product of O_2^- and NO, might have had a protective effect with respect to glomerular permeability under baseline conditions, we administered 10 mg/kg of FeTPPS ($n = 5$), a peroxynitrite scavenger, and after 5 min, followed the effects for 30 min. There were no changes from baseline in glomerular permeability obtained with any of the compounds tested (Fig. 6).

DISCUSSION

NO plays a central role in a large number of biological processes, most notably in regulation of vascular tone and prevention of platelet aggregation, leukocyte adhesion, and in wound healing and inflammation. Furthermore, NO is of importance in regulating vascular barrier permeability. The present study demonstrated that systemic competitive inhibition of NOS in vivo using L-NAME rapidly increased glomerular permeability, an effect that could be abrogated by the SOD

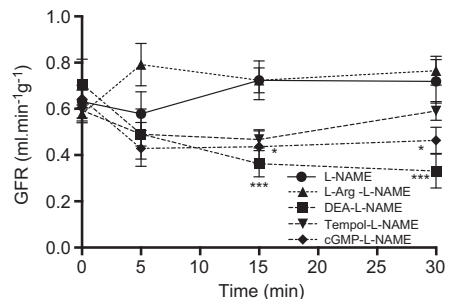


Fig. 5. Glomerular filtration rate (GFR) as a function of time in the experimental groups. There were significant reductions in GFR at 15 min (and 30 min) vs. baseline only for the DEA-NONOate-L-NAME group ($P < 0.001$) and for the 8-bromo-cGMP-L-NAME group ($P < 0.05$). Symbols are explained in Figs. 3 and 4.

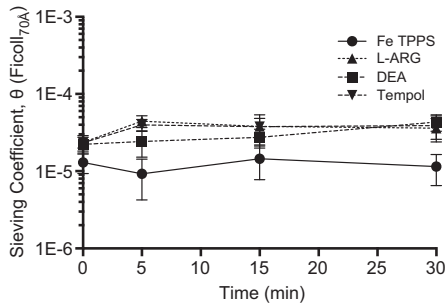


Fig. 6. Theta (θ) for Ficoll_{70A} as a function of time for (control) groups in which Tempol (inverted triangles and dotted line, $n = 7$), L-arginine (triangles and dashed line, $n = 6$), DEA-NONOate (filled squares and dashed-dotted line, $n = 6$), and FeTPPS (filled circles and solid line, $n = 5$) were given alone. There were no significant changes in θ for Ficoll_{70A} for any of the compounds given.

mimetic Tempol, and also the natural NOS substrate L-arginine, and by the cGMP agonist 8-bromo-cGMP. Under *in vivo* conditions, NO thus seems to exhibit a protective effect on glomerular permeability, conceivably by antagonizing ROS, and acting through the NO-sGC-cGMP pathway. This is largely in accordance with previous results obtained in isolated, nonperfused glomeruli *in vitro* (44, 45) and with the original observations by Kubes and Granger (24, 25) in feline mesenteric microvessels *in vivo*.

However, the role of NO and eNOS in regulating vascular permeability is controversial. Although there is agreement that moderate levels of NO release have a protective effect on vascular permeability, the role of elevated NO levels has been under intense debate for more than two decades. NO depletion in vessels or organs perfused with cell-free perfusates containing albumin seems to reduce permeability instead of increasing vascular permeability, and to be partly protective with respect to vascular integrity, especially after agonist stimulation with, for example, histamine or platelet-activating factor (21, 28, 40, 52, 53). In that respect, NO can be regarded as a “dual-edged sword”.

A number of factors and processes govern the activity of eNOS, the most well known perhaps being vascular shear stress, the level of intracellular Ca^{2+} , and chemical modification of the enzyme through phosphorylation (13, 14). A major regulator of eNOS activity is caveolin-1, which normally has an inhibitory effect. Caveolin-1 and eNOS are mostly colocalized in caveolae (lipid rafts). We have previously demonstrated that in caveolin-1 knockout ($Cav1^{-/-}$) mice that show increased eNOS activity and enhanced endothelial NO production, the glomerular permeability to HMW Ficoll (and albumin) remained normal, despite the fact that $Cav1^{-/-}$ mice showed a doubling in GFR (16). However, all in all, $Cav1^{-/-}$ mice showed an increased extravasation of macromolecules in a large number of vascular beds (39). This has been interpreted as reflecting an increased microvascular permeability following eNOS-induced NO overproduction. However, because eNOS activation (and increases in NO bioavailability) leads to precapillary vasodilatation, these changes are more likely to be consistent with increases in microvascular pressure, and hence, in pressure-induced macromolecular extravasation, rather than

due to an increased microvascular permeability (16, 36). It should be noted in this context that glomerular-sieving coefficients (θ) to macromolecules as assessed in the present study and, for example, in that by Grände et al. (16), are theoretically independent of capillary surface area and hydrostatic pressure, in contrast to assessments of just the rate of extravasation of macromolecules from the plasma to the tissues or to the urine.

In vivo, the activity of ROS is counteracted not only by NO, but also by a number of other endogenous antioxidants, the balance between ROS and their antagonists being delicate. Despite the *in vivo* conditions in the present study, implying the presence of a multitude of interacting oxidative and anti-oxidative processes, a reduction in glomerular NO production by NOS inhibition produced at least moderate and transient increases in glomerular permeability. Furthermore, the induced dysbalance between NO and ROS following NOS inhibition, which would create a relative increase in ROS bioavailability, could be efficiently restored by ROS (O_2^-) scavenging. In that respect, the present *in vivo* observations are similar to those made in isolated glomeruli *in vitro*. However, *in vitro*, there is no flow-mediated NO release, and, furthermore, normal plasma concentrations of oxidants/antioxidants or vasoconstrictors/vasodilators are not present. This may be the reason why in our *in vivo* study, the response to L-NAME was not as dramatic as that observed *in vitro*.

It should be pointed out that oxidative stress can negatively interact with NO in multiple ways, either directly or via NO generation through NOS and/or via the NO-sGC-cGMP pathway, and that these processes are not simply additive. BH_4 is a cofactor required for NO synthesis by NOS, and there is a stoichiometric relationship between BH_4 and NOS at which NO is produced in adequate quantities. If the BH_4 /NOS relationship is essentially lowered, as during oxidative stress, NOS will produce ROS (O_2^-) instead of NO, so-called NOS uncoupling. Oxidative stress will also affect the NO-sGC-cGMP pathway at the sGC level. Thus, oxidation of the heme group of sGC during oxidative stress will prevent the binding of NO to the sGC molecule, and hence, halt the downhill activation of cGMP. In the present study, the normal production of ONOO⁻ from NO and O_2^- apparently did not affect basal glomerular permeability, which remained intact even after scavenging of peroxynitrite.

The L-NAME-induced permeability alterations in the present *in vivo* study were reversible. Indeed, such a reversibility is commonly noted in peripheral microvascular beds after various permeability challenges (19, 29). A number of processes responsible for the restoration of barrier integrity have been described, such as receptor desensitization, activation of signaling pathways opposing endothelial retraction, activation of small GTPases (for reassembly of adherence junctions), release of endothelial barrier-stabilizing agents (26, 30), and increases in endogenous scavengers (e.g., endogenous SOD or catalase), etc. Many of these mechanisms, however, warrant further study.

We have previously demonstrated that the glomerular permeability changes occurring after, for example, systemic Ang II infusions or atrial natriuretic peptide infusions, are largely independent of glomerular hemodynamics (4, 6). In fact, after inhibiting the hemodynamic actions of systemic Ang II infusions, the Ang II-induced glomerular hyperpermeability remained entirely unaffected (4). In the present study we could competitively inhibit the permeability increases induced by

L-NAME by L-arginine in doses that did not cause major hemodynamic alterations compared with baseline. However, using the potent NO donor DEA-NONOate, systemic reductions in MAP, and particularly in GFR, occurred during coinfusion with L-NAME. Because MAP reductions more than 15 mmHg were not allowed, dose titration to levels of DEA-NONOate that would counteract the effects of L-NAME could not be performed. This may explain why DEA-NONOate was not found to be effective in antagonizing L-NAME in the present study. Conceivably, the threshold for eliciting vasodilatation might be lower than that for reducing an enhanced glomerular permeability. Indeed, quite high levels of NO may be needed to reverse an enhanced permeability, given the marked inhibition of sGC and the reduction in BH₄/NOS ratio that oxidative stress can produce.

The permeability of the GFB has been shown to be highly dynamic, in that θ for HMW Ficoll and albumin can reversibly increase by one or two orders of magnitude within just a few minutes (2–6, 47, 48). The precise nature of these acute permeability alterations is not known. The consensus today is that changes in any of the sequential barriers of the GFB (i.e., the endothelium with its glycocalyx, the glomerular basement membrane [GBM], and the podocyte layer with its slit diaphragms) can each induce marked changes in the permeability of the GFB. Although there is good evidence that the ultimate sieving barrier to proteins is not at the podocyte level (27, 37), podocytes are important for the barrier function in toto through their interactions with the rest of the GFB. Podocytes are anchored to the GBM by integrins, whereby they can, for example, mediate pressure on upstream layers of the GFB, and hence, modify its function without gross changes in cell shape occurring. The endothelial layer is also likely to be involved in regulation of glomerular permeability. This is in analogy with the formation of paracellular gaps in peripheral venules in response to various permeability challenges (9, 29). Paracellular gaps can open and close with a cycle time between 10 and 30 min (19, 29). To what extent the endothelial surface layer and its innermost part, the glycocalyx, is involved in the permeability changes observed in this study, is not known. However, the pattern of very dynamic and reversible alterations in glomerular permeability observed here makes the glomerular glycocalyx a less plausible morphological candidate to be affected by NOS inhibition.

In this study we followed θ for HMW FITC Ficoll (Ficoll_{70Å}), not θ for albumin, as a marker of glomerular permeability. The prerequisite for using radiolabeled albumin (e.g., ¹²⁵I-albumin) as a permeability marker in, for example, tissue uptake studies (2, 38), is that it must remain intact in the circulation and that the level of free label can be reduced to less than 0.1% of total marker activity. Because this could not be achieved in the present study, θ for albumin could not be accurately determined. However, in a number of previous studies we have shown a near-complete coupling of θ values for Ficoll_{70Å} and that for albumin whenever the permeability of the GFB has been altered (2, 6, 38). Thus, θ for Ficoll_{70Å} can be regarded as a sensitive and adequate marker of glomerular permeability.

Contrary to the established view (i.e., that the GFB is a very highly restrictive barrier to macromolecules compatible with a θ for albumin on the order of 10⁻⁴) (20), recent data based mainly on multiphoton electron microscopy of fluorescent albumin (or dextran) filtering across the GFB in superficial

glomeruli, have indicated that albumin θ values may be much higher; namely, 0.03–0.07 (11, 42). In that case, intact albumin has to be continually retrieved from the filtrate to the plasma by tubular reabsorption of 200–300 g albumin daily. Such a retrieval mechanism of intact albumin has yet to be discovered. Anyway, the concept of a leaky GFB and massive albumin retrieval has over the last decade started a heated debate on the fundamental mechanisms of proteinuria. The results from our group, however, entirely support the established view, which is also supported by micropuncture studies (12, 33, 50), results of inhibition of proximal tubular protein reabsorption (PTR) by lysine (49) or by studies in megalin-knockout mice (8). If the low permeability of the GFB to HMW Ficoll demonstrated here had been due to a high degree of PTR, then inhibition of PTR, as in the cooled isolated perfused kidney, would markedly increase θ for HMW Ficoll, which it does not. On the contrary, very low θ values for Ficoll_{55Å–70Å}, which are similar to the low θ value measured for albumin, are regularly obtained in the cooled isolated perfused kidney (20, 32).

In summary, acute systemic NOS inhibition in intact rats produced reversible increases in glomerular permeability, which were abrogated by the SOD mimetic Tempol and by L-arginine and the cGMP agonist 8-bromo-cGMP. Thus, it seems safe to conclude that NO plays an important role in maintaining normal glomerular permeability during in vivo conditions, and that these effects are partly exerted through ROS antagonism.

ACKNOWLEDGMENTS

We gratefully acknowledge Kerstin Wihlborg for skillfully typing the manuscript.

GRANTS

This study was supported by the Swedish Heart and Lung Foundation and the Medical Faculty at Lund University.

DISCLOSURES

No conflicts of interest, financial or otherwise, are declared by the authors.

AUTHOR CONTRIBUTIONS

K.S. and B.R. conceived and designed research; J.D. and A.R. performed experiments; J.D., A.R., C.M.Ö., and B.R. analyzed data; J.D., K.S., A.R., C.M.Ö., and B.R. interpreted results of experiments; A.R. prepared figures; J.D. and B.R. drafted manuscript; J.D., K.S., A.R., C.M.Ö., and B.R. edited and revised manuscript; J.D., K.S., A.R., C.M.Ö., and B.R. approved final version of manuscript.

REFERENCES

1. Asgerirsson D, Venturoli D, Rippe B, Rippe C. Increased glomerular permeability to negatively charged Ficoll relative to neutral Ficoll in rats. *Am J Physiol Renal Physiol* 291: F1083–F1089, 2006.
2. Axelsson J, Mahmutovic I, Rippe A, Rippe B. Loss of size selectivity of the glomerular filtration barrier in rats following laparotomy and muscle trauma. *Am J Physiol Renal Physiol* 297: F577–F582, 2009.
3. Axelsson J, Rippe A, Sverrisson K, Rippe B. Scavengers of reactive oxygen species, paricalcitol, RhoA and Rac-1 inhibitors and tacrolimus inhibit angiotensin II induced actions or glomerular permeability. *Am J Physiol Renal Physiol* 305: F237–F243, 2013.
4. Axelsson J, Rippe C, Öberg CM, Rippe B. Rapid, dynamic changes in glomerular permeability to macromolecules during angiotensin II (Ang II) infusion in rats. *Am J Physiol Renal Physiol* 303: F790–F799, 2012.
5. Axelsson J, Rippe A, Rippe B. mTOR inhibition with temsirolimus causes acute increases in glomerular permeability, but inhibits the dynamic permeability actions of puromycin aminonucleoside. *Am J Physiol Renal Physiol* 308: F1056–F1064, 2015.

6. Axelsson J, Rippe A, Rippe B. Transient and sustained increases in glomerular permeability following ANP infusion in rats. *Am J Physiol Renal Physiol* 300: F24–F30, 2011.
7. Baylis C. Nitric oxide deficiency in chronic kidney disease. *Am J Physiol Renal Physiol* 294: F1–F9, 2008.
8. Christensen EL, Birn H, Rippe B, Maunsbach AB. Controversies in nephrology: renal albumin handling, facts, and artifacts! *Kidney Int* 72: 1192–1194, 2007.
9. Curry FR, Adamson RH. Vascular permeability modulation at the cell, microvessel, or whole organ level: towards closing gaps in our knowledge. *Cardiovasc Res* 87: 218–229, 2010.
10. Daehn I, Casalena G, Zhang T, Shi S, Frenninger F, Barasch N, Yu L, D'Agati V, Schlondorff D, Kriz W, Haraldsson B, Bottinger EP. Endothelial mitochondrial oxidative stress determines podocyte depletion in segmental glomerulosclerosis. *J Clin Invest* 124: 1608–1621, 2014.
11. Dickson LE, Wagner MC, Sandoval RM, Molitoris BA. The proximal tubule and albuminuria: really! *J Am Soc Nephrol* 25: 443–453, 2014.
12. Eisenbach GM, Liew JB, Boylan JW, Manz N, Muir P. Effect of angiotensin on the filtration of protein in the rat kidney: a micropuncture study. *Kidney Int* 8: 80–87, 1975.
13. Féltóu M, Köhler R, Vanhoutte PM. Nitric oxide: orchestrator of endothelium-dependent responses. *Ann Med* 44: 694–716, 2012.
14. Féltóu M, Vanhoutte PM. Endothelial dysfunction: a multifaceted disorder (The Wiggers Award Lecture). *Am J Physiol Heart Circ Physiol* 291: H985–H1002, 2006.
15. Ferrario R, Takahashi K, Fogo A, Badr KF, Munger KA. Consequences of acute nitric oxide synthesis inhibition in experimental glomerulonephritis. *J Am Soc Nephrol* 4: 1847–1854, 1994.
16. Grande G, Rippe C, Rippe A, Rahman A, Swärd K, Rippe B. Unaltered size selectivity of the glomerular filtration barrier in caveolin-1 knockout mice. *Am J Physiol Renal Physiol* 297: F257–F262, 2009.
17. Granqvist A, Nilsson UA, Ebefors K, Haraldsson B, Nyström J. Impaired glomerular and tubular antioxidative defense mechanisms in nephrotic syndrome. *Am J Physiol Renal Physiol* 299: F898–F904, 2010.
18. Gwinner W, Landmesser U, Brandes RP, Kubat B, Plasger J, Eberhard O, Koch KM, Olbricht CJ. Reactive oxygen species and antioxidant defense in puromycin aminonucleoside glomerulopathy. *J Am Soc Nephrol* 8: 1722–1731, 1997.
19. Haraldsson B, Zackrisson U, Rippe B. Calcium dependence of histamine-induced increases in capillary permeability, studied in isolated rat hindlimbs. *Acta Physiol Scand* 128: 247–258, 1986.
20. Haraldsson B, Nyström J, Deen WM. Properties of the glomerular barrier and mechanisms of proteinuria. *Physiol Rev* 88: 451–487, 2008.
21. Hatakeyama T, Pappas PJ, Hobson RW 2nd, Boric MP, Sessa WC, Duran WN. Endothelial nitric oxide synthase regulates microvascular hyperpermeability in vivo. *J Physiol* 574: 275–281, 2006.
22. Hölschermann H, Noll T, Hempel A, Piper HM. Dual role of cGMP in modulation of macromolecule permeability of aortic endothelial cells. *Am J Physiol Heart Circ Physiol* 272: H91–H98, 1997.
23. Kietadorn R, Juni RP, Moens AL. Tackling endothelial dysfunction by modulating NOS uncoupling: new insights into its pathogenesis and therapeutic possibilities. *Am J Physiol Endocrinol Metab* 302: E481–E495, 2012.
24. Kubes P. Nitric oxide affects microvascular permeability in the intact and inflamed vasculature. *Microcirculation* 2: 235–244, 1995.
25. Kubes P, Granger DN. Nitric oxide modulates microvascular permeability. *Am J Physiol Heart Circ Physiol* 262: H611–H615, 1992.
26. Lum H, Malik AB. Mechanisms of increased endothelial permeability. *Can J Physiol Pharmacol* 74: 787–800, 1996.
27. Lund U, Rippe A, Venturoli D, Tenstad O, Grubb A, Rippe B. Glomerular filtration rate dependence of sieving of albumin and some neutral proteins in rat kidneys. *Am J Physiol Renal Physiol* 284: F1226–F1234, 2003.
28. Mayhan WG. Nitric oxide accounts for histamine-induced increases in macromolecular extravasation. *Am J Physiol Heart Circ Physiol* 266: H2369–H2373, 1994.
29. McDonald DM. Endothelial gaps and permeability of venules in rat tracheas exposed to inflammatory stimuli. *Am J Physiol Lung Cell Mol Physiol* 266: L61–L83, 1994.
30. Mehta D, Malik AB. Signaling mechanisms regulating endothelial permeability. *Physiol Rev* 86: 279–367, 2006.
31. Nagasu H, Satoh M, Kiyokage E, Kidokoro K, Toida K, Channon KM, Kanwar YS, Sasaki T, Kashiwara N. Activation of endothelial NAD(P)H oxidase accelerates early glomerular injury in diabetic mice. *Lab Invest* 96: 25–36, 2016.
32. Ohlson M, Sorensson J, Haraldsson B. Glomerular size and charge selectivity in the rat as revealed by FITC-Ficoll and albumin. *Am J Physiol Renal Physiol* 279: F84–F91, 2000.
33. Oken DE, Flamenbaum W. Micropuncture studies of proximal tubule albumin concentrations in normal and nephrotic rats. *J Clin Invest* 50: 1498–1505, 1971.
34. Persson J, Ekelund U, Grande PO. Nitric oxide and prostacyclin play a role in the regulation of microvascular protein and hydraulic permeability in cat skeletal muscle. *Microcirculation* 10: 233–243, 2003.
35. Predescu D, Predescu S, Shimizu J, Miyawaki-Shimizu K, Malik AB. Constitutive eNOS-derived nitric oxide is a determinant of endothelial junctional integrity. *Am J Physiol Lung Cell Mol Physiol* 289: L371–L381, 2005.
36. Rippe B, Haraldsson B. Transport of macromolecules across microvascular walls. The two-pore theory. *Physiol Rev* 74: 163–219, 1994.
37. Rippe C, Asgerisson D, Venturoli D, Rippe A, Rippe B. Effects of glomerular filtration rate on Ficoll sieving coefficients (theta) in rats. *Kidney Int* 69: 1326–1332, 2006.
38. Rippe C, Rippe A, Torffvit O, Rippe B. Size and charge selectivity of the glomerular filter in early experimental diabetes in rats. *Am J Physiol Renal Physiol* 293: F1533–F1538, 2007.
39. Rosengren BI, Rippe A, Rippe C, Venturoli D, Swärd K, Rippe B. Transvascular protein transport in mice lacking endothelial caveolae. *Am J Physiol Heart Circ Physiol* 291: H1371–H1377, 2006.
40. Rumbaut RE, McKay MK, Huxley VH. Capillary hydraulic conductivity is decreased by nitric oxide synthase inhibition. *Am J Physiol Heart Circ Physiol* 268: H1856–H1861, 1995.
41. Rumbaut RE, Wang J, Huxley VH. Differential effects of L-NAME on rat venular hydraulic conductivity. *Am J Physiol Heart Circ Physiol* 279: H2017–H2023, 2000.
42. Russo LM, Sandoval RM, McKee M, Osicka TM, Collins AB, Brown D, Molitoris BA, Comper WD. The normal kidney filters nephrotic levels of albumin retrieved by proximal tubule cells: retrieval is disrupted in nephrotic states. *Kidney Int* 71: 504–513, 2007.
43. Schulz A, Schütten-Faber S, Schulte L, Unland J, Kossmehl P, Kreutz R. Genetic variants on rat chromosome 8 exhibit profound effects on hypertension severity and survival during nitric oxide inhibition in spontaneously hypertensive rats. *Am J Hypertens* 27: 294–298, 2014.
44. Sharma M, Zhou Z, Miura H, Papapetropoulos A, McCarthy ET, Sharma R, Savin VJ, Lianos EA. ADMA injures the glomerular filtration barrier: role of nitric oxide and superoxide. *Am J Physiol Renal Physiol* 296: F1386–F1395, 2009.
45. Sharma M, McCarthy ET, Savin VJ, Lianos EA. Nitric oxide preserves the glomerular protein permeability barrier by antagonizing superoxide. *Kidney Int* 68: 2735–2744, 2005.
46. Suttorp N, Hippenstiel S, Fuhrmann M, Krull M, Podzuweit T. Role of nitric oxide and phosphodiesterase isoenzyme II for reduction of endothelial hyperpermeability. *Am J Physiol Cell Physiol* 270: C778–C785, 1996.
47. Sverrisson K, Axelsson J, Rippe A, Asgerisson D, Rippe B. Acute reactive oxygen species (ROS)-dependent effects of IL-1 β , TNF- α , and IL-6 on the glomerular filtration barrier (GFB) in vivo. *Am J Physiol Renal Physiol* 309: F800–F806, 2015.
48. Sverrisson K, Axelsson J, Rippe A, Gram M, Åkerström B, Hansson SR, Rippe B. Extracellular fetal hemoglobin induces increases in glomerular permeability: inhibition with α 1-microglobulin and tempol. *Am J Physiol Renal Physiol* 306: F442–F448, 2014.
49. Tencer J, Frick IM, Öqvist BW, Alm P, Rippe B. Size-selectivity of the glomerular barrier to high molecular weight proteins: upper size limitations of shunt pathways. *Kidney Int* 53: 709–715, 1998.
50. Tojo A, Endou H. Intrarenal handling of proteins in rats using fractional micropuncture technique. *Am J Physiol Renal Fluid Electrolyte Physiol* 263: F601–F606, 1992.
51. Yang B, Rizzo V. Shear stress activates eNOS at the endothelial apical surface through I containing integrins and caveolae. *Cell Mol Bioeng* 6: 346–354, 2013.
52. Yuan Y, Granger HJ, Zawieja DC, DeFily DV, Chilian WM. Histamine increases venular permeability via a phospholipase C-NO synthase-guanylate cyclase cascade. *Am J Physiol Heart Circ Physiol* 264: H1734–H1739, 1993.
53. Zhou X, He P. Endothelial [Ca²⁺]_i and caveolin-1 antagonistically regulate eNOS activity and microvessel permeability in rat venules. *Cardiovasc Res* 87: 340–347, 2010.

Paper II



RESEARCH ARTICLE | *Translational Physiology*

Glomerular hyperpermeability after acute unilateral ureteral obstruction: effects of Tempol, NOS, RhoA, and Rac-1 inhibition

Julia Dolinina,¹ Anna Rippe,¹ Peter Bentzer,^{2,3} and Carl M. Öberg¹

¹Department of Nephrology, Clinical Sciences Lund, Lund University, Lund, Sweden; ²Department of Anesthesiology and Intensive Care, Clinical Sciences Lund, Lund University, Lund, Sweden; and ³Department of Anesthesia and Intensive Care, Helsingborg Hospital, Helsingborg, Sweden

Submitted 11 December 2017; accepted in final form 16 February 2018

Dolinina J, Rippe A, Bentzer P, Öberg CM. Glomerular hyperpermeability after acute unilateral ureteral obstruction: Effects of Tempol, NOS, RhoA, and Rac-1 inhibition. *Am J Physiol Renal Physiol* 315: F445–F453, 2018. First published February 21, 2018; doi:10.1152/ajprenal.00610.2017.—It is well known that proteinuria following urinary tract obstruction is mainly of a tubular nature. However, it is unknown whether there are also changes in glomerular permeability. In this study, we compared glomerular sieving coefficients (θ) of polydisperse fluorescein isothiocyanate (FITC)-Ficoll 70/400 following a 120- or 180-min unilateral ureteral obstruction (UO) in anesthetized Sprague-Dawley rats. Samples were collected from the obstructed kidney at 5, 15, and 30 min postrelease and analyzed by means of high-pressure size-exclusion chromatography. After 120-min UO, mean θ for Ficoll_{70A} was increased ($P < 0.01$) from $2.2 \pm 0.5 \times 10^{-5}$ (baseline) to $10.6 \pm 10 \times 10^{-5}$ 15 min postrelease (highest value). After 180-min UO, mean θ for Ficoll_{70A} was further increased ($P < 0.001$) from $1.4 \pm 0.5 \times 10^{-5}$ (baseline) to $40 \pm 10 \times 10^{-5}$ at 5 min postrelease (highest value). Administration of a reactive oxygen species (ROS) scavenger (Tempol; $1 \text{ mg} \cdot \text{kg}^{-1} \cdot \text{min}^{-1}$) partly abrogated the permeability effects following 120-min UO but not after 180 min. Moreover, administration of the RhoA kinase inhibitor Y-27632, the nitric oxide synthase inhibitor *N*^G-nitro-L-arginine methyl ester, or Rac-1 inhibition did not ameliorate glomerular hyperpermeability following 180-min UO. We show, for the first time, that acute UO results in marked elevations in glomerular permeability. In addition, our data suggest a time-dependent pathophysiology of UO-induced hyperpermeability, where reactive oxygen species generation may play an important role in the early stages.

filtration barrier; glomerular; pore model; ureteral obstruction

INTRODUCTION

Complete, acute, urinary tract obstruction represents a medical emergency and will commonly result in severe flank pain and radiating pain to the thigh or groin region while a partial or nonacute obstruction that develops over time may go completely unnoticed. Nearly 20% of community-acquired cases of acute kidney injury have a postrenal etiology (8). If the obstruction is removed within a sufficiently short amount of time, the prognosis is generally good, suggesting that many of the pathophysiological changes that occur are of a reversible nature. After acute unilateral ureteral obstruction (UO), there is

an immediate rise in ureteral pressure with a subsequent rise in renal parenchymal (18) and tubular pressures (12, 42). Initially, there is an increase in renal blood flow (RBF) in the obstructed kidney (12, 18, 34, 40), as well as an increase in glomerular capillary pressure (12, 18), possibly leading to an essentially unchanged glomerular filtration rate (GFR) in this phase of obstruction (12). After a short intermediate phase with rising ureteral pressure and declining RBF, the ureteral pressure starts to decrease followed by severe renal vasoconstriction, and if the obstruction is not removed, complete failure of the obstructed kidney is unavoidable (40). Pioneering experiments using angiotensin II type 1 receptor blockade did not ameliorate this late phase vasoconstriction (23). By contrast, the initial vasodilation could be completely abrogated by nitric oxide synthase (NOS) inhibition while the late phase vasoconstriction could be counteracted by L-arginine infusion (a nitric oxide donor) (17, 40). In addition to hemodynamic alterations, one of the hallmark pathophysiological mechanisms in UO is that of interstitial fibrosis characterized by an increased production and deposition of extracellular matrix proteins, mainly collagen (13).

It is well established that tubular mechanisms contribute to the proteinuria observed following urinary tract obstruction (16, 41). It is however unknown whether alterations in glomerular permeability also occur following UO. In addition, while the hemodynamic effects of UO have been investigated before at some length (40), studies of glomerular permeability in UO are lacking. In this study, we investigate the effects on glomerular permeability induced by acute and 120- and 180-min unilateral ureteral obstruction (UO). We show that UO leads to marked increases in glomerular permeability for large Ficoll molecules in the range of 50–80 Å. Neither treatment with the reactive oxygen species (ROS) scavenger 4-hydroxytempo (Tempol) nor nitro-L-arginine methyl ester (L-NAME) had any effect on the glomerular hyperpermeability following 180-min UO while Tempol partly attenuated the glomerular hyperpermeability observed after 120-min UO. Indeed, oxidative stress has been identified as an important pathophysiological mechanism in UO (22). Furthermore, previous studies from our group have shown that ROS play an integral role in glomerular permeability (4, 36, 37). Similarly, Rho family GTPases such as RhoA and Rac-1 kinase have been shown to play an important role in maintaining glomerular filtration barrier integrity (39) as well as angiotensin II-mediated glomerular hyperpermeability (4). However, in the current study, neither RhoA nor Rac-1 kinase inhibition had any beneficial

Address for reprint requests and other correspondence: C. M. Öberg, Dept. of Nephrology, Alwall House, Barnagatan 2, Skåne Univ. Hospital, SE-211 85 Lund, Sweden (e-mail: carl.oberg@med.lu.se).

effect on 180-min UO. Our current findings support the view of a dynamic pathophysiology in UO where ROS are involved in the early stages.

METHODS

Animals. The experimental studies were performed in 32 male Sprague-Dawley rats (Møllegaard, Lille Stensved, Denmark) having a median body weight of 276 g (262–293 g) with free access to food and water. All procedures were approved by the local Animal Ethics Committee at Lund University.

Surgery. Anesthesia was induced by an intraperitoneal injection with pentobarbital (Pentobarbitalnatrium veterinary applied at 60 mg/ml), 90 mg/kg body wt, and maintained, if necessary, by administration of pentobarbital (3–6 mg) via the tail artery. A heating pad was used to maintain the body temperature at 37°C. A tracheotomy was performed (using a PE-240 tube) to facilitate breathing. The tail artery was cannulated (using a PE-50 cannula) and used for administration of furosemide (Furosemid Recip, Årsta, Sweden), maintenance of anesthesia, and continuous monitoring and registration of mean arterial blood pressure and heart rate (HR) on a data acquisition system (BioPack Systems model MP150 with AcqKnowledge software version 4.2.0; BioPack Systems, Goleta, CA). The left carotid artery was cannulated (PE-50) and used for blood sampling. The left and right internal jugular vein was cannulated (PE-50) for the administration of Ficoll and pharmacological interventions [Tempol, Rac-1 inhibitor (RAC1i), or Rho kinase inhibitor (RHOi)], respectively. A small abdominal incision (6–8 mm) was made to gain access to the left ureter. After a small dose of furosemide (0.375 mg/kg) to facilitate urine production (and cannulation), the ureter was dissected free and cannulated using a PE-10 cannula (connected to a PE-50 cannula), which was used for urine sampling. All connectors, cannulas, and tubes in contact with the circulation were prepared and flushed post-administration with a dilute heparin (Heparin LEO; 5,000 IU/ml) solution (~25 IU/ml in NaCl aqueous at 9 mg/ml) to prevent clotting.

Experimental procedure. All experiments started with a resting period of 20 min after the cannulation of the left ureter. After an initial 5-min period for control (baseline) measurements, the left ureter was carefully obstructed using a thin rubber band to avoid any trauma to the ureter. After either 120- or 180-min UO, the obstruction was released and followed by measurements of GFR, θ_{Ficoll} , MAP, and HR.

120-min UO groups. For 120-min UO the rats were divided into two groups: UO only and UO + Tempol. In the UO + Tempol group, the superoxide O_2^- scavenger Tempol (Sigma-Aldrich, St. Louis, MO) was given as a continuous infusion (1.2 mg·kg⁻¹·min⁻¹ iv) starting directly after ureteral obstruction.

180-min UO groups. For 180-min UO, the rats were divided into four separate experimental groups: UO only, UO + Tempol, UO + RAC1i, and UO + RHOi. The Tempol group received the same intravenous dose of Tempol as the 120-min group *vide infra*. Inhibitors of small GTPases, RHOi (Y-27632; Mitsubishi Pharma, Osaka, Japan) and RAC1i (NSC-23766, Calbiochem, San Diego, CA), were given as an intravenous bolus (RHOi: $n = 6$, bolus of 15 μg ; and RAC1i, $n = 6$, bolus of 12.5 μg) followed by continuous infusion (RHOi: 8.9 $\mu\text{g}\cdot\text{kg}^{-1}\cdot\text{min}^{-1}$ iv and RAC1i: 9.3 $\mu\text{g}\cdot\text{kg}^{-1}\cdot\text{min}^{-1}$ iv).

In a separate group, the competitive NOS inhibitor L-NAME (Sigma-Aldrich) was given as an initial bolus (470 $\mu\text{g}/\text{kg}$ iv) followed by a continuous infusion (93 $\mu\text{g}\cdot\text{kg}^{-1}\cdot\text{min}^{-1}$ iv) 10 min before release of the ureteral obstruction.

Determination of the glomerular sieving coefficient for Ficoll. During the entire course of the experimental procedure, a continuous intravenous infusion (10 ml·kg⁻¹·h⁻¹) of FITC-Ficoll (FITC-Ficoll-70, 20 $\mu\text{g}/\text{ml}$; FITC-Ficoll-400, 480 $\mu\text{g}/\text{ml}$; FITC-Inulin, 500 $\mu\text{g}/\text{ml}$; and ⁵¹Cr-EDTA, 0.3 MBq/ml) was given after an initial bolus dose (FITC-Ficoll-70, 40 μg ; FITC-Ficoll-400, 960 μg ; FITC-Inulin 0.5 mg; and ⁵¹Cr-EDTA 0.3 MBq). This 1:24 mixture of Ficoll provides

a broad range of molecular sizes. Sieving measurements were performed by a 5-min collection of urine from the left ureter with a midpoint (2.5 min) plasma sample.

Determination of GFR in the left kidney. ⁵¹Cr-EDTA (Amersham Biosciences, Buckinghamshire, UK) was given throughout the experiment (see above). Radioactivity in blood (CPM_{blood}) and urine (CPM_{urine}) was detected using a γ -counter (Wizard 1480, LKP; Wallac, Turku, Finland). The GFR for the left kidney was estimated from the plasma to urine clearance of ⁵¹Cr-EDTA.

High-performance size-exclusion chromatography. To determine the concentration and size distribution of the FITC-Ficoll samples, a HPLC system (Waters, Milford, MA) was used. The plasma and urine samples were size-separated using an Ultrahydrogel 500 column (Waters) connected to a guard column (Waters) using a phosphate buffer (0.15 M NaCl, pH 7.4) as the mobile phase. The mobile phase was driven by a pump (Waters 1525). Fluorescence was detected at an excitation wavelength of 492 nm and emission wavelength of 518 nm. An autosampler (Waters 717 plus) was used to load samples onto the system. The system was controlled by Breeze Software 3.3 (Waters). The system was calibrated using narrow Ficoll, Dextran, and protein standards as is described at some length in a previous article (2). The urine FITC-Ficoll concentration for each size (a_n) was divided by the urine FITC inulin concentration to obtain the concentration of Ficoll in primary urine (C_u). The glomerular sieving coefficient was then calculated by dividing C_u by the plasma concentration of Ficoll.

Distributed two-pore model. A distributed two-pore model (25) was used to analyze the θ -data for FITC-Ficoll (15–100 Å). Data were analyzed by means of nonlinear least squares regression to obtain the best curve fit as described previously (33).

Statistical analysis. Values are presented as means \pm SE unless otherwise stated. Main and interaction effects (time \times treatment) were assessed using a nonparametric factorial omnibus test as provided in the nparLD (24) package (version 2.1) for R (version 3.4.0, The R Foundation for Statistical Computing) giving a nonparametric ANOVA-type statistic and a Wald Type Statistic. In the presence of significant main effects without interactions, post hoc testing was performed using either a Friedman test (for time main effects) or a Kruskal-Wallis test (for treatment main effects) followed by pairwise comparisons using either a Wilcoxon-Nemenyi-McDonald-Thompson test (for Friedman test; see also Ref. 20, p. 296) or Wilcoxon tests (for Kruskal-Wallis) when appropriate. Significant interactions were tested using a 2 \times 2-factorial design (again using the nparLD package). Holm-Bonferroni corrections for multiple comparisons were made when applicable. Significance levels were set at $P < 0.05$, $P < 0.01$, and $P < 0.001$. All statistical calculations were performed using R 3.4.0 for Windows. Power analysis based on previous data (25) (using the pwr package for R) showed that four was the minimal number of animals needed to detect a difference in sieving coefficients by a factor of at least 2 using a two-tailed *t*-test assuming a statistical power of 0.80.

RESULTS

Glomerular hyperpermeability is induced in the obstructed kidney after 120-min UO, which is ameliorated by Tempol.

To determine the effects of acute UO on glomerular permeability, we studied the fractional clearance of polydisperse FITC-Ficoll in rats at baseline conditions and after 120-min UO. Figure 1 shows the glomerular sieving coefficients for 70 Å Ficoll (Ficoll_{70Å}) vs. time (baseline and 5, 15, and 30 min postrelease) for 120-min UO alone (solid line) compared with 120-min UO combined with treatment with Tempol (dashed line). A marked hyperpermeability was induced in the obstructed kidney with maximal increase in θ occurring 15 min postrelease. As can be seen, treatment with Tempol partly abrogated the hyperpermeability induced by UO at 15 and 30

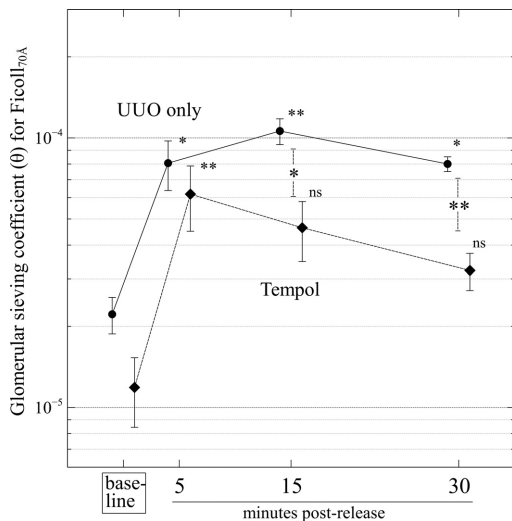


Fig. 1. Glomerular sieving coefficients for Ficoll_{70A} vs. time (baseline and 5, 15, and 30 min postrelease) for 120-min unilateral ureteral obstruction (UO) alone (solid line) compared with 120-min UO with an intervention of Tempol (dashed line).

min postrelease. No difference in sieving coefficients was observed at 5 min postrelease. Using the nonparametric omnibus test for longitudinal data (nparLD), the hypotheses of no effect for treatment (Tempol) and time (postrelease) were rejected at the 1 and 0.1% level, respectively. The hypothesis of no interaction was not rejected ($P = 0.08$). Post hoc testing revealed significant differences between untreated and Tempol-treated animals at 15 min ($P < 0.05$) and 30 min ($P < 0.01$) postrelease in addition to significant Friedman tests for both untreated ($P < 0.01$) and Tempol treated groups ($P < 0.05$) with respect to time (baseline, 5, 15, and 30 min postrelease). In Fig. 2, sieving curves (θ vs. Stokes-Einstein radius) are plotted for Ficoll molecules ranging from 15 to 80 Å in radius at baseline and 5, 15, and 30 min postrelease following 120-min UO. No sham group was included here; however, in previous publications (3, 5), rats receiving just saline for 120 min had no increase in permeability.

Pore model analysis after 120-min UO. A distributed two-pore model was used to analyze the sieving data, describing the glomerular filtration barrier (GFB) as a porous membrane having two log-normal pore size distributions having radii r_S (small-pore mean radius) and r_L (large-pore mean radius), respectively, and (geometric) standard deviations s_S (small-pore spread) and s_L (large-pore spread), respectively. The optimal parameters, obtained by means of nonlinear regression, providing the best curve fits of θ vs. a_e to the theoretical model, are shown in Table 1. In line with the above findings, a marked increase was observed in the relative water flux across the large-pore population (J_{V1}/GFR) indicating mainly an increase in the number of large pores. In contrast to the analysis of 70 Å sieving coefficients, the hypothesis of no interaction was rejected at the 5% level for J_{V1}/GFR . Post hoc

testing showed that Tempol ameliorated the hyperpermeability induced by UO at 15 and 30 min postrelease. Additionally there were small but significant changes in the large-pore radius and distribution spread.

Changes in MAP, HR, and GFR following 120-min UO. The MAP, HR, and GFR are shown in Table 2 at baseline and 5, 15, and 30 min postrelease following 120-min UO. GFR was increased following 120-min UO compared with baseline at 5 min for both groups whereas for the UO only group there were significant differences in GFR at all time points postrelease. The heart rate was significantly lower in both treatment groups at all time points postrelease. No differences in MAP between the groups and time points were observed.

Marked transient glomerular hyperpermeability is induced in the obstructed kidney after 180-min UO. We also studied the fractional clearance of polydisperse FITC-Ficoll in rats at baseline conditions and after 180-min UO. First, following 180-min UO, we however noted that Tempol did not seem to have any effect on the increased glomerular permeability. To investigate other possible mechanisms of UO-induced glomerular hyperpermeability, interventions in the form of RhoAi and RAC1i as well as a NOS inhibitor were tested. Figure 3 shows the glomerular θ for 70 Å Ficoll (Ficoll_{70A}) vs. time (baseline and 5, 15, and 30 min postrelease) for 180-min UO alone compared with 180-min UO with an intervention of either Tempol, RAC1i, or RHOi or endothelial nitric oxide synthase inhibitor. With the use of the nonparametric test for longitudinal data (nparLD), the hypothesis of no interaction (time \times treatment), i.e., parallel time profiles, was rejected at the 0.1% level ($P \approx 4.6 \cdot 10^{-4}$; $P < 0.001$). The main effect of time (baseline vs. 5, 15, and 30 min postrelease) was also

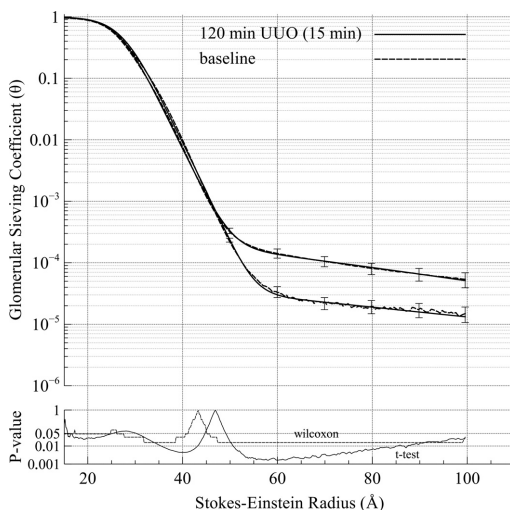


Fig. 2. Glomerular sieving coefficient (θ) vs. Stokes-Einstein radius at baseline and at 15 min following 120-min unilateral ureteral obstruction (UO). In a separate graph below the plotted sieving curve are P values from a common t -test (Welch's t -test) and a nonparametric (Wilcoxon signed-rank test) test comparing sieving coefficients in the 2 groups (baseline vs. 15 min postrelease).

Table 1. Two-pore parameters at baseline and 5, 15 and 30 min postrelease following 120-min UO

Treatment/Time	$r_s, \text{\AA}$	ss	$A_0/\Delta x, \ddagger \text{ cm} \times 10^5$	$r_L, \text{\AA}$	s_L	$J_{vL}/\text{GFR}, \times 10^{-1}$
UO only ($n = 7$)						
Baseline	36.3 ± 0.5	1.15 ± 0.00	9 ± 1	76 ± 10	1.5 ± 0.1	6 ± 1
5 min	35.0 ± 0.6	1.15 ± 0.00	12 ± 1	71 ± 4	1.44 ± 0.05	33 ± 8 ^a
15 min	34.8 ± 0.3	1.16 ± 0.00	12 ± 1	81 ± 6	1.43 ± 0.04	31 ± 4 ^{aa}
30 min	34.2 ± 0.3 ^{aaa}	1.16 ± 0.00 ^a	12 ± 1	90 ± 4	1.37 ± 0.02	25 ± 4
Tempol ($n = 7$)						
Baseline	36.5 ± 0.3	1.14 ± 0.00	7 ± 0	110 ± 20	1.50 ± 0.04	4 ± 1
5 min	35.0 ± 0.4 ^a	1.15 ± 0.00	10 ± 1	76 ± 5	1.38 ± 0.07	24 ± 5 ^{aa}
15 min	35.7 ± 0.4 ^a	1.15 ± 0.00	11 ± 1	82 ± 6	1.45 ± 0.06	16 ± 2 ^{#a}
30 min	34.7 ± 0.4	1.16 ± 0.00	12 ± 1 ^{aaa}	73 ± 8	1.48 ± 0.04 [#]	11 ± 2 ^{##}
ANOVA-type statistic						
Treatment	NS	NS	NS	NS	NS	*
Time	***	***	***	NS	NS	***
Interaction	NS	NS	NS	*	*	*

Values are given as means ± SE. UO, unilateral ureteral obstruction; r_s , small-pore mean radius; ss , small-pore distribution spread; r_L , large-pore radius; s_L , large-pore spread; α_L , fractional ultrafiltration coefficient accounted for by large pores; J_{vL}/GFR , fractional fluid flow through large pores/glomerular filtration rate; $A_0/\Delta x$ effective pore area over unit diffusion path length. †Refers to the left kidney. ^a $P < 0.05$, ^{aa} $P < 0.01$, compared with baseline within the same treatment group. [#] $P < 0.05$, ^{##} $P < 0.01$, compared with the same time point (baseline and 5, 15, and 30 min postrelease) in the UO-only group.

highly significant ($P < 0.001$). To investigate the question of whether the hypothesis of no interaction is rejected for each treatment group, multiple post hoc comparisons were performed by using the test repeatedly with the UO-only group vs. the other groups. The hypothesis of no interaction (parallel time profiles) was rejected for the RAC1i group vs. UO-only group ($P < 0.05$) and for the L-NAME group vs. UO-only group ($P < 0.01$). The GFR for the left kidney vs. time (baseline and 5, 15, and 30 min postrelease) is shown in Fig. 4 for UO-only group compared with the different interventions. There were no significant interactions for the different interventions compared with UO-only group ($P = 0.25$), but there were significant main effects for treatment ($P < 0.01$) and time (baseline vs. 5, 15, and 30 min postrelease; $P < 0.001$). Post hoc tests revealed a higher GFR at 5 min postrelease compared with baseline in both groups treated with the GTPase inhibitors RHOi (baseline vs. 5 min, $P < 0.05$) and RAC1i (baseline vs. 5 min $P < 0.05$). Additionally, GFR returned to baseline 30 min postrelease in the RHOi group (5 vs. 30

min $P < 0.01$). MAP, GFR and HR for the different groups are shown in Table 3.

Sieving curves at baseline vs. 5 min postrelease following 180-min UO. Figure 5 shows the glomerular sieving curves, i.e., the glomerular θ vs. the molecular Stokes-Einstein radius, for Ficoll molecules ranging from 15 to 100 Å in radius assessed at baseline and at 5 min postrelease. As can be seen, a marked glomerular hyperpermeability was observed 5 min postrelease after 180-min UO for large Ficolls. Shown in a separate graph below the sieving curve graph are P values from

Table 2. MAP, HR, and GFR at baseline and 5, 15, and 30 min postrelease following UO 120 min

Time	MAP, mmHg	HR, min ⁻¹	GFR, † ml/min
UO only ($n = 7$)			
Baseline	110 ± 6	355 ± 9	0.6 ± 0.1
5 min	106 ± 3	288 ± 9 ^a	0.8 ± 0.0 ^a
15 min	130 ± 20	330 ± 50 ^{aa}	0.7 ± 0.1 ^{aa}
30 min	112 ± 4	292 ± 8 ^a	0.7 ± 0.1 ^a
Tempol ($n = 6$)			
Baseline	108 ± 5	310 ± 20	0.5 ± 0.0
5 min	113 ± 3	250 ± 10 ^{aaa}	0.6 ± 0.1 ^{aa}
15 min	106 ± 4	260 ± 20	0.7 ± 0.1
30 min	104 ± 4	260 ± 20	0.7 ± 0.1
ANOVA-type statistic			
Treatment	NS	*	NS
Time	NS	***	**
Interaction	NS	NS	NS

Values are given as means ± SE. MAP, mean arterial pressure; HR, heart rate; GFR, glomerular filtration rate; UO, unilateral ureteral obstruction. †Refers to the left kidney. ^a $P < 0.05$, ^{aa} $P < 0.01$, compared with baseline in the same treatment group. [#] $P < 0.05$, compared with the same time point (baseline and 5, 15, and 30 min postrelease) in the UO-only group.

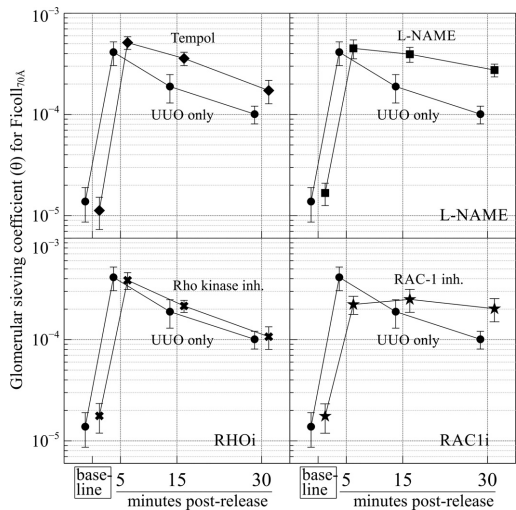


Fig. 3. Glomerular sieving coefficients for Ficoll_{100Å} vs. time (baseline and 5, 15, and 30 min postrelease) for 180-min unilateral ureteral obstruction (UO) alone (solid line) compared with 180-min UO with an intervention of either Tempol (dashed line), Rac-1 inhibitor (RAC1i; dotted line), Rho kinase inhibitor (RHOi; dash-dot line), or endothelial nitric oxide synthase inhibitor (eNOSi; dash-dot-dot line).

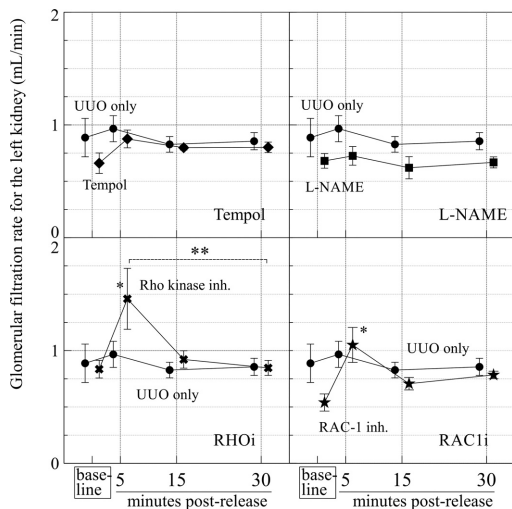


Fig. 4. Glomerular filtration rate (GFR) vs. time (baseline and 5, 15 and 30 min postrelease) for 180-min unilateral ureteral obstruction (UO) alone (filled circle) compared with 180-min UO with an intervention of either Tempol (diamond), Rac-1 inhibitor (RAC1i), (star); Rho kinase inhibitor (RHOi), (cross); or endothelial nitric oxide synthase inhibitor (eNOSi; square).

parametric (Welch's *t*-test) and nonparametric (Wilcoxon signed-rank test) tests comparing sieving coefficients in the two groups (baseline vs. 5 min postrelease) (Fig. 6). Both tests were significant for Ficolls larger than ~44 Å.

Pore model analysis after 180-min UO. For the pore analysis of 180-min UO, shown in Table 4, the hypothesis of no interaction (parallel time profiles) was rejected for the RAC1i group vs. UO only group ($P < 0.01$) for J_{vL}/GFR . Post hoc analysis shows a transient increase in the number of large pores, with the maximum increase in the fractional large-pore fluid flux (J_{vL}/GFR) occurring 5 min postrelease. By contrast, there were no significant differences in the mean large-pore radius (r_L) or the large-pore distribution spread (s_L) indicating that the size-selective properties of the large-pore pathway seem to be unchanged following 180-min UO. There were also small, but significant, differences in the small-pore mean radius (r_s) and the small-pore distribution spread (s_s).

Comparison of glomerular hyperpermeability following 120- vs. 180-min UO. In a separate analysis, we compared the sieving coefficients as a function time (baseline and 5, 15 and 30 min postrelease) following 120- vs. 180-min UO. As can be seen, the longer duration of obstruction caused a larger increase in permeability. In a small number of animals, we also tested 90 min UO which gave a smaller increase than that found following 120-min UO (data not shown). In addition to a larger increase in permeability, 180-min UO apparently has a different time course compared with 120-min UO. Between the groups, the hypothesis of no interaction was rejected at the 0.1% level ($P < 0.001$), indicating a slower recovery in the group of animals receiving 120-min UO.

DISCUSSION

In the current study we show, for the first time, that acute UO results in a marked, transient, glomerular hyperpermeability for large molecules. The observed changes in permeability were partly ameliorated by the ROS scavenger Tempol after 120 min but not after 180 min, indicating a dynamic, time-dependent, pathophysiology of UO where ROS may play an important role in the early stages. In addition, small but significant changes in the small-pore population, being more pronounced following 180-min UO, indicate early structural damage to the GFB following UO.

ROS, formed by the incomplete reduction of oxygen, have been shown to play an important role in a number of different disease processes such as diabetic nephropathy (27), ischemic acute kidney injury, and renal graft rejection (9). Furthermore, ROS are involved in regulating normal biological processes such as cell defense, gene expression, and activation of G protein-coupled receptors. The mechanisms by which ROS induce glomerular hyperpermeability may, in part, be elucidated from *in vitro* studies and could involve ROS-induced prostaglandin E_2 production (10, 11, 32), facilitation of TNF- α production (10, 36), and direct structural damages by direct oxidation of membrane lipids and other cellular components (9). Moreover, it is well established that angiotensin II can induce glomerular hyperpermeability (4, 6, 31) (independ-

Table 3. MAP, HR, and GFR at baseline and 5, 15, and 30 min postrelease following 180-min UO

Treatment/Time	MAP, mmHg	HR, min ⁻¹	GFR,† ml/min
UO only (<i>n</i> = 7)			
Baseline	108 ± 5	340 ± 10	0.9 ± 0.2
5 min	113 ± 5	300 ± 20	1.0 ± 0.1
15 min	111 ± 5	290 ± 20	0.8 ± 0.1
30 min	108 ± 5	320 ± 30	0.9 ± 0.1
Tempol (<i>n</i> = 6)			
Baseline	106 ± 4	340 ± 20	0.7 ± 0.1
5 min	113 ± 3	290 ± 30	0.9 ± 0.1
15 min	110 ± 4	290 ± 30	0.8 ± 0.0
30 min	106 ± 4	280 ± 20	0.8 ± 0.0
RHOi (<i>n</i> = 6)			
Baseline	113 ± 4	330 ± 20	0.8 ± 0.1
5 min	102 ± 7	300 ± 30	1.5 ± 0.2 ^a
15 min	101 ± 6	300 ± 30	0.9 ± 0.1
30 min	102 ± 5	300 ± 30	0.8 ± 0.1 ^{bb}
RAC1i (<i>n</i> = 6)			
Baseline	105 ± 3	320 ± 10	0.5 ± 0.1
5 min	105 ± 4	260 ± 20	1.1 ± 0.1 ^a
15 min	102 ± 5	270 ± 20	0.7 ± 0.1
30 min	101 ± 4	270 ± 20	0.8 ± 0.0
L-NAME (<i>n</i> = 7)			
Baseline	102 ± 4	310 ± 10	0.7 ± 0.1
5 min	125 ± 6	270 ± 20	0.7 ± 0.1
15 min	120 ± 6	270 ± 20	0.6 ± 0.1
30 min	121 ± 8	270 ± 20	0.7 ± 0.0
ANOVA-type statistic			
Treatment	NS	NS	**
Time	NS	***	***
Interaction	*	NS	NS

Values are given as means ± SE. MAP, mean arterial pressure; HR, heart rate; GFR, glomerular filtration rate; UO, unilateral ureteral obstruction; RAC1i, Rac-1 inhibitor; RHOi, Rho kinase inhibitor; L-NAME, nitro-L-arginine methyl ester. †Refers to the left kidney. ^a $P < 0.05$, compared with baseline within the same treatment group. ^{bb} $P < 0.01$, compared with 5 min postrelease within the same treatment group.

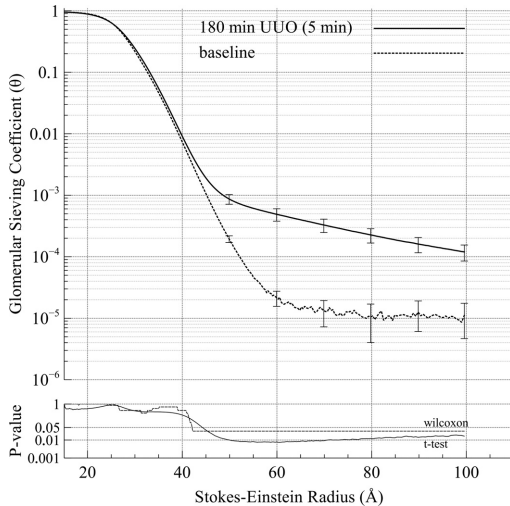


Fig. 5. Glomerular sieving coefficient (θ) vs. Stokes-Einstein radius at baseline and at 5 min following 180-min of unilateral ureteral obstruction (UUO). In a graph below the plotted sieving curve are P values from a common t -test (Welch's t -test) and a nonparametric (Wilcoxon signed-rank test) test comparing sieving coefficients in the t2 groups (baseline vs. 5 min postrelease).

dent of intraglomerular pressure) and it is possible that activation of the renin-angiotensin-aldosterone system (RAAS) is involved in the permeability changes caused by UUO. In a previous study from our group, we demonstrated that glomerular hyperpermeability induced by angiotensin II (6) could be inhibited both by Tempol as well as inhibitors of Rac-1 and RhoA (4). From a mechanistic standpoint, it is conceivable that acute UUO leads to the release of renin in the obstructed kidney following decreased sodium delivery to the macula densa. However, while it is possible that RAAS activation may play a role in the early phases following obstruction, several studies have failed to show any effects of RAAS blockade on the afferent arteriolar vasoconstriction occurring in long-term obstruction (1). Additionally, the current finding that neither Tempol nor RhoA inhibition had any effect after 180-min UUO implies that the observed increases in glomerular permeability both after 120 and 180 min are not mediated by angiotensin II since the renin activity has a half-life well over 1 h (9). By contrast, there is evidence that the RAAS system is activated after as little as 1 h of UUO (28). Moreover, angiotensin II seems to modulate the inflammatory response in UUO (15) and has been implied in the pathogenesis of the tubulo-interstitial fibrosis occurring in the obstructed kidney (21). Following 180-min UUO, RAC-1 but not RhoA inhibition affected the time course of the changes in glomerular permeability indicating a possible involvement of the actin cytoskeleton (38). Lastly, NOS inhibition using L-NAME appears to lead to a slower recovery of the hyperpermeability caused by 180-min UUO but had no effect on the initial increase in permeability. In a recent study from our group (14), we showed that NOS inhibition per se induced glo-

merular hyperpermeability, which may explain the current findings.

Loss of statistical power due to correction for multiple comparisons (e.g., using Bonferroni correction) is a common problem when measurements are performed at several time points. Here we used a nonparametric omnibus test for longitudinal data (24), which enabled us to compare entire time profiles of an observed main effect (e.g., MAP, θ) for two or more interventions instead of comparing individual time points. Since the intervention is not given until after the first measurement timepoint (baseline), any significant treatment effect will cause the time profiles (intervention vs. UUO only) to be nonparallel, leading to a significant interaction (time \times effect). In addition, nonparametric methods do not require distributional assumptions and are generally assumed to be more robust to small sample sizes and outliers. A very common misconception is that parametric tests inflate the type I (false positive) error rate. This belief may have originated from the superior power of parametric tests for normal data. This superiority however does not seem to extend to nonnormal data. By contrast, for several nonnormal distributions, nonparametric tests have been found to have superior power compared with parametric tests (43). Additionally, empirical studies have demonstrated that t -tests do not inflate the type I (false positive) error rate even when the data are clearly nonnormal and sample sizes are small (19, 35). Thus concerns over the relative advantages of parametric vs. nonparametric tests should focus on the type II (false negative) error rate, i.e., the application of nonparametric tests on normal data. Regardless of what sort of test one may favor, in the present study both parametric and nonparametric tests showed an increased fractional clearance of Ficoll_{70A} larger than 44 Å after UUO,

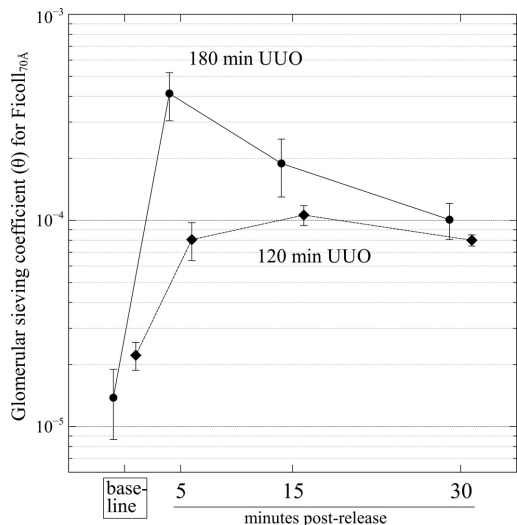


Fig. 6. Glomerular sieving coefficients for Ficoll_{70A} vs. time (baseline and 5, 15 and 30 min postrelease) for 180-min unilateral ureteral obstruction (UUO) (solid line) compared with 120-min UUO (dashed line).

Table 4. Two-pore parameters at baseline and 5, 15, and 30 min postrelease at baseline and after 180-min UO

Treatment/Time	r_s , Å	s_s	$A_0/\Delta x$, \uparrow cm $\times 10^5$	r_L , Å	s_L	J_{vL}/GFR , $\times 10^{-5}$
UUO only ($n = 7$)						
baseline	34.2 \pm 0.6	1.16 \pm 0.00	15 \pm 2	70 \pm 10	1.5 \pm 0.1	3 \pm 1
5 min	36.2 \pm 0.7	1.14 \pm 0.01	14 \pm 2	72 \pm 4	1.40 \pm 0.02	160 \pm 30 ^{aaa}
15 min	34.3 \pm 0.4	1.16 \pm 0.00	14 \pm 1	75 \pm 3	1.40 \pm 0.01	60 \pm 10 ^a
30 min	32.8 \pm 0.6 ^b	1.18 \pm 0.01 ^b	16 \pm 2	75 \pm 6	1.45 \pm 0.03	31 \pm 6 ^b
Tempol ($n = 6$)						
baseline	34.0 \pm 0.4	1.16 \pm 0.00	11 \pm 1	70 \pm 20	1.50 \pm 0.04	7 \pm 3
5 min	35.9 \pm 0.6	1.15 \pm 0.01	13 \pm 1	68 \pm 2	1.46 \pm 0.03	200 \pm 20 ^{aaa}
15 min	33.8 \pm 0.4 ^b	1.17 \pm 0.00	14 \pm 0	82 \pm 7	1.45 \pm 0.06	110 \pm 20 ^a
30 min	33.2 \pm 0.4 ^{bb}	1.17 \pm 0.01 ^{bb}	14 \pm 1	80 \pm 20	1.44 \pm 0.06	47 \pm 7 ^b
RHOi ($n = 6$)						
baseline	34.8 \pm 0.3	1.16 \pm 0.00	13 \pm 1	90 \pm 20	1.5 \pm 0.1	4 \pm 1
5 min	34.0 \pm 0.6	1.16 \pm 0.01	25 \pm 5 ^{aaa}	73 \pm 6	1.54 \pm 0.08	110 \pm 20 ^{aaa}
15 min	32.9 \pm 0.6	1.17 \pm 0.01 ^b	17 \pm 2	75 \pm 5	1.48 \pm 0.05	64 \pm 6 ^a
30 min	32.3 \pm 0.6 ^{aa,b}	1.18 \pm 0.00 ^{aa,bb}	16 \pm 2	66 \pm 1 ^{##}	1.55 \pm 0.03	32 \pm 7
RACi ($n = 6$)						
baseline	36.2 \pm 0.4	1.15 \pm 0.00	8 \pm 1	70 \pm 10	1.37 \pm 0.3	15 \pm 3
5 min	36.5 \pm 0.5	1.14 \pm 0.00	15 \pm 2 ^{aaa}	62 \pm 2	1.50 \pm 0.05	100 \pm 30 ^{aaa}
15 min	34.5 \pm 0.2 ^b	1.16 \pm 0.00	12 \pm 1	66 \pm 3	1.52 \pm 0.07	80 \pm 20
30 min	33.7 \pm 0.3 ^{aa,bb}	1.16 \pm 0.00 ^{bb}	13 \pm 1 ^a	68 \pm 2	1.55 \pm 0.02	53 \pm 9
L-NAME ($n = 7$)						
baseline	36.1 \pm 0.3	1.15 \pm 0.00	10 \pm 1	70 \pm 10	1.6 \pm 0.1	4 \pm 0
5 min	36.7 \pm 0.4	1.14 \pm 0.00	10 \pm 1	80 \pm 8	1.37 \pm 0.03	150 \pm 30 ^{aa}
15 min	35.0 \pm 0.6 ^b	1.16 \pm 0.01	10 \pm 2	90 \pm 10	1.38 \pm 0.05	120 \pm 30 ^{aaa}
30 min	33.9 \pm 0.4 ^{a,b}	1.18 \pm 0.00 ^{a,bb}	11 \pm 1	130 \pm 20	1.36 \pm 0.05	70 \pm 20
ANOVA-type statistic						
Treatment	**	*	***	*	NS	NS
Time	***	***	***	**	NS	***
Interaction	NS	NS	NS	NS	*	*

Values are given as means \pm SE. UUO, unilateral ureteral obstruction; RACi, Rac-1 inhibitor; RHOi, Rho kinase inhibitor (RHOi); L-NAME, nitro-L-arginine methyl ester; r_s , small-pore mean radius; s_s , small-pore distribution spread; r_L , large-pore radius; s_L , large-pore spread; α_L , fractional ultrafiltration coefficient accounted for by large pores; J_{vL}/GFR , fractional fluid flow through large pores; GFR, glomerular filtration rate; $A_0/\Delta x$ effective pore area over unit diffusion path-length. \uparrow Refers to the left kidney. ^a $P < 0.05$, ^{aa} $P < 0.01$, ^{aaa} $P < 0.001$, compared with baseline within the same treatment group. ^b $P < 0.05$, ^{bb} $P < 0.01$, compared with 5 min postrelease within the same treatment group. ^{##} $P < 0.01$, compared with the same time point (baseline and 5, 15, and 30 min postrelease) in the UUO-only group.

implying that the size-selective “small-pore” pathway excludes Ficolls smaller than this size.

For more than three decades the two-pore model (29, 30) has been applied for the quantification of solute and water transport across renal microvascular walls (6) and recently also to dialyzer filters (7). The phenomenological nature of the two-pore model means that it gives no information about the actual anatomical structure of the GFB, being highly complex, but rather, describes the GFB in terms of an equivalent porous membrane having a small- and large-pore population. In the current work we used both parametric and nonparametric statistical tests comparing normal and elevated UUO-induced permeability showing that the transition between the large- and small-pore population occurs at ~ 44 Å. It is hypothesized that the selective pathway (the small pores) is nearly completely impermeable to serum albumin where charge selectivity may play an important role via a so called “fringe effect” (26). Thus the main filtration barrier in the kidney is represented by the small-pore population, and changes in the properties of the small-pore population are typically associated with structural damage. By contrast, the large-pore population is highly dynamic and its properties can change dramatically within a short period of time. It is presently unknown what mechanisms regulate large-pore permeability, but alterations in podocyte cytoskeletal structures have been implied (6).

Much remains to be learned about the complex and dynamic pathophysiology of UUO-induced kidney injury. We here provide evidence that marked glomerular hyperpermeability is induced by acute UUO, where a longer duration leads to more pronounced alterations in permeability, which may in part be of a structural nature. There is growing evidence that ultrafiltrated proteins contribute to the tubulointerstitial damage and fibrosis when the permeability of the GFB is compromised (1). Increases in glomerular permeability may thus be an important driving mechanism in the progressive renal injury occurring during urinary tract obstruction. While early changes in permeability seem to be mediated by ROS, the mechanisms leading to glomerular hyperpermeability following obstruction for longer time periods remain to be elucidated.

GRANTS

This study was supported by the Swedish Heart and Lung Foundation and the Medical Faculty at Lund University.

DISCLOSURES

No conflicts of interest, financial or otherwise, are declared by the authors.

AUTHOR CONTRIBUTIONS

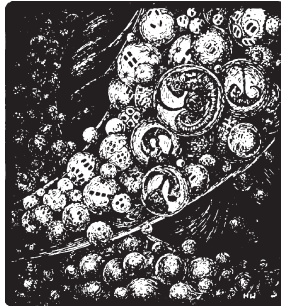
J.D. and C.M.x. conceived and designed research; J.D. and A.R. performed experiments; A.R. and C.M.x. analyzed data; J.D., P.B., and C.M.x. interpreted results of experiments; C.M.x. prepared figures; J.D. and C.M.x. drafted

manuscript; J.D., A.R., P.B., and C.M.x. edited and revised manuscript; J.D., A.R., P.B., and C.M.x. approved final version of manuscript.

REFERENCES

- Abbate M, Zoja C, Remuzzi G. How does proteinuria cause progressive renal damage? *J Am Soc Nephrol* 17: 2974–2984, 2006. doi:10.1681/ASN.2006040377.
- Asgerirsson D, Venturoli D, Rippe B, Rippe C. Increased glomerular permeability to negatively charged Ficoll relative to neutral Ficoll in rats. *Am J Physiol Renal Physiol* 291: F1083–F1089, 2006. doi:10.1152/ajprenal.00488.2005.
- Axelsson J, Mahmutovic I, Rippe A, Rippe B. Loss of size selectivity of the glomerular filtration barrier in rats following laparotomy and muscle trauma. *Am J Physiol Renal Physiol* 297: F577–F582, 2009. doi:10.1152/ajprenal.00246.2009.
- Axelsson J, Rippe A, Sverrisson K, Rippe B. Scavengers of reactive oxygen species, paracalcitol, RhoA, and Rac-1 inhibitors and tacrolimus inhibit angiotensin II-induced actions on glomerular permeability. *Am J Physiol Renal Physiol* 305: F237–F243, 2013. doi:10.1152/ajprenal.00154.2013.
- Axelsson J, Rippe A, Venturoli D, Swärd P, Rippe B. Effects of early endotoxemia and dextran-induced anaphylaxis on the size selectivity of the glomerular filtration barrier in rats. *Am J Physiol Renal Physiol* 296: F242–F248, 2009. doi:10.1152/ajprenal.90263.2008.
- Axelsson J, Rippe A, Öberg CM, Rippe B. Rapid, dynamic changes in glomerular permeability to macromolecules during systemic angiotensin II (ANG II) infusion in rats. *Am J Physiol Renal Physiol* 303: F790–F799, 2012. doi:10.1152/ajprenal.00153.2012.
- Axelsson J, Öberg CM, Rippe A, Krause B, Rippe B. Size-selectivity of a synthetic high-flux and a high cut-off dialyzing membrane compared to that of the rat glomerular filtration barrier. *J Membr Sci* 413: 29–37, 2012. doi:10.1016/j.memsci.2012.03.001.
- Basile DP, Anderson MD, Sutton TA. Pathophysiology of acute kidney injury. *Compr Physiol* 2: 1303–1353, 2012. doi:10.1002/cphy.c110041.
- Baud L, Ardaillou R. Reactive oxygen species: production and role in the kidney. *Am J Physiol Renal Fluid Electrolyte Physiol* 251: F765–F776, 1986. doi:10.1152/ajprenal.1986.251.5.F765.
- Baud L, Fouqueray B, Philippe C, Ardaillou R. Reactive oxygen species as glomerular autacoids. *J Am Soc Nephrol* 2, Suppl: S132–S138, 1992.
- Chizzolini C, Brembilla NC. Prostaglandin E2: igniting the fire. *Immunol Cell Biol* 87: 510–511, 2009. doi:10.1038/icc.2009.56.
- Dal Canton A, Stanziale R, Corradi A, Andreucci VE, Migone L. Effects of acute ureteral obstruction on glomerular hemodynamics in rat kidney. *Kidney Int* 12: 403–411, 1977. doi:10.1038/ki.1977.131.
- Ding Y, Kim S, Lee SY, Koo JK, Wang Z, Choi ME. Autophagy regulates TGF- β expression and suppresses kidney fibrosis induced by unilateral ureteral obstruction. *J Am Soc Nephrol* 25: 2835–2846, 2014. doi:10.1681/ASN.2013101068.
- Dolinina J, Sverrisson K, Rippe A, Öberg CM, Rippe B. Nitric oxide synthase inhibition causes acute increases in glomerular permeability in vivo, dependent upon reactive oxygen species. *Am J Physiol Renal Physiol* 311: F984–F990, 2016. doi:10.1152/ajprenal.00152.2016.
- Esteban V, Lorenzo O, Rupérez M, Suzuki Y, Mezzano S, Blanco J, Kretzler M, Sugaya T, Egido J, Ruiz-Ortega M. Angiotensin II, via AT1 and AT2 receptors and NF- κ B pathway, regulates the inflammatory response in unilateral ureteral obstruction. *J Am Soc Nephrol* 15: 1514–1529, 2004. doi:10.1097/01.ASN.0000130564.75008.F5.
- Everaert K, Kerckhaert W, Delanghe J, Lameire N, Sturley W, Van de Wiele C, Dieckers RA, Van de Voorde J, Oosterlinck W. Elevated tubular proteinuria, albuminuria and decreased urinary N-acetyl-beta-D-glucosaminidase activity following unilateral total ureteral obstruction in rats. *Urol Res* 26: 285–289, 1998. doi:10.1007/s002400050059.
- Felsen D, Schulzinger D, Gross SS, Kim FY, Marion D, Vaughan ED Jr. Renal hemodynamic and ureteral pressure changes in response to ureteral obstruction: the role of nitric oxide. *J Urol* 169: 373–376, 2003. doi:10.1016/S0022-5347(05)64130-4.
- Gilmore JP. Influence of tissue pressure on renal blood flow autoregulation. *Am J Physiol* 206: 707–713, 1964.
- Heeren T, D'Agostino R. Robustness of the two independent samples t-test when applied to ordinal scaled data. *Stat Med* 6: 79–90, 1987. doi:10.1002/sim.478006110.
- Hollander M, Wolfe DA. *Nonparametric Statistical Methods*. New York: John Wiley & Sons, 1999.
- Ishidoya S, Morrissey J, McCracken R, Reyes A, Klahr S. Angiotensin II receptor antagonist ameliorates renal tubulointerstitial fibrosis caused by unilateral ureteral obstruction. *Kidney Int* 47: 1285–1294, 1995. doi:10.1038/ki.1995.183.
- Kawada N, Moriyma T, Ando A, Fukunaga M, Miyata T, Kurokawa K, Imai E, Hori M. Increased oxidative stress in mouse kidneys with unilateral ureteral obstruction. *Kidney Int* 56: 1004–1013, 1999. doi:10.1046/j.1523-1755.1999.00612.x.
- Moody TE, Vaughan ED Jr, Wyker AT, Gillenwater JY. The role of intrarenal angiotensin II in the hemodynamic response to unilateral obstructive uropathy. *Invest Urol* 14: 390–397, 1977.
- Noguchi K, Gel YR, Brunner E, Konietzschke F, nparLD: an R software package for the nonparametric analysis of longitudinal data in factorial experiments. *J Stat Softw* 50: 1–23, 2012. doi:10.18637/jss.v050.i12.
- Öberg CM, Rippe B. A distributed two-pore model: theoretical implications and practical application to the glomerular sieving of Ficoll. *Am J Physiol Renal Physiol* 306: F844–F854, 2014. doi:10.1152/ajprenal.00366.2013.
- Öberg CM, Rippe B. Quantification of the electrostatic properties of the glomerular filtration barrier modeled as a charged fiber matrix separating anionic from neutral Ficoll. *Am J Physiol Renal Physiol* 304: F781–F787, 2013. doi:10.1152/ajprenal.00621.2012.
- Palm F, Cederberg J, Hansell P, Liss P, Carlsson PO. Reactive oxygen species cause diabetes-induced decrease in renal oxygen tension. *Diabetologia* 46: 1153–1160, 2003. doi:10.1007/s00125-003-1155-z.
- Pimentel JL Jr, Montero A, Wang S, Yosivip I, el-Dahr S, Martínez-Maldonado M. Sequential changes in renal expression of renin-angiotensin system genes in acute unilateral ureteral obstruction. *Kidney Int* 48: 1247–1253, 1995. doi:10.1038/ki.1995.408.
- Rippe B, Haraldsson B. Fluid and protein fluxes across small and large pores in the microvasculature. Application of two-pore equations. *Acta Physiol Scand* 131: 411–428, 1987. doi:10.1111/j.1748-1716.1987.tb08257.x.
- Rippe B, Haraldsson B. Transport of macromolecules across microvascular walls: the two-pore theory. *Physiol Rev* 74: 163–219, 1994. doi:10.1152/physrev.1994.74.1.163.
- Schiefl IM, Castro P. H. Angiotensin II AT2 receptor activation attenuates AT1 receptor-induced increases in the glomerular filtration of albumin: a multiphoton microscopy study. *Am J Physiol Renal Physiol* 305: F1189–F1200, 2013. doi:10.1152/ajprenal.00377.2013.
- Schlondorff D, Ardaillou R. Prostaglandins and other arachidonic acid metabolites in the kidney. *Kidney Int* 29: 108–119, 1986. doi:10.1038/ki.1986.13.
- Sivertsson E, Friederich-Persson M, Öberg CM, Fasching A, Hansell P, Rippe B, Palm F. Inhibition of mammalian target of rapamycin decreases intrarenal oxygen availability and alters glomerular permeability. *Am J Physiol Renal Physiol* 314: F864–F872, 2018. doi:10.1152/ajprenal.00033.2017.
- Suki WN, Guthrie AG, Martínez-Maldonado M, Eknoyan G. Effects of ureteral pressure elevation on renal hemodynamics and urine concentration. *Am J Physiol* 220: 38–43, 1971. doi:10.1152/ajplegacy.1971.220.1.38.
- Sullivan LM, D'Agostino RB. Robustness of the t test applied to data distorted from normality by floor effects. *J Dent Res* 71: 1938–1943, 1992. doi:10.1177/00220345920710121601.
- Sverrisson K, Axelsson J, Rippe A, Asgerirsson D, Rippe B. Acute reactive oxygen species (ROS)-dependent effects of IL-1 β , TNF- α , and IL-6 on the glomerular filtration barrier (GFB) in vivo. *Am J Physiol Renal Physiol* 309: F800–F806, 2015. doi:10.1152/ajprenal.00111.2015.
- Sverrisson K, Axelsson J, Rippe A, Gram M, Åkerström B, Hansson SR, Rippe B. Extracellular fetal hemoglobin induces increases in glomerular permeability: inhibition with α 1-microglobulin and Tempol. *Am J Physiol Renal Physiol* 306: F442–F448, 2014. doi:10.1152/ajprenal.00502.2013.
- Tian D, Jacobo SM, Billing D, Rozkalne A, Gage SD, Anagnostou T, Pavenstädt H, Hsu HH, Schlondorff J, Ramos A, Greka A. Antagonistic regulation of actin dynamics and cell motility by TRPC5 and TRPC6 channels. *Sci Signal* 3: ra77, 2010. doi:10.1126/scisignal.2001200.
- Wang L, Ellis MJ, Gomez JA, Eisner W, Fennell W, Howell DN, Ruiz P, Fields TA, Spurney RF. Mechanisms of the proteinuria induced by Rho GTPases. *Kidney Int* 81: 1075–1085, 2012. doi:10.1038/ki.2011.472.
- Vaughan ED Jr, Marion D, Poppas DP, Felsen D. Pathophysiology of unilateral ureteral obstruction: studies from Charlottesville to New

- York. *J Urol* 172: 2563–2569, 2004. doi:10.1097/01.ju.0000144286.53562.95.
41. **Wen L, Andersen PK, Husum DMU, Nørregaard R, Zhao Z, Liu Z, Birn H.** MicroRNA-148b regulates megalin expression and is associated with receptor downregulation in mice with unilateral ureteral obstruction. *Am J Physiol Renal Physiol* 313: F210–F217, 2017. doi:10.1152/ajprenal.00585.2016.
42. **Yarger WE, Griffith LD.** Intrarenal hemodynamics following chronic unilateral ureteral obstruction in the dog. *Am J Physiol* 227: 816–826, 1974. doi:10.1152/ajplegacy.1974.227.4.816.
43. **Zimmerman DW, Zumbo BD.** Effect of outliers on the relative power of parametric and nonparametric statistical tests. *Percept Mot Skills* 71: 339–349, 1990. doi:10.2466/pms.1990.71.1.339.



Paper III



RESEARCH ARTICLE | *Translational Physiology*

Sustained, delayed, and small increments in glomerular permeability to macromolecules during systemic ET-1 infusion mediated via the ET_A receptor

Julia Dolinina, Anna Rippe, and  Carl M. Öberg

Department of Nephrology, Skåne University Hospital, Clinical Sciences Lund, Lund University, Lund, Sweden

Submitted 29 January 2019; accepted in final form 10 March 2019

Dolinina J, Rippe A, Öberg CM. Sustained, delayed, and small increments in glomerular permeability to macromolecules during systemic ET-1 infusion mediated via the ET_A receptor. *Am J Physiol Renal Physiol* 316: F1173–F1179, 2019. First published March 13, 2019; doi:10.1152/ajprenal.00040.2019.—Emerging evidence indicates that endogenous production of endothelin (ET)-1, a 21-amino acid peptide vasoconstrictor, plays an important role in proteinuric kidney disease. Previous studies in rats have shown that chronic administration of ET-1 leads to increased glomerular albumin leakage. The underlying mechanisms are, however, currently not known. Here, we used size-exclusion chromatography to measure glomerular sieving coefficients for neutral FITC-Ficoll (molecular Stokes-Einstein radius: 15–80 Å, molecular weight: 70 kDa/400 kDa) in anesthetized male Sprague-Dawley rats ($n = 12$) at baseline and at 5, 15, 30, and 60 min after intravenous administration of ET-1. In separate experiments, ET-1 was given together with the selective ET type A (ET_A) or ET type B (ET_B) receptor antagonists JKC-301 and BQ-788, respectively. At both 15 and 30 min postadministration, the glomerular sieving coefficient for macromolecular Ficoll (70 Å) was significantly increased to $4.4 \times 10^{-5} \pm 0.7 \times 10^{-5}$ ($P = 0.024$) and $4.5 \times 10^{-5} \pm 0.8 \times 10^{-5}$ ($P = 0.007$), respectively, compared with baseline ($2.2 \times 10^{-5} \pm 0.4 \times 10^{-5}$). Decreased urine production after ET-1 prevented the use of higher doses of ET-1. Data analysis using the two-pore model indicated changes in large-pore permeability after ET-1, with no changes in the small-pore pathway. Administration of ET_A blocker abrogated the permeability changes induced by ET-1 at 30 min, whereas blockade of ET_B receptors was ineffective. Mean arterial pressure was only significantly increased at 60 min, being 123 ± 4 mmHg compared with 111 ± 2 mmHg at baseline ($P = 0.02$). We conclude that ET-1 evoked small, delayed, and sustained increases in glomerular permeability, mediated via the ET_A receptor.

endothelin-1; endothelin receptor blocker; proteinuria

INTRODUCTION

More than 30 yr ago, Yanagisawa et al. (46) identified endothelin (ET) as the most potent and long-lasting vasoconstrictor in humans (40). Being mainly produced in endothelial cells (23), ET-1, the predominant member of the ET family (23), confers its biological effects in an abluminal fashion via binding to G protein-coupled ET type A and B (ET_A and ET_B) receptors (Fig. 1A), eliciting a biphasic increase in intracellular Ca²⁺ (33). Both ET_A and ET_B receptors are expressed on vascular wall smooth muscle cells, and their activation induces an initial, transient vasodilation followed by marked, sustained

vasoconstriction. The ET_B receptor is predominantly expressed on the vascular endothelium, where it induces the production of nitric oxide and prostacyclin (PGI₂), mediating the initial vasodilatation phase (19), whereas the vasoconstrictor response seems to be mainly regulated via ET_A receptors, however, apparently with the exception of the renal microvasculature (33). Much like ANG II, the formation of ET-1 is critically dependent on the presence of a converting enzyme (endothelin-converting enzyme-1) (34) to convert its 38-amino acid prohormone big ET-1 to ET-1 (Fig. 1). In addition to its hemodynamic effects, ET-1 is also involved in cell proliferation and growth via the MAPK pathway, which would imply its role in angiogenesis (23). In the kidney, ET-1 seems to have differential effects, perhaps in part because of the heterogeneity in receptor expression. Thus, in podocytes, the ET_B receptor predominates, with only a small amount of ET_A receptors, whereas mesangial cells appear to express only ET_A receptors but not ET_B receptors (11). In the collecting duct, ET_B receptor activation counteracts aldosterone-mediated Na⁺ reuptake in a negative feedback fashion (20, 25), and, thus, in the clinic, unspecific ET blockade may lead to water and Na⁺ retention.

Over the last decade, ET receptor blockers have been investigated as potential antiproteinuric and antihypertensive treatments (37). Although most patients with hypertension do not have pharmacologically relevant plasma concentrations of ETs, it is still possible that local paracrine effects could be important, and clinical studies have revealed a potent effect of ET receptor blockers similar to that of ANG receptor blockers (19). A pioneering clinical study by Wenzel and colleagues (44) showed that administration of the ET_A antagonist avosentan significantly reduces urinary albumin excretion in patients with diabetes. These findings were confirmed in a randomized controlled study that, however, had to be stopped prematurely because of an increased incidence of cardiovascular events (26). The potential positive effects of ET antagonists have been hampered by side effects (37), and there is uncertainty over the receptor specificity of current ET receptor inhibitors, which may influence the occurrence of side effects such as fluid retention and peripheral edema (31, 32, 37). Indeed, ET_B receptor-null mice retain water and Na⁺, likely because of the abolition of effects of ET on aldosterone-sensitive collecting duct cells (16). Also, recent experimental data suggest that ET_B receptor signaling in the diabetic kidney improves intrarenal tissue oxygenation (15). Hence, the most likely successful drug candidate would be a highly selective antagonist of ET_A receptors (21).

Here, we used a well-established rat model of glomerular permeability to investigate the actions of intravenous ET-1 on

Address for reprint requests and other correspondence: C. M. Öberg, Dept. of Nephrology, Skåne Univ. Hospital, Alwall House, Barnåtgatan 2, Lund SE-21185, Sweden (e-mail: carl.oberg@med.lu.se).

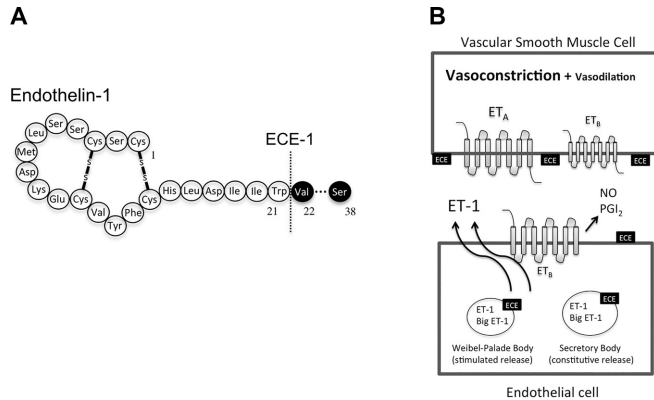


Fig. 1. Endothelin (ET)-1 is a 21-amino acid vasoactive peptide hormone (A) mainly produced by endothelial cells in an abuminal fashion. It exerts its physiological actions via ET type A (ET_A) and type B (ET_B) receptors, mediating vasoconstriction and vasodilation, respectively, in vascular smooth muscle cells (B). Biosynthesis of ET-1 is accomplished by proteolytic cleavage by a unique endothelin-converting enzyme (ECE), removing 18 amino acids from the precursor, referred to as big ET. NO, nitric oxide; PGI₂, prostacyclin.

the permselective properties of the glomerular filtration barrier. We also studied the effects of selective antagonism of ET_A receptors and ET_B receptors to elucidate whether any of the observed effects are mediated via one or both of these receptors.

METHODS

Animals. Experiments were conducted in 29 male Sprague-Dawley rats (Møllegaard, Lille Stensved, Denmark) with a median body weight of 269 g (250–313 g) with free access to food and water. The local Animal Ethics Committee at Lund University (Lund, Sweden) approved all experimental procedures.

Surgery. Anesthesia was induced by means of an intraperitoneal injection with pentobarbital (Pentobarbitalnatrium vet. APL 60 mg/ml) at 90 mg/kg body wt. Anesthesia was maintained by administration of pentobarbital (3–6 mg) via the tail artery as needed. A tracheotomy was conducted (using a PE-240 tube) to facilitate breathing. A heating pad was used to maintain body temperature at 37°C. The tail artery was cannulated using a PE-50 cannula and used for the administration of furosemide (Furosemid Recip, Årsta, Sweden) and for the continuous monitoring and registration of heart rate (HR) and mean arterial pressure (MAP) on a data-acquisition system (model MP150, BioPack Systems, with AcqKnowledge software, version 4.2.0, BioPack Systems, Goleta, CA). The left and right internal jugular vein was cannulated (PE-50) for the administration of Ficoll and pharmacological interventions, respectively. The left carotid artery was cannulated (PE-50) and used for arterial blood sampling. A minimal abdominal incision (6–8 mm) was performed to gain access to the left ureter. After a very small dose of furosemide [0.375 mg/kg, corresponding to a human dose of ~3 mg (17)] to facilitate ureteral cannulation, the ureter was dissected free and thereafter cannulated using a small PE-10 cannula (connected to a PE-50 cannula), which was used for urine sampling. All cannulas, connectors, and tubes in contact with the circulation were prepared and flushed postadministration with a dilute heparin (5,000 IE/ml Heparin LEO) solution (~25 IE/ml in NaCl aq. 9 mg/ml) to prevent clotting.

Experimental procedures. All experiments commenced with a resting period of 20 min after the cannulation of the left ureter. After an initial 5-min period for control (baseline) measurements, a nonpressor dose of ET-1 (Sigma-Aldrich, St. Louis, MO) was administered as a bolus (0.41 µg/kg, 166 pmol/kg) followed by a continuous infusion (0.14 µg·min⁻¹·kg⁻¹, 55 pmol·kg⁻¹·min⁻¹). In separate animals ($n = 2$), a higher pressor dose of ET-1 was given, bolus (0.83 µg/kg, 333 pmol/kg) followed by infusion (0.28 µg·min⁻¹·kg⁻¹, 111

pmol·kg⁻¹·min⁻¹), which led to prompt anuria. In two experimental groups, equimolar doses (200 nmol/kg) of the ET_A receptor antagonist JKC-301 (Sigma-Aldrich, $n = 8$) or the ET_B receptor antagonist BQ-788 ($n = 9$) were given before the administration of the nonpressor dose of ET-1. Sham experiments were performed in a previous investigation (3). After the experimental period, animals were euthanized with an overdose of KCl intravenously under deep anesthesia.

Determination of the glomerular sieving coefficient for Ficoll. During the entire length of the experimental procedure, an intravenous infusion (10 ml·kg⁻¹·h⁻¹) of FITC-Ficoll [FITC-Ficoll-70, 20 µg/ml; FITC-Ficoll-400, 480 µg/ml; FITC-inulin, 500 µg/ml; and ⁵¹Cr-labeled EDTA (⁵¹Cr-EDTA), 0.3 MBq/ml] was given subsequent to an initial bolus dose (FITC-Ficoll-70, 40 µg; FITC-Ficoll-400, 960 µg; FITC-inulin, 0.5 mg; and ⁵¹Cr-EDTA, 0.3 MBq). This 1:24 combination of Ficoll (70 kDa/400 kDa) provides a wide range of different molecular sizes. Sieving measurements were conducted by means of a 5-min collection of urine from the left ureter with a midpoint (2.5 min) plasma sample.

Determination of the glomerular filtration rate in the left kidney. ⁵¹Cr-EDTA (Amersham Biosciences, Buckinghamshire, UK) was given continuously during the experiment (see above). Radioactivity in blood and urine samples was detected using a gamma-counter (Wizard 1480, LKP, Wallac, Turku, Finland). The glomerular filtration rate (GFR) for the left kidney was approximated from the plasma-to-urine clearance of ⁵¹Cr-EDTA.

High-performance size-exclusion chromatography. To assess the concentration and size distribution of the FITC-Ficoll samples, a HPLC system (Waters, Milford, MA) was used. Plasma and urine samples were size separated on an Ultrahydrogel 500 column (Waters), which was connected to a guard column (Waters). The mobile phase was phosphate buffer (0.15 M NaCl, pH 7.4) driven by a binary HPLC pump (Waters 1525). Fluorescence was measured at an excitation wavelength of 492 nm and an emission wavelength of 518 nm. To load samples onto the system, an autosampler (Waters 717 plus) was used. The HPLC system was controlled by Breeze software 3.3 (Waters) and precalibrated using narrow Ficoll and protein standards, as described in a previous study (1). The urine concentration of FITC-Ficoll for each size was divided by the FITC-inulin concentration in urine to obtain the concentration of Ficoll in primary urine (C_u); the glomerular sieving coefficient (θ) was then calculated by dividing C_u by the plasma concentration of Ficoll.

Two-pore model analysis. The distributed pore model by Deen and colleagues (9), modified using two pore size distributions (29), was used to analyze the θ data for FITC-Ficoll (molecular radius: 15–80 Å) by means of weighted nonlinear least-squares regression to obtain

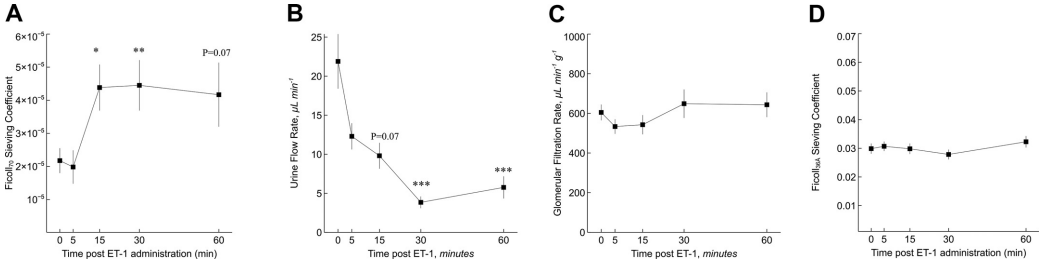


Fig. 2. A: sieving coefficients for 70 Å (7.0 nm) Ficoll (Ficoll_{70Å}) at baseline and at 5, 15, 30, and 60 min after endothelin (ET)-1 administration. B: decrement in urine flow rate after ET-1. C: glomerular filtration rate. * $P < 0.05$, ** $P < 0.01$, and *** $P < 0.001$ compared with baseline.

the best curve fit, as previously described (28). The solution of the model differential equations and calculation of renal plasma flow are described at some length in Ref. 28. Thus, renal plasma flow was estimated from the decay of the local filtration rate, $dQ/dy = -J_v(y)$, along the capillary length ($y = L$) applying the principle of the mass balance: $GFR = Q(0) - Q(L)$, where Q is renal plasma flow, J_v is filtrate flux, and L is length.

Statistical analysis. Values are presented as means \pm SE unless otherwise stated. A power calculation for the present experimental setup has been previously performed (10), showing that four rats are sufficient to detect a difference of at least a factor of 2 between two independent groups for a statistical power of 80%. Differences between samples taken at different time points were assessed using a Friedman test. In the case of a significant omnibus test, post hoc testing was performed using a Wilcoxon-Nemenyi-McDonald-Thompson test. Significance levels were set at $P < 0.05$, $P < 0.01$, and $P < 0.001$. Post hoc nonparametric 2×2 ANOVA was performed using the nparLD package for R. All statistical calculations were performed using R 3.5.1 for macOS (The R Foundation for Statistical Computing).

RESULTS

ET-1 induced a small, delayed, and sustained increase in glomerular permeability to large Ficolls. To determine the effects of ET-1 on glomerular permeability, we studied sieving coefficients of polydisperse FITC-Ficoll in Sprague-Dawley rats ($n = 12$) under baseline conditions and at 5, 15, 30, and 60 min after the administration of ET-1. Figure 2A shows glomerular sieving coefficients for macromolecular 70 Å (7.0 nm) Ficoll versus time (baseline and 5, 15, 30, and 60 min postad-

ministration). Small, sustained, and delayed elevations in the glomerular sieving coefficient of 70 Å (7.0 nm) Ficoll were observed, being significantly higher at 15 min ($P = 0.024$) and at 30 min ($P = 0.0073$) after ET-1 administration compared with baseline. We hypothesized that higher doses of ET-1 would elicit more pronounced alterations in glomerular permeability and therefore attempted higher doses of ET-1 (twice the dose given in the above group) in two separate animals, which, in both cases, resulted in prompt anuria. Indeed, the urine flow rate decreased as a function of time (Fig. 2B) after ET-1 was given, being severely diminished at the 30- and 60-min time points. In contrast, left kidney GFR was stable during the entire course of the experiment, and no significant changes were noted compared with baseline (Fig. 2C). In contrast to, for example, ANG II (2), there were no significant differences in the sieving coefficient of 36 Å Ficoll after ET-1 administration (Fig. 2D).

Delayed hemodynamic effects of ET-1. The null hypothesis of no difference in MAP between the different time points after ET-1 administration was rejected at the 5% level. Post hoc testing revealed no significant differences in MAP compared with baseline, except at 60 min (Fig. 3A). HR was, however, decreased at 30 min ($P = 0.027$) and 60 min ($P < 0.001$) compared with baseline (Fig. 3B), which could be an effect of an increased peripheral vascular resistance.

Pore analysis shows no alterations in the small-pore pathway after ET-1 administration. To further analyze the sieving data, we used the distributed pore model by Deen et al. (9),

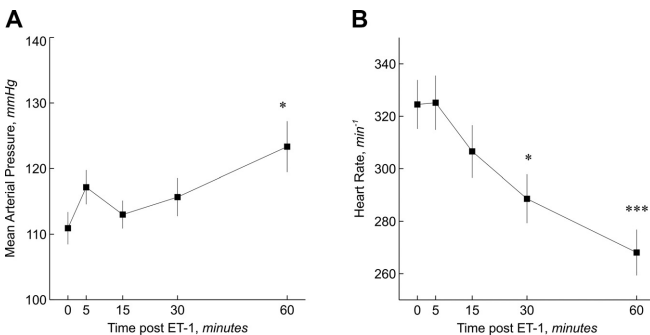


Fig. 3. Mean arterial pressure (A) and heart rate (B) at baseline and at 5, 15, 30, and 60 min after endothelin (ET)-1 administration. * $P < 0.05$ and *** $P < 0.001$ compared with baseline.

Table 1. Two-pore model results

Parameter	Baseline	5 min	15 min	30 min	60 min
Small-pore pathway					
Small-pore radius, Å	34.1 ± 0.7	34.2 ± 0.8	34.0 ± 0.6	34.6 ± 0.6	34.7 ± 0.6
Small-pore SD	1.16 ± 0.01	1.16 ± 0.01	1.16 ± 0.01	1.16 ± 0.01	1.16 ± 0.01
$A_0/\Delta x$, × 10 ⁵ cm	8.5 ± 0.3	8.5 ± 0.3	7.8 ± 0.3	8.3 ± 0.2	8.3 ± 0.2
Large-pore pathway					
Large-pore radius, Å	147 ± 15	101 ± 10*	153 ± 20	172 ± 30	123 ± 6
Large-pore SD	1.13 ± 0.02	1.14 ± 0.02	1.14 ± 0.03	1.15 ± 0.02	1.14 ± 0.02
$J_{v,L}/GFR$ × 10 ⁻⁵	5	7	9*	7	12*
Hemodynamic parameters					
Glomerular filtration pressure, mmHg‡	7.6 ± 0.5	6.7 ± 0.5	6.8 ± 0.6	8.1 ± 0.9	8.0 ± 0.8
GFR, ml/min†	0.60 ± 0.04	0.53 ± 0.04	0.54 ± 0.05	0.65 ± 0.07	0.65 ± 0.06
Renal plasma flow, ml/min†§	2.1 ± 0.2	1.8 ± 0.2	1.9 ± 0.7	2.9 ± 0.7	2.6 ± 0.5
Filtration fraction, %§	29 ± 1	30 ± 0	30 ± 1	27 ± 2	28 ± 1

$A_0/\Delta x$, unrestricted pore area (A_0) over diffusion distance (Δx); GFR, glomerular filtration rate. * $P < 0.05$ compared with baseline. †Left kidney. ‡Calculated assuming a hydraulic conductance of 0.08 ml·min⁻¹·mmHg⁻¹. §Calculated using the model of glomerular ultrafiltration by Deen et al. (9).

modified using two pore size distributions (29) having radii of r_S (small-pore mean radius) and r_L (large-pore mean radius), respectively, and geometric standard deviations of s_S (small-pore spread) and s_L (large-pore spread), respectively. The optimal parameters of the theoretical model are shown in Table 1. Thus, in contrast to, for example, glomerular hyperpermeability mediated by ANG II (2), we could not detect any alterations in the small-pore system after ET-1 infusion, whereas there were significant elevations in the large-pore permeability at 15 and 60 min postadministration (Table 1). In contrast to the analysis of 70-Å sieving coefficients, there were no significant effects at the 30-min time point. There was also a significant decrease in r_L at 5 min.

ET_A but not ET_B receptor blockade ameliorates ET-1-induced glomerular hyperpermeability. To elucidate the receptor mechanisms behind the observed alterations in glomerular permeability, we performed experiments in which both ET-1 and either a well-known selective pentapeptide ET_A receptor blocker (JKC-301; Asp-Pro-Ile-Leu-Trp) or a selective ET_B receptor blocker (BQ-788) was administered. Analysis of glomerular sieving coefficients for 70 Å (7.0 nm) Ficoll versus time (baseline and at 15 and 30 min postinjection) revealed that blockade of the ET_A receptor ($n = 8$) was effective at ameliorating ET-1-mediated glomerular hyperpermeability (Fig. 4A). However, in the group that received the ET_B receptor antagonist ($n = 9$), we noted that ET-1 still induced glomerular hyperpermeability at 30 min compared with baseline but not at

15 min ($P = 0.06$; Fig. 4B). There was an outlier ($\sim 3 \times 10^{-4}$) at 15 min in the group that received the ET_B receptor antagonist. No alterations in MAP were observed postadministration of ET-1 and ET receptor blockers (Fig. 5A), whereas HR was slightly decreased at 30 min in both intervention groups (Fig. 5B). Post hoc nonparametric 2 × 2 ANOVA factoring treatment (ET-1 only vs. ET-1 + ET_A antagonist) and time (baseline vs. 30 min) revealed a significant treatment × time interaction ($P < 0.05$).

DISCUSSION

The systemic actions of intravenous ET-1 infusions on glomerular permeability were investigated here in vivo. Our data show that ET-1 administration leads to an increased glomerular permeability to macromolecules, which is in line with a previous report using chronic ET-1 exposure (38). Furthermore, it appears that these actions on the glomerular filter are mediated chiefly via the ET_A receptor. The present and previous (38) changes in glomerular permeability are, however, small in magnitude compared with, for example, those caused by ANG II (2) and would most likely go completely unnoticed in a clinical setting. In contrast, several clinical studies have shown reduced albuminuria after treatment with ET receptor antagonists in diabetic kidney disease. Also, the selective ET_A antagonist ambrisentan attenuated the increase in urinary albumin excretion caused by overexpres-

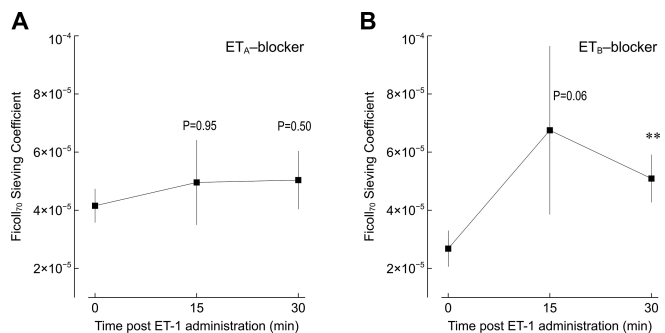


Fig. 4. Sieving coefficients for 70 Å (7.0 nm) Ficoll (Ficoll_{70A}) at baseline and at 15 and 30 min after endothelin (ET)-1 administration plus selective ET type A (ET_A) receptor inhibition (A) or selective ET type B (ET_B) receptor inhibition (B). P values represent comparisons with baseline measurements. ** $P < 0.01$ compared with baseline.

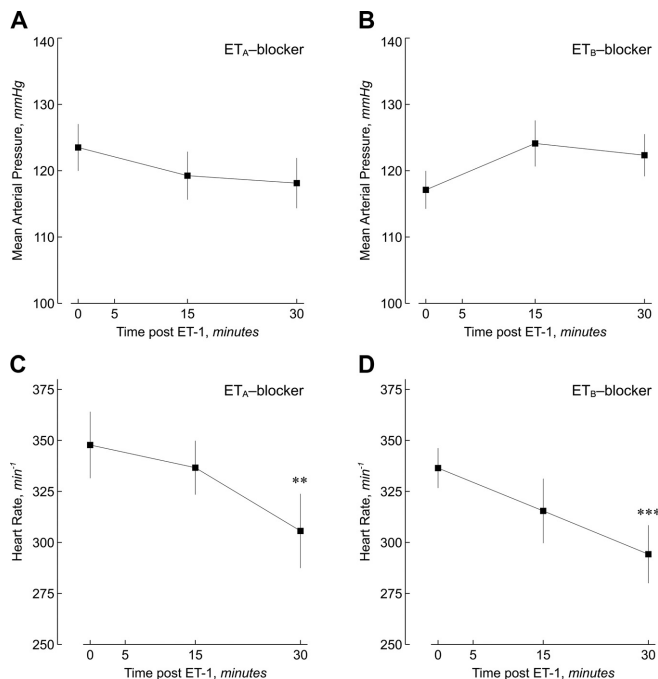


Fig. 5. Mean arterial pressure and heart rate at baseline and at 15 and 30 min after endothelin (ET)-1 administration plus selective ET type A (ET_A) receptor inhibition (A and C) or selective ET type B (ET_B) receptor inhibition (B and D). ***P* < 0.01 and ****P* < 0.001 compared with baseline.

sion of soluble fms-like tyrosine kinase-1 in mice (24). These discrepancies between the present results and clinical findings are intriguing and require special attention. Podocytes, being substantially specialized epithelial cells covering the outer aspect of glomerular capillaries, have a rather complex cytoskeleton that appears to play a crucial role in the maintenance of the renal filter (12, 39). Dysfunctional Ca²⁺ signaling is an early sign of podocyte injury (42) and is followed by disruption of the actin cytoskeleton (12), which indicates a connection between Ca²⁺ signaling and cytoskeletal alterations. Interestingly, both of these events in podocytes have been associated with proteinuric disease conditions (39). Moreover, whereas podocytes both synthesize and bind ET-1 in an autocrine fashion, endothelial cells are considered the main source of ET-1 within the glomerular filtration barrier (8), of which a substantial amount is likely transported downstream to podocytes. Conceivably, such paracrine secretion can result in far higher concentrations than those attainable by intravenous injection in the present study. Thus, it is possible that higher doses of ET-1 may produce far larger alterations in permeability. In our experimental setup, such a stimulus would have to be of a local paracrine nature, since use of higher doses of ET-1 led to prompt anuria, presumably because of renal arteriolar vasoconstriction (33). On the other hand, our data indicate that the observed alterations in permeability are mediated via the ET_A receptor and not the ET_B receptor. Since previous data have indicated that the ET_A receptor is more abundant on mesangial cells, these findings could imply a role for the mesangium in glomerular permeability.

Ficoll is a well-established and widely used marker for glomerular permeability. However, in relation to globular proteins such as albumin, Ficoll molecules are apparently hyperpermeable compared with proteins of the same hydrodynamic (Stokes-Einstein) radius (5, 13, 14). Thus, to evaluate proteinuric conditions in, for example, experimental animal studies, it would thus be valuable to also use proteins as molecular probes. However, studies of glomerular protein transport require either tissue uptake techniques or careful micropuncture of the Bowman's capsule. Thus, to assess glomerular permeability in humans, it would appear that polysaccharides such as dextran or Ficoll are the only options available. However, when using Ficoll to assess glomerular permeability, one should be aware of the hyperpermeability that polysaccharides exhibit. In terms of sieving coefficients, it appears that 55 Å Ficoll corresponds well to 36 Å albumin. The sieving coefficient of 55 Å Ficoll in this study was $5.5 \pm 0.6 \times 10^{-5}$ at baseline (and $9.1 \pm 0.9 \times 10^{-5}$ at 15 min after ET-1 administration). In a previous study by Saleh et al. (38), the glomerular sieving coefficient of albumin was estimated to >2 orders of magnitude larger at baseline, $1.7 \pm 0.3 \times 10^{-2}$ (and $2.5 \pm 0.5 \times 10^{-2}$ after ET-1 administration), compared with the results in the present study, which are more in line with results using micropuncture (6×10^{-5}) (43) or the sieving coefficient observed in Fanconi syndrome (27) (with nearly no proximal tubular uptake of proteins, as indicated by a sieving coefficient of β_2 -microglobulin, close to unity). In humans, the high glomerular sieving coefficient of albumin of 1.7×10^{-2} would lead to a profuse delivery of albumin to the proximal

tubules, of which most are reabsorbed intact because of the fact that the liver only produces ~12 g albumin daily (35). Thus, in the so-called albumin retrieval hypothesis, it is assumed that most, if not all, of the filtered albumin, corresponding to ~225 g/day in humans (45), is reabsorbed in an intact form (7). Although there have been reports of small amounts of albumin being absorbed intactly (41), there is, to date, little evidence to support the albumin retrieval hypothesis.

Much of our knowledge about the transcapillary transport of water and solute matter, especially that of macromolecules, is still obscure. It is well known that endothelial dysfunction, a systemic pathological state occurring in chronic kidney disease, diabetes, hypertension, atherosclerosis, etc., is associated with microproteinuria. Accordingly, microproteinuria has been identified as an independent risk factor for the morbidity and mortality in cardiovascular disease, suggesting that the inability of the kidneys to prevent leakage of large plasma proteins through the renal filter could act as a surrogate marker for endothelial dysfunction. Despite considerable research efforts, the exact mechanisms acting on the glomerular filtration barrier leading to proteinuria largely remain to be elucidated. The results from our laboratory suggest that the renal filter is a complex and dynamic biological filter, being weakly charge selective (30, 36) and distinctly size selective (28, 29) toward large molecules like albumin. Indeed, we previously found that the permeability of the renal glomerular barrier could increase by over 1 order of magnitude within minutes after administration of ANG II, only to return to baseline conditions shortly thereafter (2). ANG II is a powerful vasoconstrictor, being more potent than norepinephrine on a molar basis but less potent than ET-1. It was previously thought that the increase in glomerular permeability associated with ANG II was mediated by increased hydrostatic pressure. However, previous studies from our group have demonstrated that ANG II can increase glomerular permeability independently of hydrostatic pressure (2). In the present study, we found no elevations in blood pressure after ET-1, but a reduction in HR may indicate increased peripheral vascular resistance and vasoconstriction. In the theoretical modeling, we assumed that the filtration coefficient (K_f) was unchanged during ET-1 administration. This assumption may be correct (22), but there are several reports of reduced K_f during ET-1 exposure (6, 18). Either way, while it will have little impact on our conclusions in the present study, we conclude that it cannot be excluded that glomerular filtration pressure was elevated during ET-1 administration in the absence of changes in systemic pressure.

It has been well established that the severity and prognosis of kidney disease are strongly associated with the degree of proteinuria. While ANG II blockers and angiotensin-converting enzyme inhibitors are well-established antiproteinuric treatments (2, 4), blockers of ET receptors have been shown to exhibit potent antiproteinuric effects (33). Chronic exposure to ET-1 has also been shown to induce a slightly elevated glomerular sieving coefficient to albumin in rats (38). In the present study, we show that intravenous administration of ET-1 resulted in sustained, delayed glomerular hyperpermeability in Sprague-Dawley rats, being quite small in magnitude compared with other agents (2, 4, 10), in line with a previous study (38). From our analysis, we conclude that these effects on glomerular permeability are mediated chiefly via the ET_A receptor.

ACKNOWLEDGMENTS

The authors acknowledge the important contributions of Prof. Bengt Rippe (Gothenburg, 1950–Lund, 2016) to the present study.

GRANTS

This work was funded by the Swedish Heart and Lung Foundation and Medical Faculty (ALF grant) at Lund University.

DISCLOSURES

No conflicts of interest, financial or otherwise, are declared by the authors.

AUTHOR CONTRIBUTIONS

J.D. and C.M.Ö. conceived and designed research; J.D. and A.R. performed experiments; J.D., A.R., and C.M.Ö. analyzed data; J.D. and C.M.Ö. interpreted results of experiments; C.M.Ö. prepared figures; J.D. and C.M.Ö. drafted manuscript; J.D. and C.M.Ö. edited and revised manuscript; J.D., A.R., and C.M.Ö. approved final version of manuscript.

REFERENCES

1. Asgerirsson D, Venturoli D, Rippe B, Rippe C. Increased glomerular permeability to negatively charged Ficoll relative to neutral Ficoll in rats. *Am J Physiol Renal Physiol* 291: F1083–F1089, 2006. doi:10.1152/ajprenal.00488.2005.
2. Axelsson J, Rippe A, Öberg CM, Rippe B. Rapid, dynamic changes in glomerular permeability to macromolecules during systemic angiotensin II (ANG II) infusion in rats. *Am J Physiol Renal Physiol* 303: F790–F799, 2012. doi:10.1152/ajprenal.00153.2012.
3. Axelsson J, Rippe A, Rippe B. Acute hyperglycemia induces rapid, reversible increases in glomerular permeability in nondiabetic rats. *Am J Physiol Renal Physiol* 298: F1306–F1312, 2010. doi:10.1152/ajprenal.00710.2009.
4. Axelsson J, Rippe A, Sverrisson K, Rippe B. Scavengers of reactive oxygen species, paracalcitol, RhoA, and Rac-1 inhibitors and tacrolimus inhibit angiotensin II-induced actions on glomerular permeability. *Am J Physiol Renal Physiol* 305: F237–F243, 2013. doi:10.1152/ajprenal.00154.2013.
5. Axelsson J, Öberg CM, Rippe A, Krause B, Rippe B. Size-selectivity of a synthetic high-flux and a high cut-off dialyzing membrane compared to that of the rat glomerular filtration barrier. *J Membr Sci* 413: 29–37, 2012. doi:10.1016/j.memsci.2012.03.001.
6. Badr KF, Murray JJ, Breyer MD, Takahashi K, Inagami T, Harris RC. Mesangial cell, glomerular and renal vascular responses to endothelin in the rat kidney. Elucidation of signal transduction pathways. *J Clin Invest* 83: 336–342, 1989. doi:10.1172/JCI113880.
7. Comper WD. Albuminuria is controlled primarily by proximal tubules. *Nat Rev Nephrol* 10: 180, 2014. doi:10.1038/nrneph.2013.58-e1.
8. De Miguel C, Speed JS, Kasztan M, Gohar AY, Pollock DM. Endothelin-1 and the kidney: new perspectives and recent findings. *Curr Opin Nephrol Hypertens* 25: 35–41, 2016. doi:10.1097/MNH.0000000000000185.
9. Deen WM, Bridges CR, Brenner BM, Myers BD. Heteroporous model of glomerular size selectivity: application to normal and nephrotic humans. *Am J Physiol Renal Physiol* 249: F374–F389, 1985. doi:10.1152/ajprenal.1985.249.3.F374.
10. Dolinina J, Rippe A, Bentzer P, Öberg CM. Glomerular hyperpermeability after acute unilateral ureteral obstruction: effects of tempol, NOS, RhoA, and Rac-1 inhibition. *Am J Physiol Renal Physiol* 315: F445–F453, 2018. doi:10.1152/ajprenal.00610.2017.
11. Dufek B, Meehan DT, Delimont D, Cheung L, Gratton MA, Phillips G, Song W, Liu S, Cosgrove D. Endothelin A receptor activation on mesangial cells initiates Alport glomerular disease. *Kidney Int* 90: 300–310, 2016. doi:10.1016/j.kint.2016.02.018.
12. Faul C, Asanuma K, Yanagida-Asanuma E, Kim K, Mundel P. Actin up: regulation of podocyte structure and function by components of the actin cytoskeleton. *Trends Cell Biol* 17: 428–437, 2007. doi:10.1016/j.tcb.2007.06.006.
13. Fissell WH, Hofmann CL, Smith R, Chen MH. Size and conformation of Ficoll as determined by size-exclusion chromatography followed by multiangle light scattering. *Am J Physiol Renal Physiol* 298: F205–F208, 2010. doi:10.1152/ajprenal.00312.2009.
14. Fissell WH, Manley S, Dubnisheva A, Glass J, Magistrelli J, Eldridge AN, Fleischman AJ, Zydny AL, Roy S. Ficoll is not a rigid sphere. *Am*

- J Physiol Renal Physiol* 293: F1209–F1213, 2007. doi:10.1152/ajprenal.00097.2007.
15. Franzén S, Pohl L, Fasching A, Palm F. Intrarenal activation of endothelin type B receptors improves kidney oxygenation in type 1 diabetic rats. *Am J Physiol Renal Physiol* 314: F439–F444, 2018. doi:10.1152/ajprenal.00498.2017.
 16. Ge Y, Bagnall A, Stricklett PK, Strait K, Webb DJ, Kotelevtsev Y, Kohan DE. Collecting duct-specific knockout of the endothelin B receptor causes hypertension and sodium retention. *Am J Physiol Renal Physiol* 291: F1274–F1280, 2006. doi:10.1152/ajprenal.00190.2006.
 17. Hammarlund MM, Paalzow LK. Dose-dependent pharmacokinetics of furosemide in the rat. *Biopharm Drug Dispos* 3: 345–359, 1982. doi:10.1002/bdd.2510030408.
 18. Heller J, Kramer HJ, Horacek V. Action of endothelin-1 on glomerular haemodynamics in the dog: lack of direct effects on glomerular ultrafiltration coefficient. *Clin Sci (Lond)* 90: 385–391, 1996. doi:10.1042/cs0900385.
 19. Kedzierski RM, Yanagisawa M. Endothelin system: the double-edged sword in health and disease. *Annu Rev Pharmacol Toxicol* 41: 851–876, 2001. doi:10.1146/annurev.pharmtox.41.1.851.
 20. Kohan DE. Endothelin and collecting duct sodium and water transport. *Contrib Nephrol* 172: 94–106, 2011. doi:10.1159/000328687.
 21. Kohan DE, Barton M. Endothelin and endothelin antagonists in chronic kidney disease. *Kidney Int* 86: 896–904, 2014. doi:10.1038/ki.2014.143.
 22. Kon V, Yoshioka T, Fogo A, Ichikawa I. Glomerular actions of endothelin in vivo. *J Clin Invest* 83: 1762–1767, 1989. doi:10.1172/JCI114079.
 23. Lankhorst S, Danser AH, van den Meiracker AH. Endothelin-1 and antiangiogenesis. *Am J Physiol Regul Integr Comp Physiol* 310: R230–R234, 2016. doi:10.1152/ajpregu.00373.2015.
 24. Li F, Hagaman JR, Kim HS, Maeda N, Jennette JC, Faber JE, Karumanchi SA, Smithies O, Takahashi N. eNOS deficiency acts through endothelin to aggravate sFlt-1-induced pre-eclampsia-like phenotype. *J Am Soc Nephrol* 23: 652–660, 2012. doi:10.1681/ASN.2011040369.
 25. Lynch IJ, Welch AK, Gumz ML, Kohan DE, Cain BD, Wingo CS. Effect of mineralocorticoid treatment in mice with collecting duct-specific knockout of endothelin-1. *Am J Physiol Renal Physiol* 309: F1026–F1034, 2015. doi:10.1152/ajprenal.00220.2015.
 26. Mann JF, Green D, Jamerson K, Ruilope LM, Kuranoff SJ, Littke T, Viberti G; ASCEND Study Group. Avosentan for overt diabetic nephropathy. *J Am Soc Nephrol* 21: 527–535, 2010. doi:10.1681/ASN.2009060593.
 27. Norden AG, Lapsley M, Lee PJ, Pusey CD, Scheinman SJ, Tam FW, Thakker RV, Unwin RJ, Wrong O. Glomerular protein sieving and implications for renal failure in Fanconi syndrome. *Kidney Int* 60: 1885–1892, 2001. doi:10.1046/j.1523-1755.2001.00016.x.
 28. Öberg CM, Groszek JJ, Roy S, Fissell WH, Rippe B. A distributed solute model: an extended two-pore model with application to the glomerular sieving of Ficoll. *Am J Physiol Renal Physiol* 314: F1108–F1116, 2018. doi:10.1152/ajprenal.00066.2017.
 29. Öberg CM, Rippe B. A distributed two-pore model: theoretical implications and practical application to the glomerular sieving of Ficoll. *Am J Physiol Renal Physiol* 306: F844–F854, 2014. doi:10.1152/ajprenal.00366.2013.
 30. Öberg CM, Rippe B. Quantification of the electrostatic properties of the glomerular filtration barrier modeled as a charged fiber matrix separating anionic from neutral Ficoll. *Am J Physiol Renal Physiol* 304: F781–F787, 2013. doi:10.1152/ajprenal.00621.2012.
 31. Packer M, McMurray J, Massie BM, Caspi A, Charlton V, Cohen-Solal A, Kiowski W, Kostuk W, Krum H, Levine B, Rizzon P, Soler J, Swedberg K, Anderson S, Demets DL. Clinical effects of endothelin receptor antagonism with bosentan in patients with severe chronic heart failure: results of a pilot study. *J Card Fail* 11: 12–20, 2005. doi:10.1016/j.cardfail.2004.05.006.
 32. Packer M, McMurray JVV, Krum H, Kiowski W, Massie BM, Caspi A, Pratt CM, Petrie MC, DeMets D, Kobrin I, Roux S, Swedberg K; ENABLE Investigators and Committees. Long-term effect of endothelin receptor antagonism with bosentan on the morbidity and mortality of patients with severe chronic heart failure: primary results of the ENABLE trials. *JACC Heart Fail* 5: 317–326, 2017. doi:10.1016/j.jchf.2017.02.021.
 33. Pollock DM, Keith TL, Highsmith RF. Endothelin receptors and calcium signaling. *FASEB J* 9: 1196–1204, 1995. doi:10.1096/fasebj.9.12.7672512.
 34. Pupilli C, Romagnani P, Lasagni L, Bellini F, Misciglia N, Emoto N, Yanagisawa M, Rizzo M, Mannelli M, Serio M. Localization of endothelin-converting enzyme-1 in human kidney. *Am J Physiol Renal Physiol* 273: F749–F756, 1997. doi:10.1152/ajprenal.1997.273.5.F749.
 35. Rippe B, Öberg CM. Albumin turnover in peritoneal and hemodialysis. *Semin Dial* 29: 458–462, 2016. doi:10.1111/sdi.12534.
 36. Rippe B, Öberg CM. Counterpoint: defending pore theory. *Perit Dial Int* 35: 9–13, 2015. doi:10.3747/pdi.2014.00110.
 37. Ritz E, Wenzel RR. Endothelin antagonist as add-on treatment for proteinuria in diabetic nephropathy: is there light at the end of the tunnel? *J Am Soc Nephrol* 22: 593–595, 2011. doi:10.1681/ASN.2011020158.
 38. Saleh MA, Sandoval RM, Rhodes GJ, Campos-Bilderback SB, Mollitoris BA, Pollock DM. Chronic endothelin-1 infusion elevates glomerular sieving coefficient and proximal tubular albumin reuptake in the rat. *Life Sci* 91: 634–637, 2012. doi:10.1016/j.lfs.2012.06.007.
 39. Schiffer M, Teng B, Gu C, Shechedrina VA, Kasaikina M, Pham VA, Hanke N, Rong S, Gueler F, Schroder P, Tossidou I, Park JK, Staggs L, Haller H, Erschow S, Hilffiker-Kleiner D, Wei C, Chen C, Tardi N, Hakroush S, Selig MK, Vasilyev A, Merscher S, Reiser J, Sever S. Pharmacological targeting of actin-dependent dynamin oligomerization ameliorates chronic kidney disease in diverse animal models. *Nat Med* 21: 601–609, 2015. doi:10.1038/nm.3843.
 40. Shihoya W, Nishizawa T, Okuta A, Tani K, Dohmae N, Fujiyoshi Y, Nureki O, Doi T. Activation mechanism of endothelin ET_B receptor by endothelin-1. *Nature* 537: 363–368, 2016. doi:10.1038/nature19319.
 41. Tenten V, Menzel S, Kunter U, Sicking E-M, van Roeyen CR, Sanden SK, Kaldenbach M, Boor P, Fuss A, Uhlir S, Lanzmich R, Willemssen B, Dijkman H, Greppl M, Wild K, Kriz W, Smeets B, Floege J, Moeller MJ. Albumin is recycled from the primary urine by tubular transcytosis. *J Am Soc Nephrol* 24: 1966–1980, 2013. doi:10.1681/ASN.2013010018.
 42. Tian D, Jacobo SM, Billing D, Rozkalne A, Gage SD, Anagnostou T, Pavenstädt H, Hsu HH, Schlondorff J, Ramos A, Greka A. Antagonistic regulation of actin dynamics and cell motility by TRPC5 and TRPC6 channels. *Sci Signal* 3: ra77, 2010. [Erratum in *Sci Signal* 3: er11, 2010.] doi:10.1126/scisignal.2001200.
 43. Tojo A, Endou H. Intrarenal handling of proteins in rats using fractional micropuncture technique. *Am J Physiol Renal Physiol* 263: F601–F606, 1992. doi:10.1152/ajprenal.1992.263.4.F601.
 44. Wenzel RR, Littke T, Kuranoff S, Jürgens C, Bruck H, Ritz E, Philipp T, Mitchell A; SPP301 (Avosentan) Endothelin Antagonist Evaluation in Diabetic Nephropathy Study Investigators. Avosentan reduces albumin excretion in diabetics with macroalbuminuria. *J Am Soc Nephrol* 20: 655–664, 2009. doi:10.1681/ASN.2008050482.
 45. Weyer K, Andersen PK, Schmidt K, Mollet G, Antignac C, Birn H, Nielsen R, Christensen EL. Abolishment of proximal tubule albumin endocytosis does not affect plasma albumin during nephrotic syndrome in mice. *Kidney Int* 93: 335–342, 2018. doi:10.1016/j.kint.2017.07.024.
 46. Yanagisawa M, Kurihara H, Kimura S, Tomobe Y, Kobayashi M, Mitsui Y, Yazaki Y, Goto K, Masaki T. A novel potent vasoconstrictor peptide produced by vascular endothelial cells. *Nature* 332: 411–415, 1988. doi:10.1038/332411a0.

Paper IV



Inhibition of TRPC5 Ameliorates Angiotensin II-induced Glomerular Hyperpermeability *In* *Vivo* Without Hemodynamic Effects

Julia Dolinina¹, Anna Rippe¹, Carl M. Öberg¹

¹ Department of Nephrology, Clinical Sciences Lund, Lund University, Lund, Sweden

Correspondence:

Carl Öberg, Department of Nephrology, Alwall House, Barngatan 2, SE-21185 Lund, Sweden. E-mail: carl.oberg@med.lu.se

Running head: Ang II-signaling via TRPC-channels

Words:

- Abstract: 246 words,
- main text excl. methods: 1808 words, incl. methods: 2695 words

Keywords: Glomerular permeability, Angiotensin II, Proteinuria

SIGNIFICANCE STATEMENT

Angiotensin II receptor blockers are widely used as anti-proteinuric treatments. Unraveling the underlying mechanisms of their action is thus crucial to identify potential novel anti-proteinuric drugs. Several lines of evidence indicate that podocyte calcium signaling via TRPC5 and TRPC6 plays a critical role in angiotensin II induced glomerular hyperpermeability, but the effects on glomerular permeability of modulating glomerular calcium signaling via these channels has not been studied *in vivo*. Our current data highlight the critical role of TRPC5 in angiotensin II mediated glomerular hyperpermeability. They also show that blocking TRPC5 does not affect the hemodynamic effects of angiotensin II making it a promising target for new anti-proteinuric drugs, potentially being a safer alternative compared to conventional RAS inhibitors.

ABSTRACT

Background: Angiotensin II (Ang II) induces marked, dynamic increases in the permeability of the glomerular filtration barrier (GFB) in rats. After binding to its receptor, Ang II elicits Ca^{2+} influx into cells, mediated by TRPC5 and TRPC6 (transient receptor potential canonical type 5 and 6). We here identified TRPC5 and TRPC6 as regulators of Ang II induced glomerular hyperpermeability.

Methods: Anesthetized male Sprague-Dawley rats were infused with Ang II ($80 \text{ ng kg}^{-1} \text{ min}^{-1}$) alone, or together with a potent TRPC5 blocker (clemizole) or low dose La^{3+} (activates TRPC5, blocks TRPC6) or high dose La^{3+} (blocks both TRPC5 and TRPC6). Plasma and urine samples were taken during baseline and at 5 min after the start of the infusions and analyzed by high-performance size-exclusion chromatography for determination of glomerular sieving coefficients for Ficoll 10-80Å (1-8 nm).

Results: Ang II infusion evoked glomerular hyperpermeability to large Ficolls (50–80Å), which was ameliorated by the TRPC5 blocker clemizole, having no effect on glomerular filtration rate (GFR) or Ang II mediated increase in mean arterial pressure (ΔMAP). In contrast, high and low dose La^{3+} significantly lowered ΔMAP but also reduced Ang II induced hyperpermeability.

Conclusion: Our data unveil differential effects of Ca^{2+} signaling via TRPC5 and TRPC6 following Ang II stimulation. Especially, it appears that inhibition of TRPC5 in rats can ameliorate AngII-induced glomerular hyperpermeability without affecting GFR or Ang II induced increases in MAP. Inhibition of TRPC5 may thus be a potential target for a novel anti-proteinuric agent.

INTRODUCTION

Inhibitors of the renin-angiotensin system (RAS), particularly angiotensin (Ang) II receptor blockers (ARBs) and angiotensin converting enzyme (ACE) inhibitors, are widely adopted anti-proteinuric and anti-hypertensive agents that prevent the progression of chronic kidney disease¹. However, in conditions where systemic blood pressure is compromised, such as in hypovolemia or shock, RAS inhibitors may critically reduce glomerular filtration pressure by reducing efferent arteriolar tone, leading to AKI^{2,3}.

Podocytes, being highly specialized epithelial cells covering the outer aspect of glomerular capillaries, have a contractile cytoskeleton that appears to play an important role for the integrity of the renal filter^{4,5}. Dysregulation of Ca²⁺ homeostasis is an early sign of podocyte injury⁶ and is followed by disruption of the actin cytoskeleton⁴ indicating a link between Ca²⁺ signaling and cytoskeletal alterations. Importantly, these events in podocytes have been closely associated with proteinuric kidney disease⁵. After binding to its receptor, Ang II elicits Ca²⁺ influx via the classic transient receptor potential channel (TRPC) type 5 and 6⁶ triggering a complex cascade of intra-cellular signaling events⁷.

We have previously shown that Ang II infusion causes rapid, dynamic changes in the glomerular permeability to macromolecules in Wistar rats, independent of blood pressure^{8,9}. In the current work we sought to interact with Ang II induced Ca⁺⁺ signaling via TRPC5 and TRPC6 channels in Sprague-Dawley rats. We studied sieving coefficients of fluorescein isothiocyanate (FITC) Ficoll, a polydisperse polysaccharide that does not undergo tubular processing, and is therefore a robust marker of glomerular permeability. Our data show that both TRPC5 and TRPC6 inhibition is effective against the acute increments in glomerular permeability induced by Ang II. Furthermore, we find that TRPC5 inhibition does not affect the hemodynamic effects of Ang II.

METHODS

Animals: Experiments were performed in 37 male Sprague-Dawley rats (Møllegaard, Lille Stensved, Denmark) having an average body weight (BW) of 275 g (256 - 302 g) with access to food and water *ad libitum*. Approval by the local Animal Ethics Committee at Lund University, Sweden, was obtained for all procedures.

Surgery: Induction of anesthesia was established by means of an intraperitoneal injection of sodium pentobarbital (Pentobarbitalnatrium vet. APL 60 mg/ml), 1.5 mL/kg BW, and maintained, if necessary, by further administration of pentobarbital (~50-100 μ L) as needed. The body temperature was maintained at 37°C using a heating pad. A tracheotomy was performed by means of a small incision on the lower anterior aspect of the trachea (intubation using a PE-240 tube). The tail artery was cannulated (using a PE-50 cannula) and used for the maintenance of anesthesia and for continuous registration and monitoring of heart rate (HR) and mean arterial blood pressure (MAP) using a data acquisition system (BioPack Systems model MP150 with AcqKnowledge software version 4.2.0, BioPack Systems Inc., Goleta, CA). The left and right internal jugular veins were cannulated (PE-50) for the iv infusion of Ficoll and the different pharmacological interventions (La^{3+} and clemizole), respectively. For blood sampling, the left carotid artery was cannulated (PE-50). Access to the left ureter was established via a small abdominal incision (6-8 mm). For urine sampling, the left ureter was cannulated using a small PE-10 cannula (connected to a PE-50 cannula). A small dose of furosemide (0.375 mg/kg) was given to facilitate the cannulation procedure.

Experimental procedure: All experimental procedures were initiated by a resting period of 20 min following the cannulation of the left ureter. After an initial 5 min period for control (baseline) measurements (GFR, θ_{Ficoll} , MAP and HR), new measurements were performed following administration of different pharmacological challenges as described below.

Glomerular hyperpermeability was induced by a bolus dose (160 ng/kg) Ang II followed by an iv infusion (80 ng kg⁻¹ min⁻¹). The animals were divided into 5 experimental groups: Ang II only, Ang II + Hi La³⁺, Ang II + Lo La³⁺, AngII+clemizole and Ang II + Low La³⁺ + clemizole. In the AngII+La³⁺ groups, lanthanum(III)chloride heptahydrate (Sigma-Aldrich, St. Louis, MO) was given as an iv bolus dose (18 mg kg⁻¹ for Hi; 3 mg kg⁻¹ for Lo) followed by a continuous infusion (220 µg kg⁻¹ min⁻¹ iv for Hi; 60 µg kg⁻¹ min⁻¹ for Lo). For the AngII+TRPC5i group, we used clemizole, a potent TRPC5 inhibitor effective against both TRPC5:TRPC5 homomers and TRPC1:TRPC5 heteromers¹⁰. Clemizole (Sigma-Aldrich, St. Louis, MO), was administered as a bolus dose dose (0.4 mg kg⁻¹ iv) and a continuous infusion (24 µg kg⁻¹ min⁻¹). Serum concentrations of La³⁺ were determined using inductively coupled mass-spectrometry (ICP-MS) using a Perkin Elmer Optima 8300 (Perkin Elmer Instruments, Shelton, CT).

Determination of the glomerular sieving coefficient for Ficoll (θ_{Ficoll}): During the course of the experiment, An continuous iv infusion (10 ml kg⁻¹ h⁻¹) of FITC-Ficoll (FITC-Ficoll-70, 20 µg ml⁻¹; FITC-Ficoll-400, 480 µg ml⁻¹; FITC-Inulin, 500 µg ml⁻¹ and ⁵¹Cr-EDTA, 0.3 MBq ml⁻¹) was given, initiated by a bolus dose (FITC-Ficoll-70, 40 µg; FITC-Ficoll-400, 960 µg; FITC-Inulin 0.5 mg and ⁵¹Cr-EDTA 0.3 MBq). This 1:24 mixture of polydisperse Ficoll provides a broad range of molecular sizes. Sieving measurements were performed by means of a 5 min collection of urine and a mid-point (2.5 min) plasma sample.

Determination of glomerular filtration rate in the left kidney: ⁵¹Cr-EDTA (Amersham Biosciences, Buckinghamshire, UK) was administered throughout the experimental period (see above). A gamma counter (Wizard 1480, LKP, Wallac, Turku, Finland) was used to detect radioactivity in blood (CPM_{blood}) and urine (CPM_{urine}) samples. The glomerular filtration rate (for the left kidney) was estimated from the plasma to urine clearance of ⁵¹Cr-EDTA.

High-performance size-exclusion chromatography (HPSEC): A HPLC system (Waters, Milford, MA) was applied to quantify the concentration and size distribution of the FITC-Ficoll samples. Size-separation of the plasma and urine samples was accomplished using an Ultrahydrogel 500 column (Waters) connected to a guard column (Waters). A phosphate buffer (0.15 M NaCl, pH 7.4) was used as the mobile phase, driven by a pump (Waters 1525). Fluorescence in the samples was detected at an excitation wavelength 492 nm and emission wavelength of 518 nm. Samples were loaded onto the system using an autosampler (Waters 717 plus). As is described at some length elsewhere ¹¹ the system was calibrated using protein standards and narrow Ficoll standards. The urine FITC-Ficoll concentration for each size (a_e) was multiplied by the urine-to-plasma FITC-Inulin concentration ratio to approximate the concentration of Ficoll in primary urine (C_u). The glomerular sieving coefficient calculated by dividing C_u by the plasma concentration of Ficoll.

Statistical analysis: Values are presented as means \pm standard error. Significant differences were assessed using an ANOVA on aligned rank transformed data (using ARTool version 0.10.5), essentially performing a non-parametric test using parametric methods ¹². We used an alpha level (probability of type I error) of 0.05 and a beta level (probability of type II error) of 0.20 unless otherwise specified. Bonferroni corrections for multiple comparisons were made when applicable. A previous power analysis showed that four was the minimal number of animals needed to detect a difference in sieving coefficients by a factor of at least 2 ¹³. Statistical analysis was performed using R version 3.5.1 for macOS (The R Foundation for Statistical Computing).

RESULTS

Inhibition of TRPC5 Ameliorates Ang II induced Glomerular Hyperpermeability In Vivo Without Hemodynamic Effects

Ang II elicited rapid, dynamic elevations in glomerular sieving coefficients (θ) for large Ficolls $> 45 \text{ \AA}$, being increased more than an order of magnitude after 5 min (Fig. 1A). Small, transient, increments in θ also occurred for Ficolls $< 45 \text{ \AA}$ at 15 min. In addition, at the same time point, the left kidney glomerular filtration rate was significantly higher compared to baseline (Fig. 1C). In contrast to the changes in permeability, mean arterial pressure remained elevated through the entire experimental period (Table 1), similar to previous results⁸.

Previous work has demonstrated that the effects of Ang II on glomerular permeability and mean arterial pressure can be completely abrogated by angiotensin receptor blockade⁸. In contrast, we find that inhibition of TRPC5 did not affect the hemodynamic pressor effects of Ang II with the increase in MAP being very similar between Ang II only and Ang II + TRPC5i (Fig. 2A). TRPC5 inhibition did however effectively reduce the changes in glomerular permeability caused by Ang II (Fig. 2B) for Ficolls $> 45 \text{ \AA}$, similar to Ang II blocking⁸.

Effects of La^{3+} on Hemodynamic Effects and Glomerular Hyperpermeability Induced by Angiotensin II

Lanthanides like La^{3+} and Gd^{3+} have been shown to activate TRPC5 at micromolar concentrations while at the same time inhibiting TRPC6 in a dose dependent manner¹⁴. Here we firstly administered iv La^{3+} in a low dose (x.x mg/kg /min giving a serum concentration of $\sim 300 \text{ \mu M}$), thus activating the TRPC5 channel rather than blocking it while blocking the TRPC6 channel followed by separate experiments using millimolar concentrations of La^{3+}

(x.x mg/kg /min giving a serum concentration of ~2.4 mM) blocking both the TRPC5 and TRPC6 channel. Both La^{3+} concentrations were effective in blocking the glomerular hyperpermeability response induced by Ang II (Fig. 3a). Both low and high dose La^{3+} effectively counteracted the increases in mean arterial pressure induced by Ang II (Fig. 3b). To elucidate if the increased effect of high dose La^{3+} on MAP is due to blocking both TRPC5 and TRPC6 or simply a dose response (increased TRPC6 blocking), we administered both low dose La^{3+} and clemizole in a separate group. The combined therapy appeared less effective at reducing MAP than low dose La^{3+} . In a separate analysis, we tested the interaction treatment \times time on the sieving coefficient of Ficoll_{70Å} between the low dose La^{3+} and the combined La^{3+} + TRPC5i group. We rejected the null hypothesis at the 1% level ($F_{1,13}=9.4$, $P=0.009$) showing that the combined treatment was inferior in its ability reduce the leakage of large Ficoll_{70Å} across the glomerular filter compared to low dose La^{3+} only indicating that concomitant activation of TRPC5 potentiates the hyperpermeability reducing effect of low dose La^{3+} . Lastly, since clemizole is also an H₁R antagonist, we tested the effects of iv infusion of histamine on glomerular permeability and found no effect (data not shown), similar to previous results by Ichikawa and Brenner¹⁵. There were no significant differences in heart rate in the different experimental groups.

DISCUSSION

Is it possible to separate the hemodynamic actions of Ang II from its effects on glomerular permeability? Our data demonstrate that inhibition of TRPC5 effectively ameliorates Ang II induced glomerular hyperpermeability without affecting systemic blood pressure. These findings confirm recent results both by Zhou et al ¹⁶ and Ilatovskaya et al ¹⁷ providing further evidence that therapeutically targeting TRPC5 channels may be effective to treat glomerular proteinuric disease states. We also found that TRPC6 inhibition using La³⁺ reduced Ang II induced glomerular hyperpermeability. La³⁺ also counteracted the vasopressor effects of Ang II. However, while Ang II induced Ca²⁺ influx seems to occur mainly via TRPC5 and TRPC6 in podocytes ⁶, the observed effects on mean arterial pressure may be due to the effects of La³⁺ on other TRP channels and future experiments should be performed using a more specific TRPC6 inhibitor. Interestingly, combining blockers of TRPC5 and TRPC6, using clemizole and low dose La³⁺, respectively, had significantly less effect on glomerular hyperpermeability compared to low dose La³⁺ alone. While this finding may appear counterintuitive, it could be the result of an antagonistic relationship between these channels in podocytes ⁶. We have previously demonstrated that blocking either the TRPC5-associated GTP-ase Rac-1 or the TRPC6-associated GTP-ase RhoA is also effective to counteract Ang II effects on glomerular permeability. Thus, blocking either RhoA-kinase or TRPC6 has the same effect as blocking either Rac-1-kinase or TRPC5. From our current results it would also appear that blocking just one channel is more effective than blocking both channels, supporting the view that it is a concerted and mutually inhibitory action of both Rac-1 and RhoA signaling pathways that governs the glomerular hyperpermeability response (Fig. 4), rather than the sole action of one of the pathways.

Glomerular hyperpermeability can be induced by a number of pharmacological and experimental challenges ^{8, 18-20} often being of a transient nature such that the permeability

approaches baseline levels after the injurious stimuli is removed. While proteinuria is often associated with structural alterations in the renal filter, such reversible alterations imply that the structural changes occurring in the GFB are of a brief and non-persistent nature. While there is good evidence that podocytes play a key role in proteinuric disease, the mechanisms by which they keep the renal filter tight are still obscure. Very recently, it was hypothesized that podocytes, via their contractile cytoskeleton, maintain a tension compressing the GBM in the radial direction keeping the meshwork of the GBM in an organized state²¹. According to this hypothesis, loss of tension will disorganize the GBM, reducing its size-selective properties, leading to leakage of macromolecules across the filter. In terms of a pore model of glomerular permeability²², this would be equivalent to increasing the average pore radius or widening the pore size distribution.

We have here identified both TRPC5 and TRPC6 as potential targets for novel anti-proteinuric agents, both being effective against glomerular hyperpermeability induced by Ang II. We have previously identified several potential pharmacological targets downstream of the Ang II receptor^{8,9}. However, since TRPC-channels are partly extra-cellular, they are more easily targeted by pharmacological interventions. A limitation in the current study is the non-selective nature of La³⁺ salts, meaning that the observed effects may be due to blocking of other TRP channels. Another limitation is the acute nature of the present experiments, which prevents evaluation of chronic effects.

AUTHOR CONTRIBUTIONS

C.M.O. and J.D. designed the study; A.R. carried out experiments; C.M.O and J.D. analyzed the data; C.M.O. made the figures; C.M.O and J.D. drafted and revised the paper; all authors approved the final version of the manuscript.

ACKNOWLEDGEMENTS

This work has been funded by the Swedish Heart and Lung foundation and the medical faculty in Lund (ALF grant). The authors declare no competing interests pertaining to the current article.

REFERENCES

1. Hsu, TW, Liu, JS, Hung, SC, Kuo, KL, Chang, YK, Chen, YC, Hsu, CC, Tarng, DC:
Renoprotective effect of renin-angiotensin-aldosterone system blockade in patients with predialysis advanced chronic kidney disease, hypertension, and anemia. *JAMA Intern Med*, 174: 347-354, 2014.
2. Siew, ED, Davenport, A: The growth of acute kidney injury: a rising tide or just closer attention to detail? *Kidney Int*, 87: 46-61, 2015.
3. Palevsky, PM, Zhang, JH, Seliger, SL, Emanuele, N, Fried, LF, Study, VN-D: Incidence, Severity, and Outcomes of AKI Associated with Dual Renin-Angiotensin System Blockade. *Clin J Am Soc Nephrol*, 11: 1944-1953, 2016.
4. Faul, C, Asanuma, K, Yanagida-Asanuma, E, Kim, K, Mundel, P: Actin up: regulation of podocyte structure and function by components of the actin cytoskeleton. *Trends Cell Biol*, 17: 428-437, 2007.
5. Schiffer, M, Teng, B, Gu, C, Shchedrina, VA, Kasaikina, M, Pham, VA, Hanke, N, Rong, S, Gueler, F, Schroder, P, Tossidou, I, Park, JK, Staggs, L, Haller, H, Erschow, S, Hilfiker-Kleiner, D, Wei, C, Chen, C, Tardi, N, Hakrrouch, S, Selig, MK, Vasilyev, A, Merscher, S, Reiser, J, Sever, S: Pharmacological targeting of actin-dependent dynamin oligomerization ameliorates chronic kidney disease in diverse animal models. *Nat Med*, 21: 601-609, 2015.
6. Tian, D, Jacobo, SM, Billing, D, Rozkalne, A, Gage, SD, Anagnostou, T, Pavenstadt, H, Hsu, HH, Schlondorff, J, Ramos, A, Greka, A: Antagonistic regulation of actin dynamics and cell motility by TRPC5 and TRPC6 channels. *Sci Signal*, 3: ra77, 2010.
7. Greka, A, Mundel, P: Balancing calcium signals through TRPC5 and TRPC6 in podocytes. *J Am Soc Nephrol*, 22: 1969-1980, 2011.

8. Axelsson, J, Rippe, A, Öberg, CM, Rippe, B: Rapid, dynamic changes in glomerular permeability to macromolecules during systemic angiotensin II (ANG II) infusion in rats. *Am J Physiol Renal Physiol*, 303: F790-799, 2012.
9. Axelsson, J, Rippe, A, Sverrisson, K, Rippe, B: Scavengers of reactive oxygen species, paracalciton, RhoA, and Rac-1 inhibitors and tacrolimus inhibit angiotensin II-induced actions on glomerular permeability. *Am J Physiol Renal Physiol*, 305: F237-243, 2013.
10. Richter, JM, Schaefer, M, Hill, K: Clemizole hydrochloride is a novel and potent inhibitor of transient receptor potential channel TRPC5. *Mol Pharmacol*, 86: 514-521, 2014.
11. Asgeirsson, D, Venturoli, D, Rippe, B, Rippe, C: Increased glomerular permeability to negatively charged Ficoll relative to neutral Ficoll in rats. *American journal of physiology Renal physiology*, 291: F1083-1089, 2006.
12. Wobbrock, JO, Findlater, L, Gergle, D, Higgins, JJ: The aligned rank transform for nonparametric factorial analyses using only anova procedures. *Proceedings of the SIGCHI conference on human factors in computing systems*. ACM, 2011 pp 143-146.
13. Dolinina, J, Rippe, A, Bentzer, P, Öberg, CM: Glomerular hyperpermeability after acute unilateral ureteral obstruction: effects of Tempol, NOS, RhoA, and Rac-1 inhibition. *Am J Physiol Renal Physiol*, 315: F445-F453, 2018.
14. Jung, S, Muhle, A, Schaefer, M, Strotmann, R, Schultz, G, Plant, TD: Lanthanides potentiate TRPC5 currents by an action at extracellular sites close to the pore mouth. *J Biol Chem*, 278: 3562-3571, 2003.
15. Ichikawa, I, Brenner, BM: Mechanisms of action of hisamine and histamine antagonists on the glomerular microcirculation in the rat. *Circ Res*, 45: 737-745, 1979.
16. Zhou, Y, Castonguay, P, Sidhom, EH, Clark, AR, Dvela-Levitt, M, Kim, S, Sieber, J, Wieder, N, Jung, JY, Andreeva, S, Reichardt, J, Dubois, F, Hoffmann, SC, Basgen,

- JM, Montesinos, MS, Weins, A, Johnson, AC, Lander, ES, Garrett, MR, Hopkins, CR, Greka, A: A small-molecule inhibitor of TRPC5 ion channels suppresses progressive kidney disease in animal models. *Science*, 358: 1332-1336, 2017.
17. Ilatovskaya, DV, Palygin, O, Levchenko, V, Endres, BT, Staruschenko, A: The Role of Angiotensin II in Glomerular Volume Dynamics and Podocyte Calcium Handling. *Sci Rep*, 7: 299, 2017.
18. Axelsson, J, Rippe, A, Rippe, B: Transient and sustained increases in glomerular permeability following ANP infusion in rats. *American journal of physiology Renal physiology*, 300: F24-30, 2011.
19. Axelsson, J, Rippe, A, Venturoli, D, Sward, P, Rippe, B: Effects of early endotoxemia and dextran-induced anaphylaxis on the size selectivity of the glomerular filtration barrier in rats. *Am J Physiol Renal Physiol*, 296: F242-248, 2009.
20. Dolinina, J, Sverrisson, K, Rippe, A, Öberg, CM, Rippe, B: Nitric oxide synthase inhibition causes acute increases in glomerular permeability in vivo, dependent upon reactive oxygen species. *Am J Physiol Renal Physiol*, 311: F984-F990, 2016.
21. Fissell, WH, Miner, JH: What Is the Glomerular Ultrafiltration Barrier? *J Am Soc Nephrol*, 29: 2262-2264, 2018.
22. Öberg, CM, Rippe, B: A distributed two-pore model: theoretical implications and practical application to the glomerular sieving of Ficoll. *Am J Physiol Renal Physiol*, 306: F844-854, 2014.
23. Asanuma, K, Yanagida-Asanuma, E, Faul, C, Tomino, Y, Kim, K, Mundel, P: Synaptopodin orchestrates actin organization and cell motility via regulation of RhoA signalling. *Nat Cell Biol*, 8: 485-491, 2006.
24. Faul, C, Donnelly, M, Merscher-Gomez, S, Chang, YH, Franz, S, Delfgaauw, J, Chang, JM, Choi, HY, Campbell, KN, Kim, K, Reiser, J, Mundel, P: The actin cytoskeleton of

- kidney podocytes is a direct target of the antiproteinuric effect of cyclosporine A. *Nat Med*, 14: 931-938, 2008.
25. Reiser, J, Polu, KR, Moller, CC, Kenlan, P, Altintas, MM, Wei, C, Faul, C, Herbert, S, Villegas, I, Avila-Casado, C, McGee, M, Sugimoto, H, Brown, D, Kalluri, R, Mundel, P, Smith, PL, Clapham, DE, Pollak, MR: TRPC6 is a glomerular slit diaphragm-associated channel required for normal renal function. *Nat Genet*, 37: 739-744, 2005.
26. Robins, R, Baldwin, C, Aoudjit, L, Cote, JF, Gupta, IR, Takano, T: Rac1 activation in podocytes induces the spectrum of nephrotic syndrome. *Kidney Int*, 92: 349-364, 2017.

LEGENDS

Figure 1

A: Glomerular sieving coefficients vs. molecular Stokes-Einstein radius for Ficolls ranging from 15 Å (about the size of FITC-inulin) to 80 Å (about ~10 Å smaller than fibrinogen) at baseline and at the different timepoints post-administration of AngII. In a graph below the plotted sieving curve are P-values from post-hoc tests comparing sieving coefficients post-administration vs. baseline. *B*: Glomerular sieving coefficients for Ficoll_{70Å} and *C*: mean arterial pressure at baseline and 5, 15 and 30 min after AngII administration.

Figure 2

A: Mean arterial pressure at baseline and 5 min post Ang II administration (red) for the Ang II only group and Ang II + TRPC5i group (blue). A 2×2 ANOVA revealed no interaction between treatment (Ang II only vs. Ang II + TRPC5i) and time (baseline vs. 5 min) showing that inhibition of TRPC5 did not affect the hemodynamic effects of angiotensin II. *B*: Sieving coefficients at baseline and 5 min for the Ang II + TRPC5i group (black and blue lines) compared with the Ang II only group. A significant interaction (treatment \times time) indicates that TRPC5-inhibition significantly ameliorates Ang II mediated glomerular hyperpermeability for Ficolls > 45 Å.

Figure 3

A: Glomerular sieving coefficients for Ficoll_{70Å} at baseline and 5 min after Ang II administration for the different experimental groups. *B*: Difference in mean arterial pressure between baseline and 5 min post-Ang II. Statistical differences are between Ang II only and the groups combining Ang II with a TRPC-channel blocker. *C*: Glomerular filtration rate

(GFR) for the left kidney in the different groups. For high dose La^{3+} there was a significant decrease in GFR between baseline and 5 min.

Figure 4

A model for the mechanistic roles of TRPC5 and TRPC6 in the regulation of glomerular permeability. Under normal conditions, stimulation of AT1R activates TRPC6 and TRPC5 channels, allowing the influx of Ca^{2+} , thereby promoting activation of both RhoA and Rac1, which are mutually inhibitory⁶, which, in turn, lead to glomerular hyperpermeability. Blocking of either RhoA (directly using an inhibitor⁹ or via calcineurin inhibition^{9, 23, 24}) or Rac-1 (using Rac-1⁹ inhibition or prednisolone) ameliorates Ang II induced hyperpermeability. Several lines of evidence implicate TRPC channels in human proteinuric disease such as TRPC6 gain-of-function mutations²⁵ and Rac-1 over-expression in minimal change disease²⁶.

Fig 1

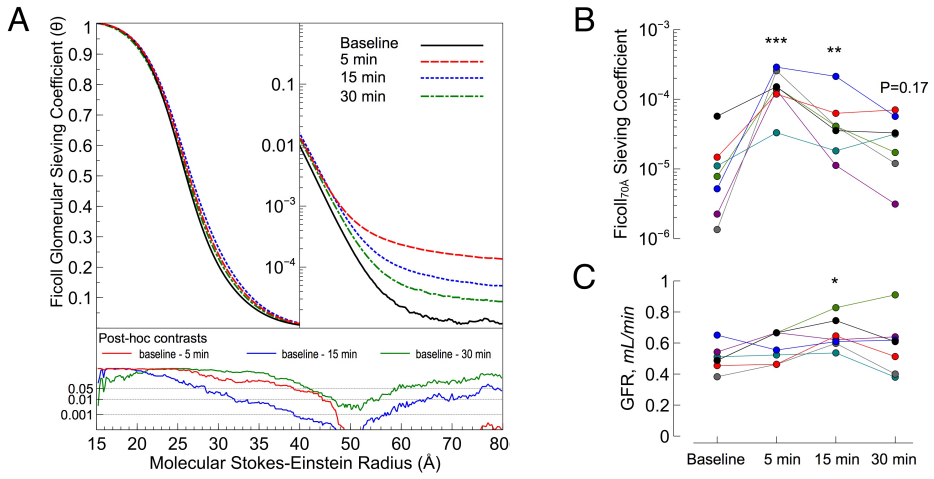


Fig 2

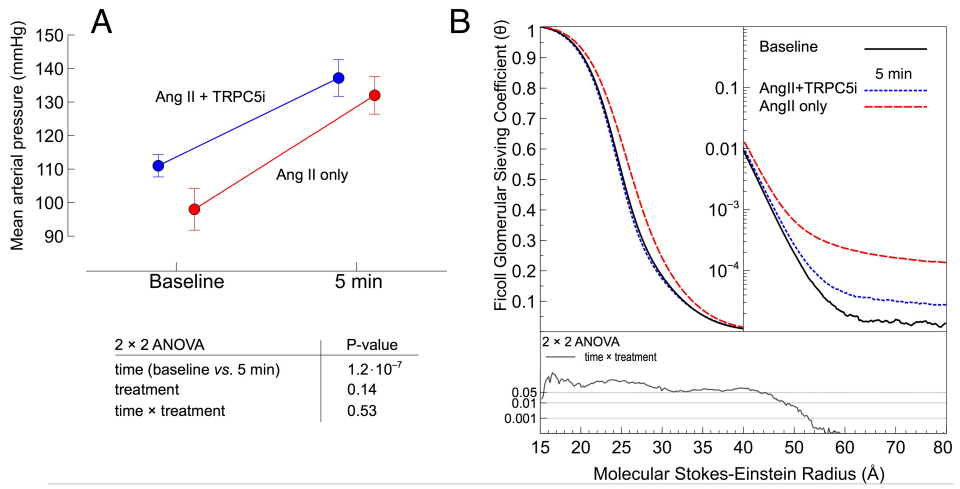


Fig 3

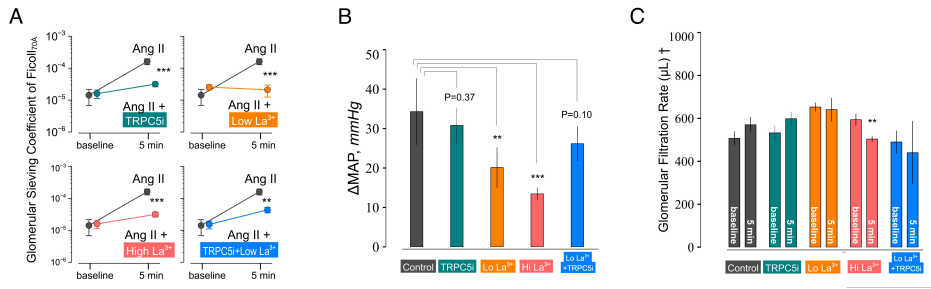
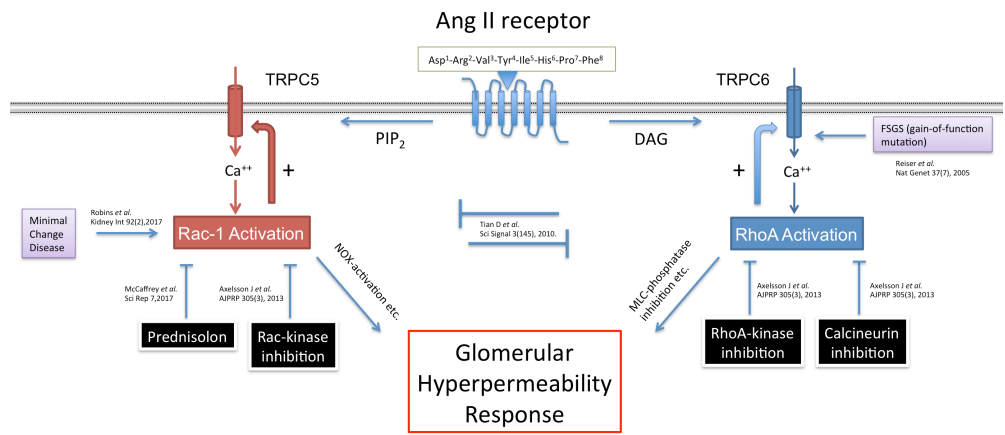


Fig 4



Supplemental Table 1

Parameter	Baseline	5 min	15 min	30 min
MAP, mmHg	98 ± 6	132 ± 6***	134 ± 5***	134 ± 4***
Heart rate, min ⁻¹	275 ± 12	263 ± 15	264 ± 17	268 ± 20

*** P < 0.001 compared to baseline



**FACULTY OF
MEDICINE**

Department of Clinical Sciences, Lund

Lund University, Faculty of Medicine
Doctoral Dissertation Series 2020:134
ISBN 978-91-8021-001-0
ISSN 1652-8220

